UBIQUITINATION IN THE UV-INDUCED DNA DAMAGE RESPONSE

from proteomics to patient

Petra Schwertman

Ubiquitination in the UV-induced DNA Damage Response

Petra Schwertman | 2014

Ubiquitination in the UV-induced DNA Damage Response

from proteomics to patient

Petra Schwertman

Layout & printing: Off Page, Amsterdam

ISBN: 978-94-6182-445-5

Ubiquitination in the UV-induced DNA Damage Response

from proteomics to patient

Ubiquitinatie in de UV-geïnduceerde DNA-schade respons

van proteomica tot patiënt

Proefschrift

ter verkrijging van de graad van doctor aan de

Erasmus Universiteit Rotterdam

op gezag van de rector magnificus Prof.dr. H.A.P. Pols

en volgens besluit van het College voor Promoties.

De openbare verdediging zal plaatsvinden op

vrijdag 6 juni om 13:30 uur.

Pieterke Schwertman

Geboren te Groningen

Promotiecommissie

Promotor:	Prof.dr. J.H.J. Hoeijmakers
Copromotoren:	Dr. W. Vermeulen
	Dr. J.A.F. Marteijn
Overige leden:	Prof.dr. L.H.F. Mullenders
	Prof.dr. T.K. Sixma
	Prof.dr. C.P. Verrijzer

TABLE OF CONTENTS

SCOPE OF THE THESIS

The integrity of DNA is continuously challenged by genotoxic agents from both internal and external origin that severely hamper vital DNA-dependent processes as genome duplication by replication and reading of the genetic code by transcription. The adverse effects of DNA damage are counteracted by a complex network of genome defence processes, referred to as the DNA damage response (DDR), which consists of different dedicated DNA repair systems and signalling pathways.

Nucleotide excision repair (NER) is the main DNA repair process in mammalian cells that removes UV-induced DNA lesions. Protein ubiquitination has emerged as a key regulatory mechanism for this pathway. However, how the entire UV-light induced DDR (UV-DDR) is controlled via ubiquitination remains largely unknown. The aim of the research described in this thesis is to better understand the ubiquitin-mediated regulation of the UV-DDR. To identify new ubiquitin modifications and proteins not previously known to be involved within the UV-DDR on a proteome-wide scale mass spectrometry (MS) was used. To provide the necessary background **Chapter 1** summarizes the current knowledge on DDR, ubiquitination and MS-based methods.

Since presumably not all proteins are ubiquitinated in any cellular response and as from those that are ubiquitinated only a fraction is usually modified at a given time, methods to enrich for these proteins are necessary to study them by MS. **Chapter 2** describes an immunoaffinity purification method for the isolation of endogenously ubiquitinated proteins, which was especially developed for the proteomic analysis of ubiquitinated protein complexes.

Quantitative proteomic strategies – such as stable isotope labelling by amino acids in cell culture (SILAC)-based MS approaches – are designed to detect and quantify the effects of a specific stimulus on relative protein abundance in a proteome-wide fashion. In **Chapter 3**, SILAC-based quantitative proteomics was combined with the method described in Chapter 2 to identify UV-induced ubiquitin modifications on proteins and protein complexes. Among the most enriched proteins in response to UV-induced DNA damage, NER factors known to be regulated by ubiquitin – including DDB2, XPC, CSB and POLR2A (the largest subunit of RNA Pol II) – were identified. The high enrichment of these NER proteins upon DNA damage validated our approach for isolating UV-induced ubiquitinated proteins.

In **Chapter 4** follow-up research is shown on one of the most enriched proteins that was identified in the MS screen presented in Chapter 3. The identification and molecular function of UVSSA and its interaction partner USP7 are described and their role in TC-NER is discussed. Of note, *UVSSA* was found to be the causative gene for UV^{S}S, an unresolved NER-deficiency disorder.

To conclude, **Chapter 5** discusses how the research on the role of UVSSA and USP7 in TC-NER contributes to a better understanding of the molecular mechanisms underlying the clinical differences between two human disorders associated with defective TC-NER: Cockayne syndrome (CS) and UV-sensitive syndrome (UV^{S}S).

1

GENERAL INTRODUCTION

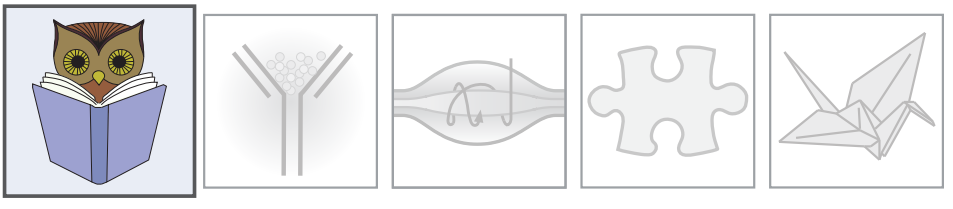

1.1 DNA DAMAGE

DNA is the blueprint for our bodies. It contains all the biological information which is needed for proper function and duplication of our cells. The DNA is stored in the nucleus as two intertwined polynucleotide chains, called the double helix, conferring high stability to our hereditary information. However, the integrity of our DNA is constantly threatened by genotoxic agents from both internal and external origin (Figure 1). Under physiological conditions spontaneous hydrolysis of nucleotides results in abasic sites and deamination. Additionally, during normal cellular metabolism reactive oxygen species (ROS) are formed that can oxidize DNA, which leads to several types of DNA damage[1]. Sources of exogenous damage are, for example: ultraviolet (UV)-light present in sunlight, ionizing radiation, genotoxic compounds present in cigarette smoke and exhaust-gasses, and chemotherapeutic drugs. Damaged DNA can lead to mutations or chromosomal aberrations, thereby increasing the risk of cancer. Alternatively, DNA damage might inhibit transcription or replication, inducing apoptosis or cellular senescence and thereby contributing to premature aging[2].

To safeguard the integrity of the genome, organisms have evolved the DNA damage response (DDR)[3,4]. This response consists of a wide variety of DNA repair systems – as discussed in section 1.2 – and complementary signalling pathways. Two key DDR signalling factors in mammalian cells are the protein kinases ATM[5] and ATR[6]. These kinases are important mediators in activating transient cell-cycle arrest, which is needed to provide an extended time window for DNA repair before replication or mitosis takes place[7,8]. Additionally, if the

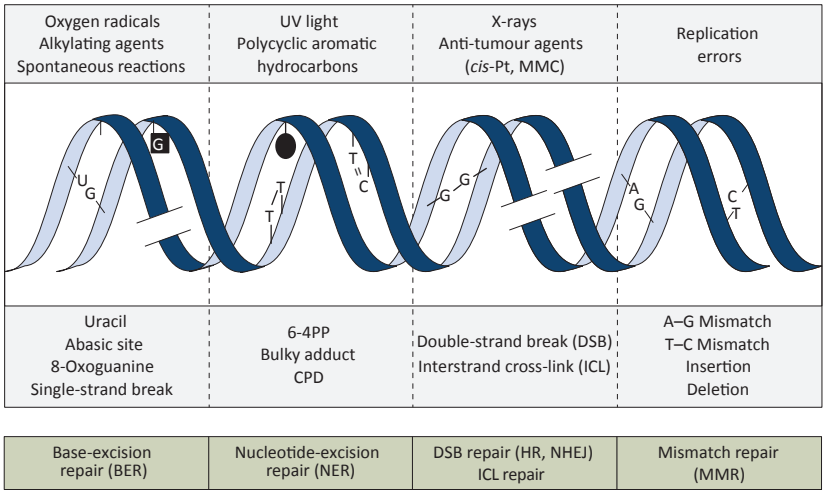

Figure 1: DNA damage and repair
DNA is constantly exposed to a wide variety of endogenous and exogenous genotoxic agents (top). These agents induce different types of DNA lesions (middle), which are recognized and repaired by distinct DNA repair mechanisms (bottom). *cis*-Pt, cisplatin; MMC, mitomycin C; 6-4PP, 6-4 photoproduct; CPD, cyclobutane-pyrimidine dimer; HR, homologous recombination; NHEJ, non-homologous end joining. Adapted from Hoeijmakers[11]

damage cannot be repaired persistent DDR signalling through these kinases can lead to cellular senescence or apoptosis-mediated cell death. The aforementioned processes are complicated by the packaging of genomic DNA into a condensed and relatively inaccessible structure called chromatin. In order to make the damaged DNA more available to DDR factors chromatin needs to be remodelled, for example by post-translational histone modifications and nucleosome remodelling[9,10].

1.2 DNA REPAIR

The first key step in initiating DNA repair is the DNA damage recognition, which is triggered by specialized lesion-sensors or by blocked transcription. Multiple, distinct DNA repair pathways exist to cope with the wide variety of DNA lesions (Figure 1)[11].

Non-homologous end joining (NHEJ) and homologous recombination (HR)

Double strand breaks (DSB), induced by e.g. X-rays and anti-tumour agents, can be repaired by either non-homologous end joining (NHEJ) or homologous recombination (HR)[12]. In NHEJ the two ends of a DSB are joined together by ligating enzymes. Since some nucleotides may be lost or added during processing of the broken ends this pathway is error-prone and therefore associated with an elevated risk of mutagenesis[13]. In HR the intact copy on the sister chromatid is used to properly align and join the broken ends in an error-free manner. Since the presence of a homologous chromatid is essential, this pathway is only active in the S and G2 phases of the cell cycle[14].

Interstrand Cross-Link (ICL) repair

Interstrand crosslinks (ICLs), which covalently link the two strands of the double helix, are highly toxic DNA lesions as they block transcription and replication. For that reason, chemical compounds that induce ICLs – such as mitomycin C (MMC) and cisplatin (*cis*-Pt) – are often used as chemotherapeutic drugs for the treatment of cancer. The molecular mechanistic details of ICL repair are not yet fully understood. However, ICL repair likely involves the participation of the Fanconi Anemia (FA) pathway proteins together with a complex coordination of homologous recombination (HR), nucleotide-excision repair (NER), and translesion synthesis (TLS)[15,16].

DNA mismatch repair (MMR)

DNA mismatch repair (MMR) recognizes and removes base-base mismatches and insertion/deletion mispairs that can arise during, for example, DNA replication and recombination. After mismatch recognition, the template and non-template strand are distinguished followed by a single-strand incision, degradation of the DNA strand past the mismatch and resynthesis of the excised tract[17].

Base excision repair (BER)

Single strand breaks (SSB) and damaged bases that arise from oxidation, alkylation, and deamination are primarily repaired by base excision repair (BER). BER is initiated by a set of lesion-specific DNA glycosylases which recognize these small, non-helix-distorting base

lesions in the genome and cleave the damaged base from the sugar-phosphate backbone. The resulting abasic site is then cleaved by an endonuclease forming a single-strand break, which is subsequently processed by short-patch (1 nucleotide) BER or to a lesser extent long-patch (2-15 nucleotides) BER. Within both sub-pathways DNA polymerases fill in the nucleotide gap, and the remaining nick is sealed by DNA ligases.[18]

Nucleotide-excision repair (NER)

Nucleotide-excision repair (NER) removes a wide range of structurally unrelated lesions which can be induced by environmental mutagens (such as benzo[a]pyrene in coal tar and cigarette smoke), certain chemotherapeutic agents (such as cisplatin) and UV-light[19]. This wide variety of lesions has in common that they are all, to some degree, helix-distorting. The remarkable ability of NER to recognize and repair all these different lesions is achieved by proteins that recognize the distortion of the DNA duplex itself instead of a certain type of lesion. To study NER, lamps that emit UV-C irradiation are often used as a convenient way to directly induce well-characterized NER lesions in cells[20]. UV-light mainly leads to the formation of dimeric photoproducts involving two adjacent pyrimidine bases. The majority of these lesions are cyclobutane-pyrimidine dimers (CPDs), and 6-4 pyrimidine-pyrimidone photoproducts (6-4PPs)[21,22]. While 6-4PPs are highly helix-distorting, CPDs are still capable of base-pairing with the opposite strand. To remove helix-distorting lesions from the DNA more than 30 proteins are involved, together forming the multistep NER pathway. The key steps in the reaction include: (1) DNA damage recognition, (2) helix unwinding and damage verification, (3) double incision of the damaged strand and, (4) gap-filling of the repair patch and sealing of the nicks[23]. NER is divided into two distinct sub-pathways which only differ in the DNA damage recognition step: global genome NER (GG-NER)[19] and transcription-coupled NER (TC-NER) (Figure 2)[24].

Damage recognition in global genome nucleotide-excision repair (GG-NER)

GG-NER recognizes and repairs DNA helix-distorting lesions located throughout the whole genome. Lesion recognition is achieved by two sensors: the XPC complex and the UV-DDB complex. The XPC complex is a heterotrimer consisting of XPC, RAD23B and CETN2[25]. XPC efficiently recognizes severe helix-distortions like 6-4PPs and binds the intact strand opposite of the damage[26]. For the recognition of certain less helix-distorting lesions (like CPDs) the UV-DDB complex is needed, which is a heterodimer consisting of DDB1 and DDB2/XPE. The DDB2 subunit binds the damaged strand and subsequently flips out the damaged nucleotides and kinks the DNA duplex[27]. The UV-DDB complex has been shown to facilitate XPC binding to lesions[28] and the DNA kinking ability of DDB2 might function to facilitate the binding of XPC to less helix-distorting lesions.

Damage recognition in transcription-coupled nucleotide-excision repair (TC-NER)

TC-NER is initiated when RNA polymerase II (RNA Pol II) is stalled during transcription by alterations in the DNA structure[24]. Lesion-stalled elongating RNA Pol II triggers the recruitment of several TC-NER specific factors to form a functional TC-NER complex; including the essential Cockayne syndrome A and B (CSA, CSB) proteins[29].

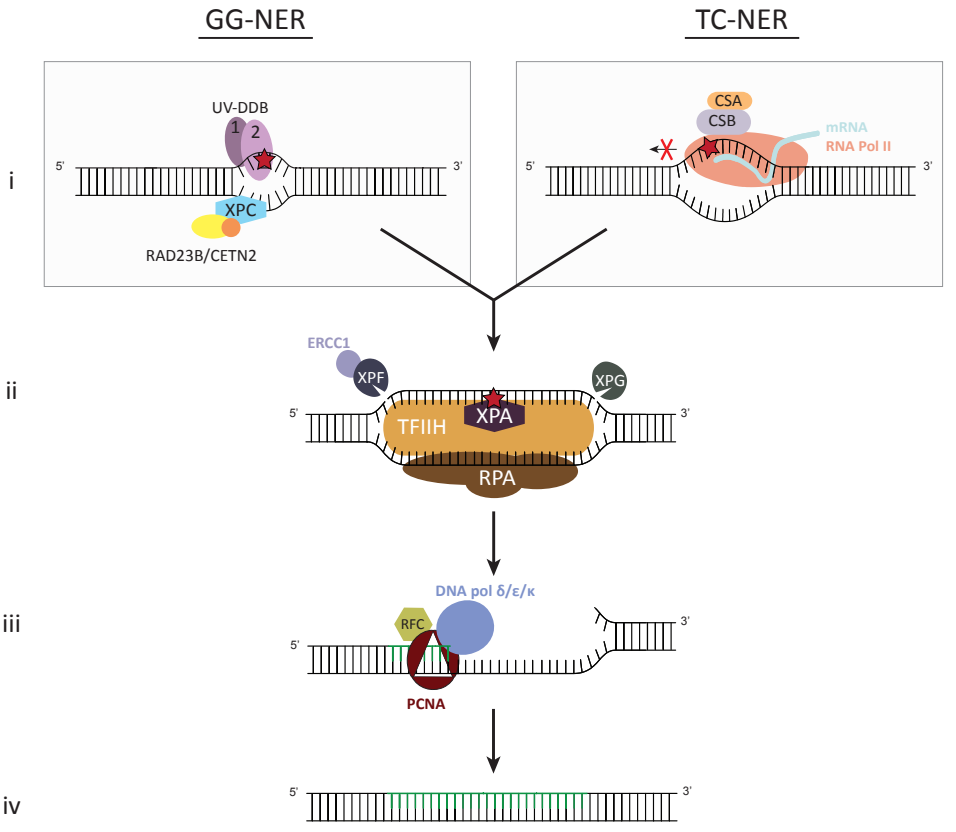

Figure 2: Nucleotide-excision repair (NER)
NER is divided into two distinct sub-pathways which only differ in the DNA damage recognition step: global genome NER (GG-NER) and transcription-coupled NER (TC-NER). (i) In GG-NER helix-distorting lesions are recognized by the XPC-complex (XPC, RAD23B and CETN2), and in some cases with the help of the UV-DDB complex (DDB1 and DDB2). TC-NER is initiated by RNA polymerase II stalled at a lesion and requires at least two TC-NER-specific factors: CSA and CSB. (ii) After the damage recognition step the two sub-pathways converge in the common NER pathway. The XPB and XPD helicases of the TFIIH complex unwind a ~30-nucleotide region around the lesion. Next, XPA and the single-stranded-binding protein RPA are recruited. Once verification of the lesion has occurred, the damaged strand is excised through double incision by ERCC1/XPF (at the 5' side) and subsequently XPG (at the 3' side). (iii) The lesion-containing oligonucleotide is released from the DNA and the gap is filled in by the replication machinery (consisting of RFC, PCNA and DNA polymerase δ, ε and/or κ). Finally, the nick is sealed by DNA ligase I or IIIα (iv) completing the repair reaction. The red star indicates DNA damage.

CSB is a member of the SNF2/SWI2 family of DNA-dependent ATPases[30] and is suggested to have chromatin remodelling abilities, possibly also through recruitment of the p300 histone acetyltransferase[31-33]. CSB transiently interacts with elongating RNA Pol II and stimulates transcription[34-39]. Upon encountering a lesion, stalled RNA Pol II stabilizes its interaction with CSB[39] and triggers, in cooperation with CSA, the recruitment of several other factors involved in NER, such as XAB2, HMGN1, TFIIS and p300[29]. Since RNA Pol II

likely shields the DNA lesion in its active pocket, the stalled transcription complex must be remodelled to enable access of the TC-NER factors to the lesion[40-45].

"Core"-nucleotide-excision repair (NER)

After the damage recognition step the two sub-pathways converge in the common NER pathway. One of the first key components to arrive is the TFIIH complex, which is a general transcription factor consisting of 10 subunits[46,47]. Two of these subunits, XPB and XPD, feature helicase activity involved in unwinding of a ~30-nucleotide region around the lesion. Next, XPA and the heterotrimer RPA are recruited. Together with TFIIH these two proteins are suggested to be involved in lesion-verification; XPA may recognize the damaged strand and single strand binding protein RPA binds the undamaged strand[48,49]. Once verification of the lesion has occurred, the damaged strand is incised by the heterodimer XPF-ERCC1 at the 5' side of the damage and subsequently by XPG at the 3' side. The lesion-containing oligonucleotide is then released from the DNA and the gap is filled in by the replication machinery (consisting of RFC, PCNA and DNA polymerase δ, ε and/or κ)[50]. Finally, the nick is sealed by DNA ligase I or IIIα[51] thereby completing the repair reaction (Figure 2).

NER-deficient disorders

The significance of NER is illustrated by several rare, autosomal recessive disorders associated with NER defects, such as xeroderma pigmentosum (XP), Cockayne syndrome (CS) and UV-sensitive syndrome ($UV^{S}S$)[52]. XP is caused by mutations in the XP genes *XPA* through *XPG*. XP patients display a dry scaly skin (xeroderma), abnormal pigmentation in sun-exposed skin areas (pigmentosum), photohypersensitivity of the skin, and an almost 10.000-fold increased risk for skin cancer in patients below 20 years of age[53]. The higher incidence of cancer in these patients is attributed to defective GG-NER. Since this pathway removes lesions throughout the genome, a defect in GG-NER would increase mutations and subsequently the risk for cancer. CS is caused by mutations in two genes essential for TC-NER, *CSA* and *CSB*. CS patients also display photohypersensitivity of the skin[54]. Additionally, in response to DNA damage, defective TC-NER results in apoptosis or senescence of cells. This effect is thought to contribute to the severe developmental, neurological, and premature aging features in patients with CS. In contrast to XP CS is not associated with increased skin cancer risk, which is probably due to the still functional GG-NER pathway[55]. $UV^{S}S$ is another disorder associated with defective TC-NER. In contrast to CS patients, $UV^{S}S$ patients express much milder features which are mostly restricted to UV hypersensitivity. $UV^{S}S$ comprises three complementation groups, which are defined by specific mutations in *CSA*, *CSB* and UV-stimulated scaffold protein A (*UVSSA*)[56]. The underlying molecular reason for the striking variety in TC-NER-deficient phenotype is still largely unknown, although several models are proposed (see Chapter 5).

1.3 UBIQUITINATION

DNA repair processes are tightly controlled to ensure appropriate function and timing at the right location. This regulation relies for a big part on post-translational modification (PTM) of the repair proteins and signalling into the DNA damage response (DDR) pathway. There are

many types of PTMs known to modulate the function of DDR proteins upon DNA damage infliction, including phosphorylation[57], ubiquitination[58], sumoylation[58], acetylation[59,60] and parylation[61,62]. Within UV-induced NER, ubiquitination plays a prominent role[63-65].

Protein ubiquitination is a PTM which plays a crucial role in many cellular processes by controlling the activity, localization and stability of proteins. The highly conserved 76-amino-acid protein ubiquitin (Ub) can be covalently attached to the ε-amino group of lysine residues in proteins[66]. In addition, less frequently also the N-terminal amine can be modified with ubiquitin[67]. Ubiquitination is a three-step enzymatic cascade, which involves Ub activating enzymes (E1), Ub conjugating enzymes (E2) and Ub ligating enzymes (E3)[68] (Figure 3). The human genome encodes two E1 enzymes for ubiquitin, which use an ATP molecule to form a high-energy thioester bond between the c-terminus of ubiquitin and an internal cysteine residue of the E1. Subsequently, the activated ubiquitin is transferred to the active-site cysteine of one of the ~30 E2s[69] in a human cell. Finally, an E3 is needed to couple the c-terminal glycine residue of ubiquitin to the substrate protein via an isopeptide bond. Humans express over 600 E3s[70], which determine substrate specificity of the ubiquitination process. The two major types of E3s are defined by the presence of either a homologous to the E6AP carboxyl terminus (HECT) domain[71] or a really interesting new gene (RING) domain[72]. For E3s harbouring a HECT domain the ubiquitin is first transferred from the E2 to form a thioester intermediate with the active-site cysteine of the E3, subsequently ubiquitin is coupled to the protein substrate. Most E3s, however, belong to the RING domain family, which mediate the direct transfer of ubiquitin from E2 to protein substrate. A third type of E3s is formed by a highly conserved, although very small family of E3s called the RING-between-RING (RBR) ligases[73]. These ligases contain two RING domains, RING1 and RING2, but combine features of both RING- and HECT-type ligases. First, RBR ligases bind a ubiquitin-conjugated E2 to their canonical RING1 domain. The ubiquitin is then transferred from the E2 to the RING2 domain, which contains a highly conserved cysteine that functions like a HECT active-site cysteine. Finally, the ubiquitin is then transferred from the RING2 domain to the protein substrate. Because of this mode of action of RBR ligases, they could be seen as RING-HECT hybrids[73].

Following addition of a single ubiquitin to a protein substrate at one or more sites (mono-ubiquitination), further ubiquitin molecules can be conjugated to the first resulting in a ubiquitin chain (poly-ubiquitination). Distinct chain-linkages can be formed at all seven internal lysine residues of ubiquitin (K6, K11, K27, K29, K33, K48 and K63) and at its N-terminus (M1). In addition to homotypic ubiquitin chains, which have a single linkage type, heterotypic chains are possible that contain mixed linkages within the same ubiquitin chain. The different poly-ubiquitin chains are structurally distinctive, which results in diverse functionalities[74,75]. The most abundant chain-linkage, through K48, is primarily a signal for proteasomal degradation, while linkage through K63 has a well-established role in cell signalling independent of degradation. In comparison, relatively little is known about possible specialized functions of the other chain-linkage types (Figure 4)[74-76].

The different topologies of ubiquitination are decoded by a large number of proteins containing ubiquitin-binding domains (UBDs)[76,77]. At least 20 different families of UBD are

identified that interact with ubiquitinated substrates to regulate the fate of these proteins[76-78]. Dedicated UBDs exist that can selectively discriminate between different types of ubiquitin chains[78]. A specialized type of proteins with UBDs are the deubiquitinating enzymes (DUBs). These enzymes can remove ubiquitin moieties from protein substrates making ubiquitination a reversible PTM. In addition to general DUBs that can disassemble ubiquitin chains non-specifically, specialized DUBs exist which can be substrate-specific or chain-linkage-specific.

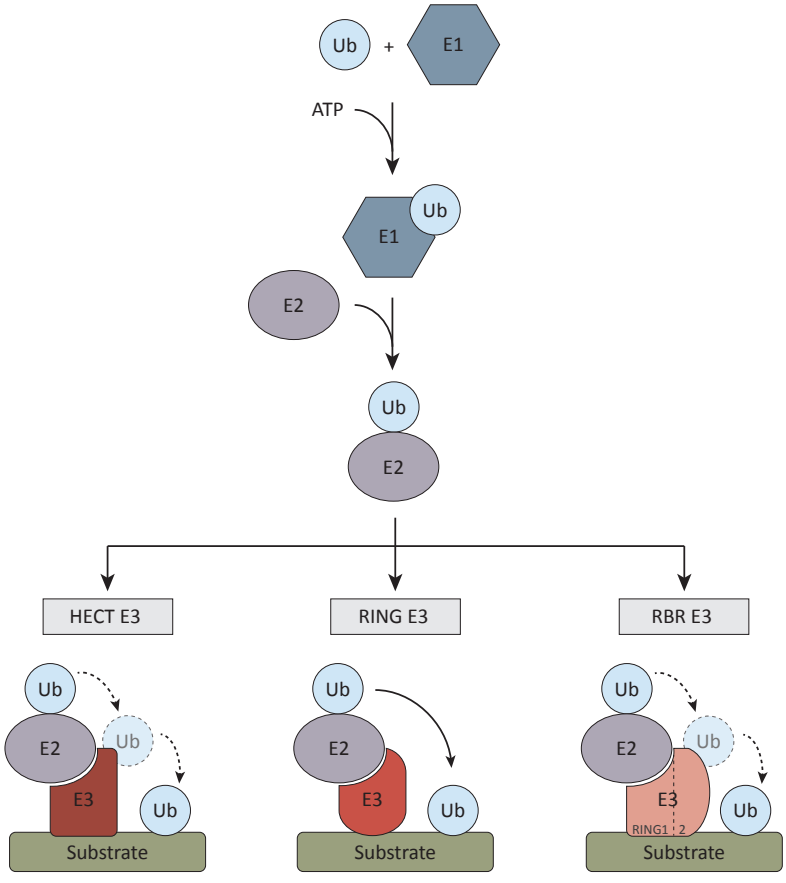

Figure 3: Ubiquitination
Ubiquitin (Ub) can be covalently attached to lysine residues in a protein, in a three-step enzymatic cascade. A Ub activating (E1) enzyme uses an ATP molecule to form a thioester bond between the c-terminus of ubiquitin and an internal cysteine residue of the E1. Subsequently, the activated ubiquitin is transferred to the active-site cysteine of a Ub conjugating (E2) enzyme. Finally, a Ub ligating (E3) enzyme then catalyses the formation of an isopeptide bond between the c-terminal glycine residue of ubiquitin to a lysine of the substrate protein. Three types of E3s are known: HECT, RING and RING-between-RING (RBR). In RING-E3-mediated ligation, Ub is transferred directly from the E2 to the substrate. In HECT-E3-mediated and RBR-E3-mediated ligation, Ub is transferred from the E2 to the E3 and then to the substrate.

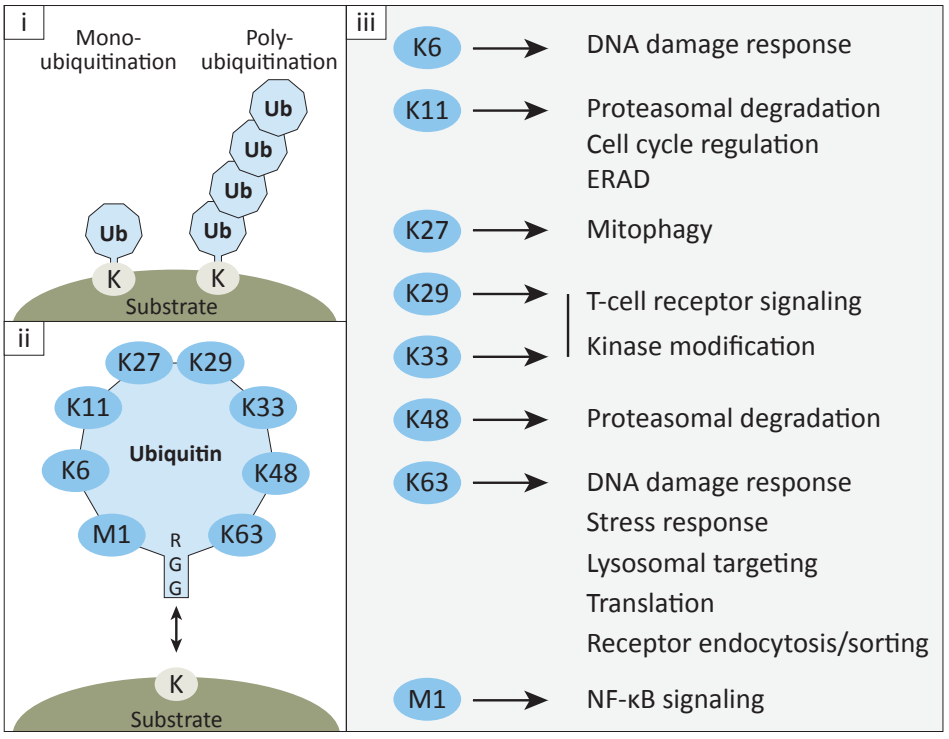

Figure 4: Topologies of ubiquitination
(i) Protein substrates can be modified by one ubiquitin (mono-ubiquitination) or a ubiquitin chain (poly-ubiquitination). (ii) Ubiquitin is coupled to a substrate by its c-terminal glycine (G) residue. Distinct ubiquitin chain-linkages can be formed at all seven internal lysine residues of ubiquitin (K6, K11, K27, K29, K33, K48 and K63) and at its N-terminus (M1). (iii) Poly-ubiquitin chains are structurally distinct, which results in diverse regulatory functions depending on the lysine residues they are linked through[74-76,140]. ERAD, endoplasmic-reticulum-associated protein degradation.

Furthermore, DUBs are involved in ubiquitin chain editing; a process in which one chain type is replaced by a chain of another topology[79-82]. Altogether, ubiquitination is a highly dynamic and versatile pathway which, through the concerted action of E3s and DUBs, is capable of strictly regulating almost all biological processes.

In addition to ubiquitin many ubiquitin-like proteins (UBLs) are identified, including NEDD8, small ubiquitin-like modifier 1 (SUMO-1), SUMO-2, SUMO-3, ISG15 and FAT10. These proteins resemble ubiquitin either by sequence homology or structural homology and are conjugated to target proteins via an enzymatic cascade that resembles ubiquitination[83,84].

1.4 REGULATION OF THE UV-DDR BY UBIQUITINATION

In response to UV irradiation many proteins are ubiquitinated or deubiquitinated in order to orchestrate the complex UV-induced DDR at different key steps. For example, repair factors need to assemble into repair complexes at the correct time and location for proper repair

to take place. Additionally, interplay with downstream signalling pathways is needed, for instance for the purpose of chromatin remodelling or activation of cell cycle checkpoints[63,65].

Regulation of GG-NER by ubiquitination

The UV-DDB complex, which recognizes mild helix-distorting lesions, forms an E3 ubiquitin ligase complex together with Cullin-4A (CUL4A) and RBX1 (also known as Roc1)[85]. The ligase activity of this complex is inhibited by the COP9 signalosome (CSN), which binds and de-neddylates the CUL4A subunit. Upon binding of the UV-DDB-E3 complex to DNA damage, CSN dissociates leading to neddylation of CUL4 and a subsequent increased E3 activity. The E3 complex can then poly-ubiquitinate XPC, which increases the affinity of XPC for DNA[28]. Another candidate for this non-proteolytical poly-ubiquitination of XPC is the recently identified SUMO-targeted ubiquitin ligase (STUbL) RNF111. In response to UV XPC is also modified by the ubiquitin-like protein SUMO. The E3 RNF111 specifically binds sumoylated XPC via its SUMO-interacting motif and together with the E2 Ubc13 attaches K63-linked ubiquitin chains to this protein[86]. Depleting cells of either DDB2 (of the UV-DDB complex) or RNF111 leads to opposing effects on XPC accumulation at UV lesions[86], indicative of differential regulatory functions of these ubiquitination events. Additionally, in response to UV irradiation XPC levels have been reported to undergo no change[28], stabilisation [87] and degradation (independent of ubiquitination)[88]. The precise timing and function of these XPC changes remain unclear, however, a strict regulation of XPC is likely an important regulation step of GG-NER. Finally, the UV-DDB-E3 complex also auto-ubiquitinates its own DDB2 subunit, which reduces its affinity for damaged DNA and ultimately leads to its degradation[89]. Recently, DDB2 was shown to undergo UV-induced PARylation as well, which inhibits its ubiquitination and subsequent degradation[90]. The opposing functional outcomes of the two PTMs seem to form a mechanism by which the stability of DDB2 is regulated during GG-NER.

Regulation of TC-NER by ubiquitination

In response to UV, CSB[91-93] and the largest subunit of RNA Pol II (POLR2A)[94-96] are poly-ubiquitinated and proteasomal degraded. POLR2A is ubiquitinated when elongating RNA Pol II is stalled at a lesion[97]. An important function of this ubiquitination could be a fail-safe mechanism; when a lesion cannot be repaired or bypassed RNA Pol II is degraded as a last resort strategy to prevent persistent transcriptional arrest[45]. Recently, also a new ubiquitinated form of RNA Pol II was identified. Interestingly, this ubiquitination does not lead to proteasomal degradation of RNA Pol II[98] and its function is currently still unknown. The E3s mediating these RNA Pol II ubiquitin modifications are still a matter of debate. Reports indicate that either the CSA-E3 complex (a complex similar to the UV-DDB complex and consisting of CSA together with DDB1, CUL4A and RBX1)[91,94], BRCA1-BARD1[95] or Nedd4[96] could be the responsible E3s. Although the exact function of these ubiquitin modifications in mammalian cells is still unclear, in yeast a complex model involving ubiquitin chain editing has been proposed for RNA Pol II regulation in response to UV (Figure 5)[45]. It is suggested that this intricate regulation mechanism of constant ubiquitination and deubiquitination may serve as a timer, to provide sufficient time for DNA repair before RNA Pol II is degraded as a last resort[45,92].

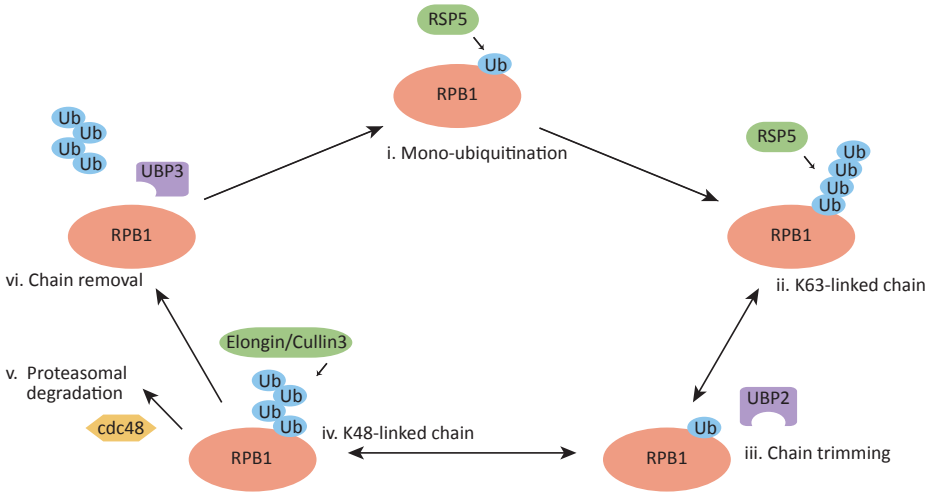

Figure 5: Model for RNA polymerase II (RNA pol II) regulation by ubiquitin chain editing
(i) The E3 RSP5 can mono-ubiquitinate the large subunit of RNA Pol II (RPB1) and (ii) form K63-linked chains. (iii)The DUB UBP2 can trim these ubiquitin chains, but is not able to remove the initial mono-ubiquitin. (iv) K48-linked ubiquitin chains can be formed on the initial ubiquitin by an Elongin/Cullin 3 complex. (v) These K48-linked ubiquitin chains can then promote RNA Pol II degradation after its extraction from chromatin by the VCP/cdc48 segregase. (vi) However, the DUB UBP3 can completely remove ubiquitin chains before a critical ubiquitin chain length is reached, restoring RNA Pol II to its unmodified form. Adapted from Nouspikel[65].

The other ubiquitinated key initiation factor of TC-NER, CSB, was shown to be a target of the CSA-E3 complex[91]. The ubiquitin-dependent degradation of CSB might function to remove CSB from the repair site in order to resume transcription after completing repair. In line with this, CSN (the negative regulator of the CSA-E3 complex) does not immediately dissociate from the CSA-E3 complex in response to UV[85], as is the case with the UV-DDB-E3 complex. Another candidate for ubiquitinating CSB in response to UV is BRCA1-BARD1, which might exist alongside the CSA-dependent pathway[93]. In addition to being ubiquitinated CSB also contains a UBD in its c-terminus which is essential for TC-NER. Mutation or deletion of this domain results in the same cellular phenotype as absence of CSB, even though TC-NER complex formation was unperturbed[99]. This indicates that ubiquitin binding is essential for CSB function and a functional TC-NER complex. The ubiquitinated target protein to which CSB binds is currently still unknown.

UV-induced ubiquitination of histones

In chromatin, the DNA is typically wrapped around an octamer of core histones (two copies each of histones H2A, H2B, H3 and H4) and these nucleosomes are further condensed by additional proteins (e.g. linker histone H1)[100]. This compact structure of chromatin limits the ability of other proteins to interact with DNA. To allow efficient damage detection and repair, the chromatin structure needs to be made more accessible[9,10,101]. Remodelling

of chromatin can be achieved by post-translational modification of histones, such as acetylation, methylation, phosphorylation and ubiquitination[102]. In response to UV-irradiation H2A, H2B, H3 and H4 have been shown to be mono-ubiquitinated[103-108], which weakens the interaction between histones and DNA facilitating histone eviction from nucleosomes[106,109]. The UV-DDB-E3 complex has been implicated in the mono-ubiquitination of H2A, H3 and H4 in response to UV, linking the DNA repair process with chromatin remodelling. Another report showed that RNF8 (E3) together with Ubc13 (E2) is responsible for the UV-induced H2A mono-ubiquitination[108]. Furthermore, the H2A mono-ubiquitination was shown to be dependent on functional NER and the DNA damage signalling kinase ATR[107,108]. Since the downstream DDR factors 53BP1 and BRCA1 are recruited to UV-damaged DNA in non-cycling cells, it was proposed that the mono-ubiquitination of H2A might serve as a recruitment signal for additional auxiliary DDR factors[108].

1.5 MS-BASED METHODS TO STUDY UBIQUITINATION

The involvement of protein ubiquitination in regulating NER, other DNA repair pathways and the DNA damage response (DDR) has extensively been shown[58,110-112]. However, it is expected that, next to the discussed ubiquitination events in section 1.4, many more proteins are involved within these processes and that ubiquitination plays an important role in their function and regulation. Antibody-based techniques, such as immunoblotting, are often used to study PTMs like ubiquitination. However, to identify new ubiquitin modifications and proteins not previously known to be involved in specific processes on a proteome-wide scale, mass spectrometry (MS) is the method of choice[113]. Moreover, various quantitative MS strategies – such as stable isotope labelling by amino acids in cell culture (SILAC) and isobaric tags for relative and absolute quantitation (iTRAQ) – are available for detecting and quantifying the effects of a specific stimulus in a proteome-wide fashion[114]. Additionally, since presumably not all proteins are ubiquitinated and as from those that are ubiquitinated only a fraction is usually modified at a given time, methods to enrich for these modified proteins will greatly enhance the detection of these PTMs by MS[115-117].

Isolation of ubiquitinated proteins using epitope-tagged ubiquitin

Initially, strategies for the isolation of ubiquitinated proteins were primarily based on the ectopic over-expression of tagged ubiquitin (Ub)[118-126]. Tagged-Ub was originally applied using a yeast strain expressing His-tagged Ub, identifying 1075 potential ubiquitinated proteins[118]. Since then different epitope tags, such as FLAG-, HA-, Myc-, V5 and biotin-tags, have been used for protein isolation from different cell lines and species. Moreover, tandem-tagged Ub was implemented to decrease non-specific protein enrichment using two-step purification protocols[121-125]. A major advantage of the epitope-tagged Ub approach is that proteins can be purified under denaturing conditions, thereby eliminating DUB and 26S proteasome activity. Additionally, since the ubiquitin modification is covalently attached to its substrate stringent washing conditions can be applied. Such conditions disrupt all protein-protein interactions thereby decreasing the isolation of non-ubiquitinated factors bound to ubiquitinated proteins and the isolation of the notorious high level of non-specific

proteins binding to isolation-matrixes. However, it cannot be excluded that exogenous over-expression of tagged Ub may lead to biased incorporation into mono-ubiquitination, certain ubiquitin chain-linkages or substrates. Furthermore, tagged Ub may also interfere with e.g. the stability, activity and localization of ubiquitinated proteins. Additionally, tagged Ub is not easily introduced in tissues and cell types that are difficult to transfect, such as primary and quiescent cells, limiting its applicability.

Isolation of endogenously ubiquitinated proteins

To overcome some of the limitations of the epitope-tagged Ub approach ubiquitin-binding domains (UBDs) and anti-ubiquitin antibodies are used for the isolation of endogenously ubiquitinated proteins.

In eukaryotic cells over 20 families of UBDs have been identified, which can recognize and bind ubiquitin modifications[77,78]. However, their natural affinity for ubiquitinated proteins is generally not sufficient for large-scale purification[127]. Therefore, recombinant UBDs were engineered fusing multiple UBDs to increase their affinity for ubiquitin[128,129]. For example, Tandem ubiquitin binding entities (TUBEs) were used under non-denaturing conditions and identified 643 proteins in MCF7 cells[128]. An added advantage of these TUBEs is that, through binding, they are able to protect ubiquitinated proteins from DUBs and proteasomal degradation. A feature of UBDs to take into account is that, given their variety, they are likely to have a preference for specific subsets of substrates. Because of this, the UBD approach might be less well suited for general isolation of all types of ubiquitinated proteins. However, this bias in binding specificity for certain substrates might be exploited for isolation of ubiquitinated proteins with a specific chain-linkage.

Next to UBDs, endogenously ubiquitinated proteins can also be isolated using high-affinity antibodies against ubiquitin. A well-known and widely used example is the monoclonal antibody FK2[130], which recognizes both mono-ubiquitinated and poly-ubiquitinated proteins and can be used for isolating ubiquitinated proteins[131-134]. However, also for antibodies against ubiquitin it is difficult to assess whether they have equal affinity for different protein substrates and for the different ubiquitin chain-linkages.

Enrichment of ubiquitinated peptides

Approaches for the isolation of ubiquitinated proteins are effective for the identification of candidate ubiquitinated substrates. However, for further functional studies, identification of the actual ubiquitinated site on the protein is very useful and can be achieved using specific characteristics of peptides derived from ubiquitinated proteins.

Generally, the protease trypsin is used for protein digestion in MS-based protein identification. It cleaves proteins at the carboxyl side of lysine and arginine, except when either is followed by a proline residue. Proteolytic digestion of ubiquitinated proteins with trypsin generates a specific di-glycine (GG) remnant on the ε amino group of the ubiquitinated lysine. Furthermore, these GG-modified lysine residues are not accessible to trypsin, leading to miscleavage in the peptide. Together, this results in a distinct monoisotopic mass shift of +114 Da in a ubiquitinated peptide that can be used to precisely identify and localize the site of ubiquitination in the peptide[118].

In digested protein mixtures the presence of ubiquitinated peptides is often masked by large amounts of non-ubiquitinated peptides from the same protein or from other, non-ubiquitinated proteins. Recently, methods to specifically isolate ubiquitinated peptides on a large scale have been successfully applied[135-139]. Using a GG-remnant antibody identification of up till ~19.000 endogenous ubiquitinated sites was reported[136,137]. However, an important notion to keep in mind for the ubiquitin remnant immunoaffinity profiling is that two Ub-like modifications – ISG15 and NEDD8 – result in the same GG-remnant as ubiquitin after cleavage with trypsin. Although the prevalence of these Ub-like modifications is estimated to be less than 6%[136], a pre-enrichment for ubiquitinated proteins might be beneficial to ensure identification of ubiquitinated peptides.

REFERENCES

1. De Bont, R. & van Larebeke, N. Endogenous DNA damage in humans: a review of quantitative data. *Mutagenesis* **19**, 169-85 (2004).
2. Hoeijmakers, J.H. DNA damage, aging, and cancer. *N Engl J Med* **361**, 1475-85 (2009).
3. Jackson, S.P. & Bartek, J. The DNA-damage response in human biology and disease. *Nature* **461**, 1071-8 (2009).
4. Ciccia, A. & Elledge, S.J. The DNA damage response: making it safe to play with knives. *Mol Cell* **40**, 179-204 (2010).
5. Shiloh, Y. ATM and related protein kinases: safeguarding genome integrity. *Nat Rev Cancer* **3**, 155-68 (2003).
6. Cimprich, K.A. & Cortez, D. ATR: an essential regulator of genome integrity. *Nat Rev Mol Cell Biol* **9**, 616-27 (2008).
7. Bartek, J. & Lukas, J. DNA damage checkpoints: from initiation to recovery or adaptation. *Curr Opin Cell Biol* **19**, 238-45 (2007).
8. Warmerdam, D.O. & Kanaar, R. Dealing with DNA damage: relationships between checkpoint and repair pathways. *Mutat Res* **704**, 2-11 (2010).
9. Lans, H., Marteijn, J.A. & Vermeulen, W. ATP-dependent chromatin remodeling in the DNA-damage response. *Epigenetics Chromatin* **5**, 4 (2012).
10. Luijsterburg, M.S. & van Attikum, H. Chromatin and the DNA damage response: the cancer connection. *Mol Oncol* **5**, 349-67 (2011).
11. Hoeijmakers, J.H. Genome maintenance mechanisms for preventing cancer. *Nature* **411**, 366-74 (2001).
12. van Gent, D.C., Hoeijmakers, J.H. & Kanaar, R. Chromosomal stability and the DNA double-stranded break connection. *Nat Rev Genet* **2**, 196-206 (2001).
13. Lieber, M.R. The mechanism of double-strand DNA break repair by the nonhomologous DNA end-joining pathway. *Annu Rev Biochem* **79**, 181-211 (2010).
14. Saleh-Gohari, N. & Helleday, T. Conservative homologous recombination preferentially repairs DNA double-strand breaks in the S phase of the cell cycle in human cells. *Nucleic Acids Res* **32**, 3683-8 (2004).
15. Deans, A.J. & West, S.C. DNA interstrand crosslink repair and cancer. *Nat Rev Cancer* **11**, 467-80 (2011).
16. Raschle, M. *et al.* Mechanism of replication-coupled DNA interstrand crosslink repair. *Cell* **134**, 969-80 (2008).
17. Jiricny, J. The multifaceted mismatch-repair system. *Nat Rev Mol Cell Biol* **7**, 335-46 (2006).
18. Hegde, M.L., Hazra, T.K. & Mitra, S. Early steps in the DNA base excision/single-strand interruption repair pathway in mammalian cells. *Cell Res* **18**, 27-47 (2008).
19. Gillet, L.C. & Scharer, O.D. Molecular mechanisms of mammalian global genome nucleotide excision repair. *Chem Rev* **106**, 253-76 (2006).
20. Vermeulen, W. Dynamics of mammalian NER proteins. *DNA Repair (Amst)* **10**, 760-71 (2011).
21. Cadet, J., Sage, E. & Douki, T. Ultraviolet radiation-mediated damage to cellular DNA. *Mutat Res* **571**, 3-17 (2005).
22. Ravanat, J.L., Douki, T. & Cadet, J. Direct and indirect effects of UV radiation on DNA and its components. *J Photochem Photobiol B* **63**, 88-102 (2001).
23. de Laat, W.L., Jaspers, N.G. & Hoeijmakers, J.H. Molecular mechanism of nucleotide excision repair. *Genes Dev* **13**, 768-85 (1999).
24. Hanawalt, P.C. & Spivak, G. Transcription-coupled DNA repair: two decades of progress and surprises. *Nat Rev Mol Cell Biol* **9**, 958-70 (2008).
25. Araki, M. *et al.* Centrosome protein centrin 2/caltractin 1 is part of the xeroderma pigmentosum group C complex that initiates global genome nucleotide excision repair. *J Biol Chem* **276**, 18665-72 (2001).
26. Maillard, O., Solyom, S. & Naegeli, H. An aromatic sensor with aversion to damaged strands confers versatility to DNA repair. *PLoS Biol* **5**, e79 (2007).
27. Scrima, A. *et al.* Structural basis of UV DNA-damage recognition by the DDB1-DDB2 complex. *Cell* **135**, 1213-23 (2008).
28. Sugasawa, K. *et al.* UV-induced ubiquitylation of XPC protein mediated by UV-DDB-ubiquitin ligase complex. *Cell* **121**, 387-400 (2005).
29. Fousteri, M., Vermeulen, W., van Zeeland, A.A. & Mullenders, L.H. Cockayne syndrome

A and B proteins differentially regulate recruitment of chromatin remodeling and repair factors to stalled RNA polymerase II in vivo. *Mol Cell* **23**, 471-82 (2006).

30. Troelstra, C. *et al.* Molecular cloning of the human DNA excision repair gene ERCC-6. *Mol Cell Biol* **10**, 5806-13 (1990).
31. Citterio, E. *et al.* ATP-dependent chromatin remodeling by the Cockayne syndrome B DNA repair-transcription-coupling factor. *Mol Cell Biol* **20**, 7643-53 (2000).
32. Newman, J.C., Bailey, A.D. & Weiner, A.M. Cockayne syndrome group B protein (CSB) plays a general role in chromatin maintenance and remodeling. *Proc Natl Acad Sci U S A* **103**, 9613-8 (2006).
33. Frontini, M. & Proietti-De-Santis, L. Cockayne syndrome B protein (CSB): linking p53, HIF-1 and p300 to robustness, lifespan, cancer and cell fate decisions. *Cell Cycle* **8**, 693-6 (2009).
34. Balajee, A.S., May, A., Dianov, G.L., Friedberg, E.C. & Bohr, V.A. Reduced RNA polymerase II transcription in intact and permeabilized Cockayne syndrome group B cells. *Proc Natl Acad Sci U S A* **94**, 4306-11 (1997).
35. Dianov, G.L., Houle, J.F., Iyer, N., Bohr, V.A. & Friedberg, E.C. Reduced RNA polymerase II transcription in extracts of cockayne syndrome and xeroderma pigmentosum/Cockayne syndrome cells. *Nucleic Acids Res* **25**, 3636-42 (1997).
36. Selby, C.P. & Sancar, A. Human transcription-repair coupling factor CSB/ERCC6 is a DNA-stimulated ATPase but is not a helicase and does not disrupt the ternary transcription complex of stalled RNA polymerase II. *J Biol Chem* **272**, 1885-90 (1997).
37. Tantin, D., Kansal, A. & Carey, M. Recruitment of the putative transcription-repair coupling factor CSB/ERCC6 to RNA polymerase II elongation complexes. *Mol Cell Biol* **17**, 6803-14 (1997).
38. van Gool, A.J. *et al.* The Cockayne syndrome B protein, involved in transcription-coupled DNA repair, resides in an RNA polymerase II-containing complex. *EMBO J* **16**, 5955-65 (1997).
39. van den Boom, V. *et al.* DNA damage stabilizes interaction of CSB with the transcription elongation machinery. *J Cell Biol* **166**, 27-36 (2004).
40. Donahue, B.A., Yin, S., Taylor, J.S., Reines, D. & Hanawalt, P.C. Transcript cleavage by RNA polymerase II arrested by a cyclobutane pyrimidine dimer in the DNA template. *Proc Natl Acad Sci U S A* **91**, 8502-6 (1994).
41. Tornaletti, S., Maeda, L.S., Lloyd, D.R., Reines, D. & Hanawalt, P.C. Effect of thymine glycol on transcription elongation by T7 RNA polymerase and mammalian RNA polymerase II. *J Biol Chem* **276**, 45367-71 (2001).
42. Brueckner, F., Hennecke, U., Carell, T. & Cramer, P. CPD damage recognition by transcribing RNA polymerase II. *Science* **315**, 859-62 (2007).
43. Fousteri, M. & Mullenders, L.H. Transcription-coupled nucleotide excision repair in mammalian cells: molecular mechanisms and biological effects. *Cell Res* **18**, 73-84 (2008).
44. Nudler, E. RNA polymerase backtracking in gene regulation and genome instability. *Cell* **149**, 1438-45 (2012).
45. Wilson, M.D., Harreman, M. & Svejstrup, J.Q. Ubiquitylation and degradation of elongating RNA polymerase II: the last resort. *Biochim Biophys Acta* **1829**, 151-7 (2013).
46. Giglia-Mari, G. *et al.* A new, tenth subunit of TFIIH is responsible for the DNA repair syndrome trichothiodystrophy group A. *Nat Genet* **36**, 714-9 (2004).
47. Ranish, J.A. *et al.* Identification of TFB5, a new component of general transcription and DNA repair factor IIH. *Nat Genet* **36**, 707-13 (2004).
48. Sugasawa, K. *et al.* Xeroderma pigmentosum group C protein complex is the initiator of global genome nucleotide excision repair. *Mol Cell* **2**, 223-32 (1998).
49. Buschta-Hedayat, N., Buterin, T., Hess, M.T., Missura, M. & Naegeli, H. Recognition of nonhybridizing base pairs during nucleotide excision repair of DNA. *Proc Natl Acad Sci U S A* **96**, 6090-5 (1999).
50. Ogi, T. *et al.* Three DNA polymerases, recruited by different mechanisms, carry out NER repair synthesis in human cells. *Mol Cell* **37**, 714-27 (2010).
51. Moser, J. *et al.* Sealing of chromosomal DNA nicks during nucleotide excision repair requires XRCC1 and DNA ligase III alpha in a cell-cycle-specific manner. *Mol Cell* **27**, 311-23 (2007).
52. Diderich, K., Alanazi, M. & Hoeijmakers, J.H. Premature aging and cancer in nucleotide excision repair-disorders. *DNA Repair (Amst)* **10**, 772-80 (2011).

53. DiGiovanna, J.J. & Kraemer, K.H. Shining a light on xeroderma pigmentosum. *J Invest Dermatol* **132**, 785-96 (2012).
54. Nance, M.A. & Berry, S.A. Cockayne syndrome: review of 140 cases. *Am J Med Genet* **42**, 68-84 (1992).
55. Pines, A. *et al.* Enhanced global genome nucleotide excision repair reduces UV carcinogenesis and nullifies strand bias in p53 mutations in Csb-/- mice. *J Invest Dermatol* **130**, 1746-9 (2010).
56. Spivak, G. UV-sensitive syndrome. *Mutat Res* **577**, 162-9 (2005).
57. Bensimon, A., Aebersold, R. & Shiloh, Y. Beyond ATM: the protein kinase landscape of the DNA damage response. *FEBS Lett* **585**, 1625-39 (2011).
58. Jackson, S.P. & Durocher, D. Regulation of DNA damage responses by ubiquitin and SUMO. *Mol Cell* **49**, 795-807 (2013).
59. Gong, F. & Miller, K.M. Mammalian DNA repair: HATs and HDACs make their mark through histone acetylation. *Mutat Res* **750**, 23-30 (2013).
60. Bennetzen, M.V. *et al.* Acetylation dynamics of human nuclear proteins during the ionizing radiation-induced DNA damage response. *Cell Cycle* **12**, 1688-95 (2013).
61. Sousa, F.G. *et al.* PARPs and the DNA damage response. *Carcinogenesis* **33**, 1433-40 (2012).
62. Pines, A., Mullenders, L.H., van Attikum, H. & Luijsterburg, M.S. Touching base with PARPs: moonlighting in the repair of UV lesions and double-strand breaks. *Trends Biochem Sci* **38**, 321-30 (2013).
63. Bergink, S., Jaspers, N.G. & Vermeulen, W. Regulation of UV-induced DNA damage response by ubiquitylation. *DNA Repair (Amst)* **6**, 1231-42 (2007).
64. Reed, S.H. & Gillette, T.G. Nucleotide excision repair and the ubiquitin proteasome pathway--do all roads lead to Rome? *DNA Repair (Amst)* **6**, 149-56 (2007).
65. Nouspikel, T. Multiple roles of ubiquitination in the control of nucleotide excision repair. *Mech Ageing Dev* **132**, 355-65 (2011).
66. Ciechanover, A. The ubiquitin-proteasome proteolytic pathway. *Cell* **79**, 13-21 (1994).
67. Ciechanover, A. & Ben-Saadon, R. N-terminal ubiquitination: more protein substrates join in. *Trends Cell Biol* **14**, 103-6 (2004).
68. Hershko, A. & Ciechanover, A. The ubiquitin system. *Annu Rev Biochem* **67**, 425-79 (1998).
69. van Wijk, S.J. & Timmers, H.T. The family of ubiquitin-conjugating enzymes (E2s): deciding between life and death of proteins. *FASEB J* **24**, 981-93 (2010).
70. Li, W. *et al.* Genome-wide and functional annotation of human E3 ubiquitin ligases identifies MULAN, a mitochondrial E3 that regulates the organelle's dynamics and signaling. *PLoS One* **3**, e1487 (2008).
71. Scheffner, M. & Kumar, S. Mammalian HECT ubiquitin-protein ligases: Biological and pathophysiological aspects. *Biochim Biophys Acta* (2013).
72. Deshaies, R.J. & Joazeiro, C.A. RING domain E3 ubiquitin ligases. *Annu Rev Biochem* **78**, 399-434 (2009).
73. Wenzel, D.M. & Klevit, R.E. Following Ariadne's thread: a new perspective on RBR ubiquitin ligases. *BMC Biol* **10**, 24 (2012).
74. Komander, D. & Rape, M. The ubiquitin code. *Annu Rev Biochem* **81**, 203-29 (2012).
75. Kulathu, Y. & Komander, D. Atypical ubiquitylation - the unexplored world of polyubiquitin beyond Lys48 and Lys63 linkages. *Nat Rev Mol Cell Biol* **13**, 508-23 (2012).
76. Husnjak, K. & Dikic, I. Ubiquitin-binding proteins: decoders of ubiquitin-mediated cellular functions. *Annu Rev Biochem* **81**, 291-322 (2012).
77. Dikic, I., Wakatsuki, S. & Walters, K.J. Ubiquitin-binding domains - from structures to functions. *Nat Rev Mol Cell Biol* **10**, 659-71 (2009).
78. Winget, J.M. & Mayor, T. The diversity of ubiquitin recognition: hot spots and varied specificity. *Mol Cell* **38**, 627-35 (2010).
79. Clague, M.J., Coulson, J.M. & Urbe, S. Cellular functions of the DUBs. *J Cell Sci* **125**, 277-86 (2012).
80. Nijman, S.M. *et al.* A genomic and functional inventory of deubiquitinating enzymes. *Cell* **123**, 773-86 (2005).
81. Komander, D., Clague, M.J. & Urbe, S. Breaking the chains: structure and function of the deubiquitinases. *Nat Rev Mol Cell Biol* **10**, 550-63 (2009).
82. Love, K.R., Catic, A., Schlieker, C. & Ploegh, H.L. Mechanisms, biology and inhibitors of

deubiquitinating enzymes. *Nat Chem Biol* **3**, 697-705 (2007).

83. van der Veen, A.G. & Ploegh, H.L. Ubiquitin-like proteins. *Annu Rev Biochem* **81**, 323-57 (2012).
84. Hochstrasser, M. Origin and function of ubiquitin-like proteins. *Nature* **458**, 422-9 (2009).
85. Groisman, R. *et al.* The ubiquitin ligase activity in the DDB2 and CSA complexes is differentially regulated by the COP9 signalosome in response to DNA damage. *Cell* **113**, 357-67 (2003).
86. Poulsen, S.L. *et al.* RNF111/Arkadia is a SUMO-targeted ubiquitin ligase that facilitates the DNA damage response. *J Cell Biol* **201**, 797-807 (2013).
87. Ng, J.M. *et al.* A novel regulation mechanism of DNA repair by damage-induced and RAD23-dependent stabilization of xeroderma pigmentosum group C protein. *Genes Dev* **17**, 1630-45 (2003).
88. Wang, Q.E. *et al.* Ubiquitylation-independent degradation of Xeroderma pigmentosum group C protein is required for efficient nucleotide excision repair. *Nucleic Acids Res* **35**, 5338-50 (2007).
89. Rapic-Otrin, V., McLenigan, M.P., Bisi, D.C., Gonzalez, M. & Levine, A.S. Sequential binding of UV DNA damage binding factor and degradation of the p48 subunit as early events after UV irradiation. *Nucleic Acids Res* **30**, 2588-98 (2002).
90. Pines, A. *et al.* PARP1 promotes nucleotide excision repair through DDB2 stabilization and recruitment of ALC1. *J Cell Biol* **199**, 235-49 (2012).
91. Groisman, R. *et al.* CSA-dependent degradation of CSB by the ubiquitin-proteasome pathway establishes a link between complementation factors of the Cockayne syndrome. *Genes Dev* **20**, 1429-34 (2006).
92. Schwertman, P., Vermeulen, W. & Marteijn, J.A. UVSSA and USP7, a new couple in transcription-coupled DNA repair. *Chromosoma* **122**, 275-84 (2013).
93. Wei, L. *et al.* BRCA1 contributes to transcription-coupled repair of DNA damage through polyubiquitination and degradation of Cockayne syndrome B protein. *Cancer Sci* **102**, 1840-7 (2011).
94. Bregman, D.B. *et al.* UV-induced ubiquitination of RNA polymerase II: a novel modification deficient in Cockayne syndrome cells. *Proc Natl Acad Sci U S A* **93**, 11586-90 (1996).
95. Starita, L.M. *et al.* BRCA1/BARD1 ubiquitinate phosphorylated RNA polymerase II. *J Biol Chem* **280**, 24498-505 (2005).
96. Anindya, R., Aygun, O. & Svejstrup, J.Q. Damage-induced ubiquitylation of human RNA polymerase II by the ubiquitin ligase Nedd4, but not Cockayne syndrome proteins or BRCA1. *Mol Cell* **28**, 386-97 (2007).
97. Somesh, B.P. *et al.* Multiple mechanisms confining RNA polymerase II ubiquitylation to polymerases undergoing transcriptional arrest. *Cell* **121**, 913-23 (2005).
98. Nakazawa, Y. *et al.* Mutations in UVSSA cause UV-sensitive syndrome and impair RNA polymerase IIo processing in transcription-coupled nucleotide-excision repair. *Nat Genet* **44**, 586-92 (2012).
99. Anindya, R. *et al.* A ubiquitin-binding domain in Cockayne syndrome B required for transcription-coupled nucleotide excision repair. *Mol Cell* **38**, 637-48 (2010).
100. Luger, K., Mader, A.W., Richmond, R.K., Sargent, D.F. & Richmond, T.J. Crystal structure of the nucleosome core particle at 2.8 A resolution. *Nature* **389**, 251-60 (1997).
101. Gong, F., Kwon, Y. & Smerdon, M.J. Nucleotide excision repair in chromatin and the right of entry. *DNA Repair (Amst)* **4**, 884-96 (2005).
102. Kouzarides, T. Chromatin modifications and their function. *Cell* **128**, 693-705 (2007).
103. Guerrero-Santoro, J. *et al.* The cullin 4B-based UV-damaged DNA-binding protein ligase binds to UV-damaged chromatin and ubiquitinates histone H2A. *Cancer Res* **68**, 5014-22 (2008).
104. Kapetanaki, M.G. *et al.* The DDB1-CUL4ADDB2 ubiquitin ligase is deficient in xeroderma pigmentosum group E and targets histone H2A at UV-damaged DNA sites. *Proc Natl Acad Sci U S A* **103**, 2588-93 (2006).
105. Giannattasio, M., Lazzaro, F., Plevani, P. & Muzi-Falconi, M. The DNA damage checkpoint response requires histone H2B ubiquitination by Rad6-Bre1 and H3 methylation by Dot1. *J Biol Chem* **280**, 9879-86 (2005).

106. Wang, H. *et al.* Histone H3 and H4 ubiquitylation by the CUL4-DDB-ROC1 ubiquitin ligase facilitates cellular response to DNA damage. *Mol Cell* **22**, 383-94 (2006).
107. Bergink, S. *et al.* DNA damage triggers nucleotide excision repair-dependent monoubiquitylation of histone H2A. *Genes Dev* **20**, 1343-52 (2006).
108. Marteijn, J.A. *et al.* Nucleotide excision repair-induced H2A ubiquitination is dependent on MDC1 and RNF8 and reveals a universal DNA damage response. *J Cell Biol* **186**, 835-47 (2009).
109. Luijsterburg, M.S. *et al.* DDB2 promotes chromatin decondensation at UV-induced DNA damage. *J Cell Biol* **197**, 267-81 (2012).
110. Bergink, S. & Jentsch, S. Principles of ubiquitin and SUMO modifications in DNA repair. *Nature* **458**, 461-7 (2009).
111. Ulrich, H.D. & Walden, H. Ubiquitin signalling in DNA replication and repair. *Nat Rev Mol Cell Biol* **11**, 479-89 (2010).
112. Al-Hakim, A. *et al.* The ubiquitous role of ubiquitin in the DNA damage response. *DNA Repair (Amst)* **9**, 1229-40 (2010).
113. Choudhary, C. & Mann, M. Decoding signalling networks by mass spectrometry-based proteomics. *Nat Rev Mol Cell Biol* **11**, 427-39 (2010).
114. Nikolov, M., Schmidt, C. & Urlaub, H. Quantitative mass spectrometry-based proteomics: an overview. *Methods Mol Biol* **893**, 85-100 (2012).
115. Low, T.Y., Magliozzi, R., Guardavaccaro, D. & Heck, A.J. Unraveling the ubiquitin-regulated signaling networks by mass spectrometry-based proteomics. *Proteomics* **13**, 526-37 (2013).
116. Shi, Y., Xu, P. & Qin, J. Ubiquitinated proteome: ready for global? *Mol Cell Proteomics* **10**, R110 006882 (2011).
117. Vertegaal, A.C. Uncovering ubiquitin and ubiquitin-like signaling networks. *Chem Rev* **111**, 7923-40 (2011).
118. Peng, J. *et al.* A proteomics approach to understanding protein ubiquitination. *Nat Biotechnol* **21**, 921-6 (2003).
119. Gururaja, T., Li, W., Noble, W.S., Payan, D.G. & Anderson, D.C. Multiple functional categories of proteins identified in an in vitro cellular ubiquitin affinity extract using shotgun peptide sequencing. *J Proteome Res* **2**, 394-404 (2003).
120. Kirkpatrick, D.S., Weldon, S.F., Tsaprailis, G., Liebler, D.C. & Gandolfi, A.J. Proteomic identification of ubiquitinated proteins from human cells expressing His-tagged ubiquitin. *Proteomics* **5**, 2104-11 (2005).
121. Hitchcock, A.L., Auld, K., Gygi, S.P. & Silver, P.A. A subset of membrane-associated proteins is ubiquitinated in response to mutations in the endoplasmic reticulum degradation machinery. *Proc Natl Acad Sci U S A* **100**, 12735-40 (2003).
122. Tagwerker, C. *et al.* A tandem affinity tag for two-step purification under fully denaturing conditions: application in ubiquitin profiling and protein complex identification combined with in vivocross-linking. *Mol Cell Proteomics* **5**, 737-48 (2006).
123. Jeon, H.B. *et al.* A proteomics approach to identify the ubiquitinated proteins in mouse heart. *Biochem Biophys Res Commun* **357**, 731-6 (2007).
124. Meierhofer, D., Wang, X., Huang, L. & Kaiser, P. Quantitative analysis of global ubiquitination in HeLa cells by mass spectrometry. *J Proteome Res* **7**, 4566-76 (2008).
125. Danielsen, J.M. *et al.* Mass spectrometric analysis of lysine ubiquitylation reveals promiscuity at site level. *Mol Cell Proteomics* **10**, M110 003590 (2011).
126. Franco, M., Seyfried, N.T., Brand, A.H., Peng, J. & Mayor, U. A novel strategy to isolate ubiquitin conjugates reveals wide role for ubiquitination during neural development. *Mol Cell Proteomics* **10**, M110 002188 (2011).
127. Hicke, L., Schubert, H.L. & Hill, C.P. Ubiquitin-binding domains. *Nat Rev Mol Cell Biol* **6**, 610-21 (2005).
128. Lopitz-Otsoa, F. *et al.* Integrative analysis of the ubiquitin proteome isolated using Tandem Ubiquitin Binding Entities (TUBEs). *J Proteomics* **75**, 2998-3014 (2012).
129. Shi, Y. *et al.* A data set of human endogenous protein ubiquitination sites. *Mol Cell Proteomics* **10**, M110 002089 (2011).
130. Fujimuro, M., Sawada, H. & Yokosawa, H. Production and characterization of monoclonal antibodies specific to multi-ubiquitin chains of polyubiquitinated proteins. *FEBS Lett* **349**, 173-80 (1994).
131. Vasilescu, J., Smith, J.C., Ethier, M. & Figeys, D. Proteomic analysis of ubiquitinated proteins from human MCF-7 breast cancer cells by immunoaffinity purification and

mass spectrometry. *J Proteome Res* **4**, 2192-200 (2005).

132. Matsumoto, M. *et al.* Large-scale analysis of the human ubiquitin-related proteome. *Proteomics* **5**, 4145-51 (2005).
133. Igawa, T. *et al.* Isolation and identification of ubiquitin-related proteins from Arabidopsis seedlings. *J Exp Bot* **60**, 3067-73 (2009).
134. Argenzio, E. *et al.* Proteomic snapshot of the EGF-induced ubiquitin network. *Mol Syst Biol* **7**, 462 (2011).
135. Xu, G., Paige, J.S. & Jaffrey, S.R. Global analysis of lysine ubiquitination by ubiquitin remnant immunoaffinity profiling. *Nat Biotechnol* **28**, 868-73 (2010).
136. Kim, W. *et al.* Systematic and quantitative assessment of the ubiquitin-modified proteome. *Mol Cell* **44**, 325-40 (2011).
137. Wagner, S.A. *et al.* A proteome-wide, quantitative survey of in vivo ubiquitylation sites reveals widespread regulatory roles. *Mol Cell Proteomics* **10**, M111 013284 (2011).
138. Udeshi, N.D. *et al.* Methods for quantification of in vivo changes in protein ubiquitination following proteasome and deubiquitinase inhibition. *Mol Cell Proteomics* **11**, 148-59 (2012).
139. Povlsen, L.K. *et al.* Systems-wide analysis of ubiquitylation dynamics reveals a key role for PAF15 ubiquitylation in DNA-damage bypass. *Nat Cell Biol* **14**, 1089-98 (2012).
140. Ye, Y. & Rape, M. Building ubiquitin chains: E2 enzymes at work. *Nat Rev Mol Cell Biol* **10**, 755-64 (2009).

2

AN IMMUNOAFFINITY PURIFICATION METHOD FOR THE PROTEOMIC ANALYSIS OF UBIQUITINATED PROTEIN COMPLEXES

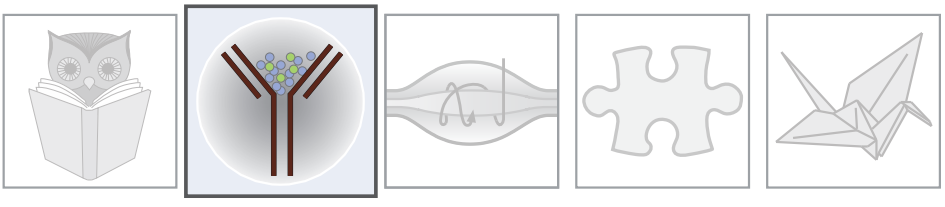

Petra Schwertman[1], Karel Bezstarosti[2], Charlie Laffeber[1], Wim Vermeulen[1], Jeroen A A Demmers[2,*] & Jurgen A Marteijn[1,*]

[1]Department of Genetics and Netherlands Proteomics Centre, Centre for Biomedical Genetics, Erasmus University Medical Centre, 3015 GE Rotterdam, The Netherlands
[2]Proteomics Centre, Erasmus University Medical Centre, 3015 GE Rotterdam, The Netherlands.
* Corresponding authors

Published in Analytical Biochemistry 2013 Sep 15; 440(2):227-36

ABSTRACT

Protein ubiquitination plays an important role in the regulation of many cellular processes, including protein degradation, cell cycle regulation, apoptosis, and DNA repair. To study the ubiquitin proteome we have established an immunoaffinity purification method for the proteomic analysis of endogenously ubiquitinated protein complexes. A strong, specific enrichment of ubiquitinated factors was achieved using the FK2 antibody bound to protein G-beaded agarose, which recognizes mono-ubiquitinated and poly-ubiquitinated conjugates. Mass spectrometric analysis of two FK2 immunoprecipitations (IPs) resulted in the identification of 296 FK2-specific proteins in both experiments. The isolation of ubiquitinated and ubiquitination-related proteins was confirmed by pathway analyses (using Ingenuity Pathways Analysis and Gene Ontology-annotation enrichment). Additionally, comparing the proteins that specifically came down in the FK2 IP with databases of ubiquitinated proteins showed that a high percentage of proteins in our enriched fraction was indeed ubiquitinated. Finally, assessment of protein-protein interactions revealed that significantly more FK2-specific proteins were residing in protein complexes than in random protein sets. This method, which is capable of isolating both endogenously ubiquitinated proteins and their interacting proteins, can be widely used for unraveling ubiquitin-mediated protein regulation in various cell systems and tissues when comparing different cellular states.

INTRODUCTION

The regulation of proteins involves posttranslational modifications (PTMs) – such as phosphorylation and ubiquitination – to control their activity, localization, stability, and assembly into protein complexes. Ubiquitination was shown to play an increasingly important role in many cellular processes, including protein degradation, cell-cycle regulation, apoptosis, and DNA repair[1-4]. The highly conserved 76-amino-acid protein ubiquitin can be covalently attached to a lysine residue in protein substrates via an E1-E2-E3 enzymatic cascade. The E1-activating enzyme uses an ATP molecule to form a high-energy thioester bond between the C-terminus of ubiquitin and an internal cysteine residue. Next, the activated ubiquitin is transferred to a ubiquitin-conjugating enzyme (E2). Finally, an E3 ubiquitin ligase is needed to transfer the ubiquitin to a lysine on the protein substrate[5]. Following addition of a single ubiquitin to a protein substrate (mono-ubiquitination), further ubiquitin molecules can be conjugated to the first, resulting in a ubiquitin chain (poly-ubiquitination). Distinct chain-linkages can be formed at all seven internal lysine residues of ubiquitin (K6, K11, K27, K29, K33, K48 and K63) and at its N-terminus (M1). Next to homotypic ubiquitin chains, which have a single linkage type, heterotypic chains exists containing mixed linkages within the same ubiquitin chain. The most abundant chain-linkage, through K48, is primarily a signal for proteasomal degradation, while linkage through K63 has a well-established role in cell signaling. In comparison, relatively little is known about the other chain-linkage types[6,7]. The ubiquitination process is highly dynamic and reversible, as illustrated by the existence of at least 80 different deubiquitinating enzymes (DUBs), which can remove ubiquitin moieties from protein substrates[8-11].

The ubiquitination status of specific proteins can be studied by immunoblotting. To study the ubiquitin proteome, also known as the ubiquitinome, on a global scale, mass spectrometry (MS)-based proteomics is used. Since presumably not all proteins are ubiquitinated and as from those that are ubiquitinated only a fraction is usually modified at a given time, methods to enrich for these proteins are necessary to study them by MS[12].

Initially, strategies for the isolation of ubiquitinated proteins were primarily based on the ectopic overexpression of tagged ubiquitin combined with a purification protocol incorporating at least one denaturing step in order to remove non-ubiquitinated interactors [13-22]. Despite its proven use, it cannot be excluded that exogenous overexpression of tagged ubiquitin may lead to biased incorporation into mono-ubiquitination or certain ubiquitin chains and/or may interfere with, e.g., the stability, activity, and localization of ubiquitinated proteins. Additionally, tagged ubiquitin is not easily introduced into tissues and cell types that are difficult to transfect, such as primary and quiescent cells, limiting its applicability.

Alternatively, some studies have made use of ubiquitin-binding domains (UBDs) or anti-ubiquitin antibodies to isolate endogenously ubiquitinated proteins[13,23-30] or peptides[31-35], thereby overcoming the above-mentioned limitations.

Proteolytic digestion of ubiquitinated proteins with trypsin generates a specific diglycine (Gly-Gly) remnant on the ε amino group of the ubiquitinated lysine. This remnant causes a distinct mass shift of the peptide mass that can be used to precisely identify and localize the site of ubiquitination in the peptide. The recent development of specific antibodies directed

against diglycine-modified peptides enables the efficient isolation of these peptides and the identification of ubiquitination sites by MS[31-35]. Because of the denaturing step that is necessary before trypsin digestion, the identification of non-ubiquitinated interactors using this approach is minimal.

Most of the methods for endogenously ubiquitinated protein isolation were performed under non-denaturing conditions, which are necessary for efficient binding of the UBDs or antibodies to the ubiquitinated proteins. Although the ubiquitinated protein pool might be exposed to residual DUB and proteasome activity under these conditions, it has the additional advantage to study protein complexes. Most biological processes mainly rely on intact, functional protein complexes[36], whose subunits, however, are not necessarily all modified by ubiquitin. Therefore, to study the biologically relevant protein modules, including the non-ubiquitinated interactors, we started out by comparing three different methods for the isolation of endogenously ubiquitinated protein complexes under non-denaturing conditions. The most efficient approach of the three, a method based on FK2 antibody immunoprecipitation (IP), was further optimized and characterized for proteomic applications.

METHODS

Cell culture

HeLa and XP2OS cells were cultured in Dulbecco's modified Eagle's medium (Invitrogen) supplemented with 10% fetal calf serum, 50 units/ml penicillin and 50 µg/ml streptomycin (Gibco) at 37°C and 5% CO_2 in a humidified cell culture incubator. Cells were grown to 90% confluence in 9 cm dishes for all experiments.

Isolation of endogenously ubiquitinated protein complexes

Cells were washed twice in ice-cold phosphate-buffered saline (PBS) and harvested by scraping in 500 µl lysis buffer. Either RIPA lysis buffer (PBS containing 1% Nonidet P-40, 0.5% sodium-deoxycholate, 0.1% SDS) or tandem ubiquitin-binding entities (TUBEs) lysis buffer (50 mM Tris-HCl, pH 7.5, 0.15 M NaCl, 1 mM EDTA, 1% NP-40, 10% glycerol) was used, both supplemented with 15 µM MG-132 (Enzo Life Sciences), 10 mM N-ethylmaleimide (Sigma), and Complete protease inhibitor cocktail (Roche). Lysates were incubated on ice for 10 min and centrifuged at 16,000g and 4°C for 15 min to remove remaining cell debris and DNA. Cleared lysates were added to the various purification resins: either 100 µl 50% slurry of agarose-TUBEs (LifeSensors), UbiQapture-Q matrix (Enzo Life Sciences), FK2 beads or control beads. The FK2 beads and control beads were prepared by incubating 100 µl 50% protein G-beaded agarose slurry (Pierce) with 87.5 µg of respectively FK2 antibody (Enzo Life Sciences) or random mouse IgG (Millipore) for 40 min at room temperature. For crosslinking FK2 to the protein G beads the Pierce Crosslink Immunoprecipitation Kit was used. All resins were washed two times with lysis buffer before use. After incubating with lysates for 4 or 16 h at 4°C, the non-bound fractions were collected and the resins were washed four times with 10 bead volumes of lysis buffer. Bound protein complexes were eluted in 1 bead volume of 2x Laemmli buffer for 5 min at 98°C and loaded onto a 4-20% SDS-PAGE precast gradient gel (Invitrogen).

Three different elution buffers compatible with a concentration-step using centrifugal filters (Amicon Ultra, Millipore) were tested for releasing ubiquitinated protein complexes from the FK2 beads: either 8 M urea buffer (8 M urea, 300 mM NaCl, 50 mM Na_2HPO_4, 0.5% NP-40; pH 8), 2% SDS or 0.1 M Glycine pH 2 was used. Proteins were eluted in four consecutive steps by shaking for 5 min at 1250 rpm in an Eppendorf Thermomixer in two bead volumes of elution buffer.

Mass spectrometric analysis

Endogenously ubiquitinated protein complexes were isolated from one 90% confluent 9 cm dish of HeLa cells for each experiment using the FK2 beads as described above. SDS-PAGE gel lanes were cut into 2 mm slices using an automatic gel slicer and subjected to in-gel reduction with dithiothreitol. Protein alkylation with iodoacetamide can produce a 2-acetamidoacetamide covalent adduct to lysine residues, which has an atomic composition and mass identical to that of the diglycine remnant present at ubiquitinated lysines after trypsin digestion[37]. To prevent false-positive identification of ubiquitinated peptides we used deuterium-labeled iodoacetamide (98%; D4; Cambridge Isotope Laboratories) for alkylation. Proteins were subsequently digested with trypsin (Promega; sequencing grade), as described previously[38]. Nanoflow liquid chromatography-tandem mass spectrometry (LC-MS/MS) was performed on an 1100 Series capillary LC system (Agilent Technologies) coupled to an LTQ-Orbitrap XL mass spectrometer (Thermo) operating in positive mode. Peptide mixtures were trapped on a ReproSil-C18 reversed-phase column (Dr Maisch GmbH; 1.5 cm × 100 µm, packed in-house) at a flow rate of 8 µl/min. Peptides were separated on a ReproSil-C18 reversed-phase column (Dr Maisch GmbH; 15 cm × 50 µm, packed in-house) using a linear gradient of 0–80% acetonitrile (in 0.1% formic acid) for 170 min at a constant flow rate of 200 nl/min using a splitter. The elution was directly sprayed into the electrospray ionization (ESI) source of the mass spectrometer. Spectra were acquired in continuum mode; fragmentation of the peptides was performed in data-dependent mode.

Raw mass spectrometry data were analyzed using the label-free algorithm of the MaxQuant software (version 1.3.0.5) with a 3 min time window for the match between runs option[39]. A false discovery rate (FDR) of 0.01 for proteins and peptides and a minimum peptide length of 6 amino acids were set. A site-specific FDR of 0.05 was applied separately. The Andromeda search engine[40] was used to search the MS/MS spectra against the Uniprot human database (release April 2013) concatenated with the reversed versions of all sequences. A maximum of two missed cleavages was allowed. The precursor mass tolerance was set to 15 ppm, the fragment mass tolerance was set to 0.6 Da. The enzyme specificity was set to trypsin. Cysteine carbamidomethylation-2D was set as a fixed modification, whereas methionine oxidation and lysine ubiquitination were set as variable modifications. Before data analysis, known contaminants and reverse hits were removed from the protein lists.

Data analysis

The Ingenuity Pathway Analysis (IPA) software (Ingenuity® Systems, www.ingenuity.com) was used to identify canonical pathways associated with the FK2-specific proteins identified in the mass spectrometric analysis. Protein-protein interactions within the FK2-specific

protein group were assessed and visualized using the GeneMANIA[41] plug-in of Cytoscape (version 2.7.0)[42]. Of the 296 FK2-specific proteins, 6 proteins were not recognized by the GeneMANIA plug-in and were therefore excluded from this analysis. Protein interaction networks were built based on physical interactions only.

Protein concentration, immunoblotting and silver staining

Protein concentration was determined using the Thermo Scientific Pierce BCA Protein Assay Kit according to the manufacturer's protocol.

For immunoblotting we used a rabbit polyclonal against ubiquitin (Code Z0458; Dako) and a mouse monoclonal against mono-ubiquitinated and poly-ubiquitinated conjugates (FK2; Enzo Life Sciences). The anti-K48-linked poly-ubiquitin antibody (Apu2.07) and the anti-K63-linked poly-ubiquitin antibody (Apu3.A8) were kindly provided by Genentech and used according to their specifications[43]. Alexa Fluor 680 donkey anti-rabbit, Alexa Fluor 795 donkey anti-mouse and Alexa Fluor 795 goat anti-human (Li-Cor Biosciences) were used to visualize the stained proteins using an infrared imaging system (Odyssey; Li-Cor Biosciences). Immunoblots were quantified with the Odyssey software (version 3.0.21). Data are expressed as integrated intensity of a specified area. The in vitro generated K48-linked and K63-linked ubiquitin chains were purchased from Enzo Life Sciences.

Total protein levels were visualized in-gel using a standard silver stain protocol. In short, gels were incubated for 16 h in 50% methanol, 12% acetic acid, 0.5 ml/L 37% HCOH. Subsequently, the gels were incubated 30 min in 50% EtOH and 1 min in 0.2 g/L $Na_2S_2O_3$. After three 30 s washes in dH_2O the gels were incubated for 45 min in 2 g/L $AgNO_3$, 0.75 ml/L 37% HCOH. Finally the gels were washed two times in dH_2O for 30 s and incubated in 60 g/L Na_2CO_3, 4 mg/L $Na_2S_2O_3$, 0.5 ml/L 37% HCOH until a desirable staining was achieved.

RESULTS

Isolation of endogenously ubiquitinated protein complexes

Our goal was to develop a method for the efficient isolation of endogenously ubiquitinated protein complexes suitable for mass spectrometry (MS)-based proteomics (Figure 1a). To this end, we compared three different affinity-based procedures under non-denaturing conditions: (1) agarose-TUBEs (Tandem Ubiquitin Binding Entities)[44], a high-affinity ubiquitin trap based on ubiquitin-binding domains (UBDs) that binds only poly-ubiquitinated conjugates; (2) UbiQapture-Q matrix, a high affinity ubiquitin trap based on UBDs that binds both mono-ubiquitinated and poly-ubiquitinated proteins; and (3) the anti-ubiquitin antibody FK2[45], which recognizes both mono-ubiquitinated and poly-ubiquitinated proteins. The three different enrichment strategies were performed in parallel using HeLa whole-cell extracts (WCEs) in RIPA lysis buffer. As a negative control – to determine nonspecific protein binding – random mouse IgGs bound to protein G beads were used. The isolation of endogenously ubiquitinated protein complexes was assessed on an immunoblot using a polyclonal α-ubiquitin antibody (Figure 1b) and quantified using Odyssey software (Figure 1c). In the negative control, the majority of ubiquitinated proteins (89%) remained present in the non-bound (NB) fraction and we observed virtually no nonspecific isolation

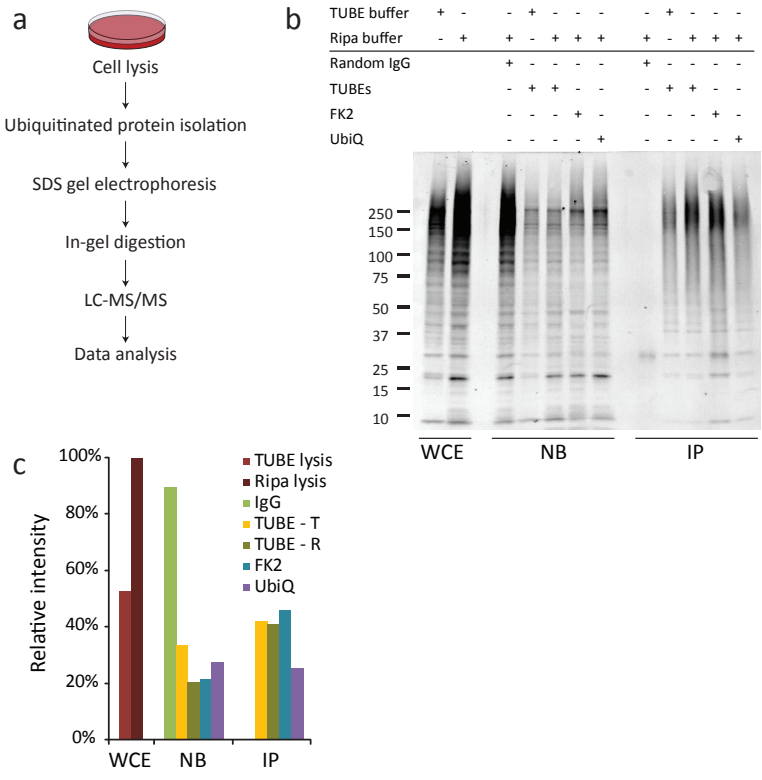

Figure 1: Isolation of endogenously ubiquitinated protein complexes
(a) Work flow for isolating endogenously ubiquitinated protein complexes for proteomic analysis. (b) Ubiquitinated proteins were isolated from HeLa WCE using either agarose-TUBEs, UbiQapture-Q matrix or FK2-beads. Protein samples were loaded on an SDS-PAGE gel in ratio and stained on an immunoblot with a polyclonal α-ubiquitin antibody to determine enrichment efficiency. (c) Odyssey quantification of Figure 1b. NB and total yield of IP of the IgG, TUBE-R, FK2 and UbiQ IPs were determined by normalization to the total of ubiquitinated proteins as shown by the WCE in RIPA buffer. The TUBE-T IP was normalized to WCE in TUBE buffer. WCE, whole-cell extract. NB, non-bound fraction. IP, immunoprecipitated proteins.

in the immunoprecipitated (IP) fraction. In contrast, in the three different enrichment procedures we observed up to 80% depletion of ubiquitinated proteins in the NB fraction, which indicates efficient binding of ubiquitinated proteins to the various purification resins. The total yield of ubiquitinated proteins isolated was highest in the methods using TUBEs (41%) or FK2 antibody (46%).

Since the manufacturer of the TUBEs has suggested that the inclusion of detergents such as SDS or deoxycholate – which are present in our RIPA lysis buffer – might have a negative impact on the overall yield of poly-ubiquitinated proteins, an enrichment experiment with the recommended TUBEs lysis buffer was performed in parallel. The relative efficiency of ubiquitinated protein isolation with TUBEs in TUBE buffer was comparable to those of the TUBEs in RIPA buffer and FK2 beads isolation procedures (Figure 1c). However,

quantification of the WCE shows that lysis in TUBE buffer led to an almost two-fold less efficient extraction of ubiquitinated proteins from cells compared when the cells were lysed in RIPA buffer. TUBE isolation using the TUBE buffer was therefore excluded from further experiments.

The efficiency of isolating ubiquitinated proteins was similar for the isolation procedures using TUBEs (in RIPA buffer) and FK2 antibody. However, the FK2 approach resulted in a slightly higher yield and has the further advantage of isolating mono-ubiquitinated proteins in addition to poly-ubiquitinated proteins[44,45]. This was also suggested by the stronger antibody staining for ubiquitinated proteins observed in the low-molecular-mass region (Figure 1b). Therefore further experiments were performed with the FK2 antibody.

Optimization of the FK2 IP

Since DUBs and the 26S proteasome might retain some residual activity under non-denaturing conditions, despite the presence of specific inhibitors, a decrease in incubation time for the IP might result in less deubiquitination and protein degradation. Figure 2a shows that a reduction in incubation time from 16 to 4 h did not change the total amount of ubiquitinated proteins isolated. Concomitantly, incubating HeLa WCE for up to 8 h at 4°C did not decrease the total amount of ubiquitinated proteins (Supplementary Figure 1a) indicating minimal loss of ubiquitinated proteins under the conditions used.

To use the FK2 antibody more efficiently, we optimized the FK2/WCE ratio by performing FK2 IPs with increasing amounts of WCE. Proteins were allowed to bind to the FK2 beads for 4 h at 4°C. Although the amount of non-bound ubiquitinated proteins increased when more WCE was added to the same amount of FK2 beads, the amount of ubiquitinated proteins in the IP fractions increased as well, up to three-fold (Figure 2a,b and Supplementary Figure 1d). This increase in the total amount of ubiquitinated proteins isolated extended linearly with the increase in WCE input up to the second highest WCE input. A maximum in the amount of recovered ubiquitinated proteins was reached for the two IPs with the highest amount of WCE input, however at the same time the amount of ubiquitinated proteins in the corresponding NB fraction increased >50% for the highest amount of WCE (Figure 2b). Together, this indicated that the maximum binding capacity of the beads was reached at the second highest amount of WCE. To exclude the possibility of a fraction of ubiquitinated proteins remaining bound to the beads after elution, a second elution from the FK2 beads was performed (Figure 2a). Although additional FK2 antibody was eluted from the beads in the second elution step for all IPs, virtually all ubiquitinated proteins were recovered from the FK2 beads in the first elution step. Taken together, based on these results we conclude that the optimal ratio of WCE to FK2 beads is 5.3 mg of WCE protein for every 100 µl of FK2 beads (50% slurry), which corresponds to 87.5 µg of FK2 antibody.

This immunoaffinity purification method has been developed for the proteomic analysis of ubiquitinated protein complexes. In such an analysis the presence of low-abundant proteins could be masked by large amounts of antibody in the IP fraction (as observed in Figure 2a, see the asterisk). This occurs when antibodies are present in the sample, either during in-solution digestion or – if proteins have the same molecular weight as the antibody – during in-gel digestion for subsequent MS analysis. Although crosslinking of the FK2

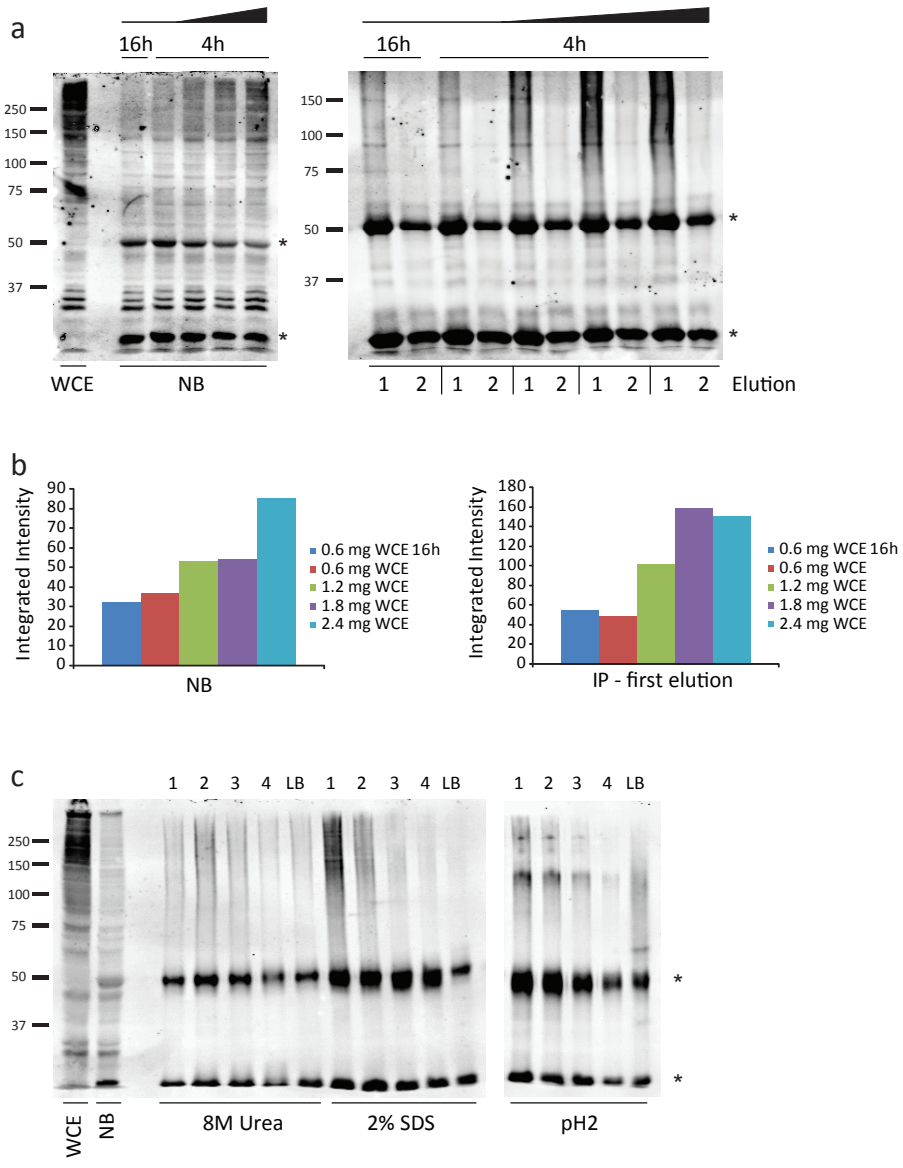

Figure 2: Optimization and elution of the FK2 IP

(a) Endogenously ubiquitinated protein complexes were isolated using 40 µl FK2-beads (50% slurry) and incubated for 4 or 16 h with an increasing amount of XP2OS WCE (0.6 – 2.4 mg). Samples were loaded on SDS-PAGE gels. Immunoblots were stained with the FK2 antibody. The left immunoblot shows the WCE and NB fractions, the right immunoblot shows the eluted IP fractions. A representative blot of this IP is shown (n = 2). (b) Odyssey quantification of Figure 2a. (c) The FK2 beads were incubated for 16 h with HeLa WCE. Bound proteins were eluted from the beads in four consecutive steps with either 8 M urea buffer, 2% SDS or 0.1 M Glycine pH 2. After elution the beads were boiled in 2x Laemmli buffer to assess residual bound proteins for elution efficiency. Protein samples were loaded on an SDS-PAGE gel in ratio and stained on immunoblot with the FK2 antibody. A representative blot of this IP is shown (n = 2). WCE, whole-cell extract. NB, non-bound fraction. LB, 2x Laemmli buffer. (*), Heavy and light antibody chains.

antibody to the protein G beads greatly decreased the amount of antibody in the IP fraction, it also decreased the affinity of the antibody for ubiquitinated substrates (Supplementary Figure 1b). Without crosslinking, the free antibody in the sample cannot be separated from the ubiquitinated proteins, rendering in-solution digestion unfavorable. Therefore, for future MS experiments we chose to perform FK2 IPs without crosslinking followed by in-gel digestion. The areas of the gel containing the bands corresponding to antibody chains were excised into separate gel slices to minimize the presence of antibody in the other gel slices.

Since only a limited volume can be loaded into a slot of an SDS-PAGE gel lane, the volume into which bound proteins are eluted from the beads is limited as well when 2x Laemmli-buffer is used. For large-scale IP experiments, elution from the beads followed by a protein concentration step is therefore necessary. The compatibility of three different elution strategies with a subsequent concentration step using centrifugal filters (Amicon Ultra, Millipore) was investigated by releasing ubiquitinated protein complexes from the FK2 beads into either (1) 8 M urea buffer, (2) 2% SDS, or (3) 0.1 M glycine pH 2 (Figure 2c and Supplementary Figure 1e). After elution the beads were boiled in 2x Laemmli buffer to assess residual bound proteins for elution efficiency. Figure 2c shows that elution with 2% SDS was the most efficient: not only was the majority (77%) of bound ubiquitinated proteins eluted within the first two rounds of elution, but also almost no residual proteins (3%) remained bound to the FK2 beads after four elution rounds, as illustrated by the absence of ubiquitinated protein signal in the LB lane (Figure 2c and Supplementary Figure 1c).

Characterization of the FK2 IP

The FK2 antibody is a mouse monoclonal recognizing both mono-ubiquitinated and poly-ubiquitinated conjugates. According to the manufacturer's data sheet the FK2 antibody can recognize various types of ubiquitin chains; however, it is unknown if it has equal affinities for all seven ubiquitin chain-linkages and for different protein substrates. If the FK2 antibody does have such a bias, then a specific fraction of ubiquitinated proteins will not be immunodepleted. To investigate this, we compared by immunoblot analysis the FK2 antibody with a polyclonal antibody that recognizes both mono-ubiquitinated and poly-ubiquitinated conjugates as well as free ubiquitin[46]. Samples of small-scale FK2 IPs with random IgG beads as negative control were separated by SDS/PAGE and immunoblotted with FK2 and the polyclonal α-ubiquitin antibody. The staining patterns for the IP samples were similar for both antibodies: we observed a strong depletion of ubiquitinated proteins in the NB fraction and a specific enrichment in the FK2 IP fraction (Figure 3a and b). The relative signal intensities in the IP fractions were also similar for both antibodies (Figure 3e), suggesting that FK2 has no bias for binding specific types of ubiquitin chain-linkages or protein substrates. To further support the notion that proteins with all ubiquitin chain-linkages may be isolated using the FK2 antibody, the immunoblots were also stained with two available chain-specific antibodies that specifically recognize K48-linked and K63-linked ubiquitin chains. The chain specificity of the antibodies was confirmed by also loading K48-linked and K63-linked ubiquitin chains that were generated in vitro onto the gels. The staining patterns and relative signal intensities of ubiquitinated proteins in the IP fractions were again very similar for the antibodies used (Figure 3a-e).

Proteolytic digestion of ubiquitinated proteins with trypsin generates a specific diglycine (Gly-Gly) remnant on the ubiquitinated lysine. This remnant causes a distinct mass shift on the peptide mass that can be used to precisely identify and localize ubiquitination sites by MS. We performed in-gel digestion on an FK2 IP fraction with trypsin and identified ubiquitin-modified peptides on positions K6, K11, K27, K29, K48 and K63 of ubiquitin, representing six of the seven possible chain-linkages of ubiquitin (Supplementary Table 1). Together with the immunoblot results this suggests that there is no bias for FK2 in binding specific types of ubiquitin chains or protein substrates under the conditions used.

To further evaluate the application of the FK2 antibody for our immunoaffinity purification method (intended for the proteomic analysis of ubiquitinated protein complexes), we performed two additional independent FK2 IP experiments with random IgG beads as a negative control for MS analysis. This replicate experiment differed only in the final washing step: beads were washed with either PBS or RIPA buffer for four times. We observed a strong, specific, and reproducible enrichment for ubiquitinated proteins, as shown by immunoblot analysis using two different antibodies (Figure 3f). Additionally, analysis of total protein levels – as visualized in-gel by silver staining – showed an enormous decrease (>200-fold) in total amount of protein in the IP fraction (Figure 3f), while most of the total ubiquitinated protein signal (Figure 3g) was recovered as shown by the immunoblot analysis. These results illustrate a high degree of specific enrichment for ubiquitinated factors.

MS analysis

To further confirm the specificity and reproducibility of our enrichment strategy, the IP fractions of the two independently executed FK2 IPs (Figure 3f) were in-gel digested and run on an LTQ-Orbitrap XL mass spectrometer. Raw mass spectrometry data were analyzed using the label-free quantitation (LFQ) algorithm of the MaxQuant software (version 1.3.0.5).

The proteins identified were considered true FK2 antibody interactors when an LFQ intensity (the total signal intensities of the peptides identifying each protein) was listed in the FK2 IP and there was either no LFQ intensity observed in the control IP or the FK2/control LFQ intensity ratio was >2. Of the identified 951 true interactors, 296 proteins were identified in both experiments (Figure 4a and Supplementary Table 2a).

To confirm that the presented enrichment method indeed isolates ubiquitinated and ubiquitination-related proteins, we performed three further analyses. First, we performed a functional pathway analysis of the 296 FK2-specific proteins found in both experiments. The Ingenuity Pathway Analysis (IPA) software (Ingenuity® Systems, www.ingenuity.com) identified 32 canonical pathways ($p<0.05$, Fisher's exact test, Supplementary Table 3) with the protein ubiquitination pathway as most significantly present (Figure 4b), indicating an enrichment for ubiquitinated and ubiquitination-related proteins. As expected, a wide variety of other pathways was also identified, indicative of the importance of ubiquitination in different pathways. In line with this, when the 296 FK2-specific proteins were subjected to a Gene Ontology (GO) enrichment analysis using the functional annotation tool DAVID[47], proteins associated with ubiquitination in the Biological Processes term were highly enriched for (Figure 4c and Supplementary Table 4). Finally, the FK2-specific protein list was compared with two large datasets of ubiquitinated proteins that were recently identified in peptide

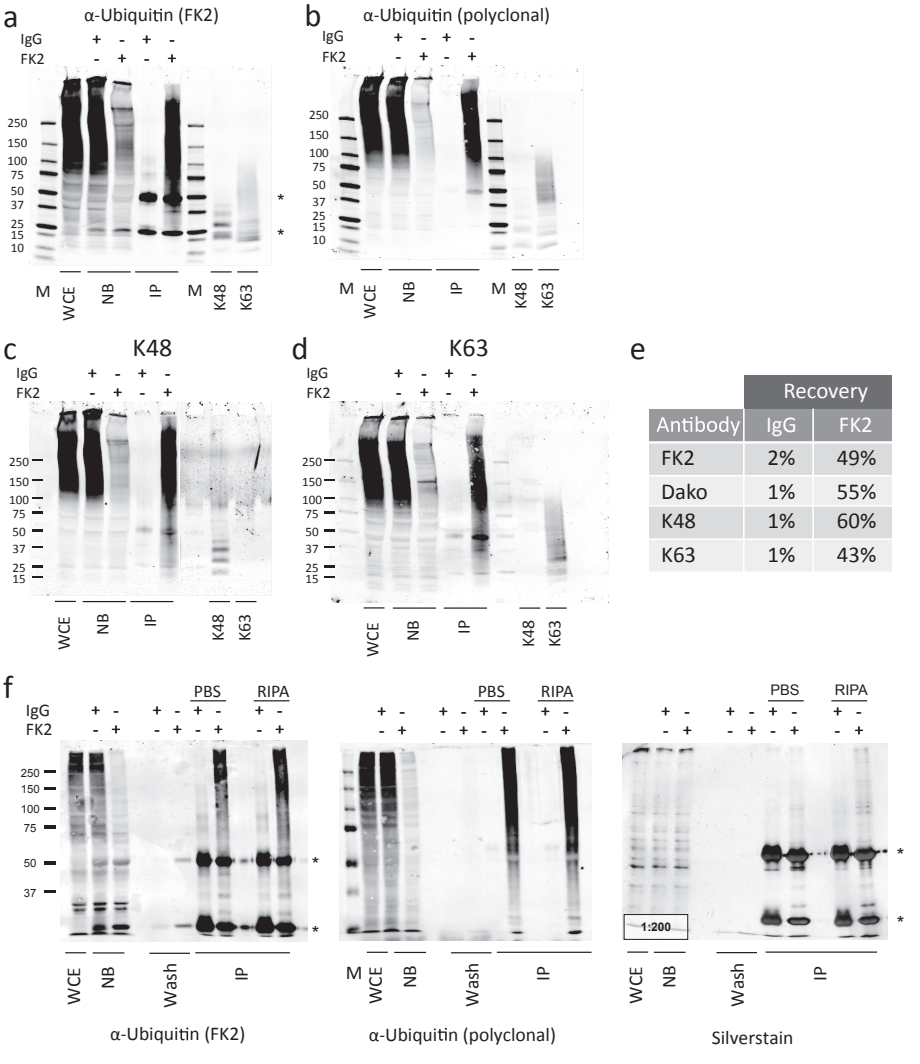

e

	Recovery	
Antibody	IgG	FK2
FK2	2%	49%
Dako	1%	55%
K48	1%	60%
K63	1%	43%

g

	WCE	NB		IP PBS		IP RIPA	
Antibody		IgG	FK2	IgG	FK2	IgG	FK2
FK2	100%	96%	17%	7%	62%	5%	69%
Dako	100%	101%	20%	0%	76%	1%	86%

Figure 3: Characterization of the FK2 IP

(a-d) Endogenously ubiquitinated protein complexes were isolated from HeLa WCE. Samples were loaded twice on SDS-PAGE gels in equal amounts compared to the WCE, IP sample was loaded at twice the amount. A representative blot of this IP is shown (n > 3). The immunoblots were stained with (a) FK2, (b) polyclonal α-ubiquitin, (c) α-K48-linked poly-ubiquitin (Apu2.07) and (d) α-K63-linked poly-ubiquitin (Apu3.A8). As specificity control for the chain-linkage specific antibodies, in vitro generated K48 and K63 ubiquitin chains (4 µg) were loaded. The last three lanes of the immunoblot in Figure 3c were scanned at a higher intensity. M, molecular weight marker. WCE, whole-cell extract. NB, non-bound

screens using antibodies recognizing the specific diglycine remnant on the ubiquitinated lysine[32,33]. There was a 62% overlap with the dataset of Kim *et al.*[32] and a 70% overlap with that of Wagner *et al.*[47], indicating that a high percentage of the isolated proteins were indeed ubiquitinated (Supplementary Table 2b).

One of the advantages of our approach is that ubiquitinated protein complexes can be isolated. To demonstrate that many of the proteins present in the FK2 IP fraction are part of protein complexes we evaluated their protein-protein interactions. Functional association data were obtained and visualized using the GeneMANIA plug-in in Cytoscape. The resulting protein network showed that 53% of the FK2-specific proteins interacted with at least one other protein within the FK2-specific protein group (Figure 4d). In contrast, when four sets of 290 proteins were randomly chosen from the Ensembl database, a significantly smaller percentage of proteins interacted (on average 15%, $p = 3.3 \times 10^{-23}$, Fisher's exact test) (Figure 4d). Since a low percentage of interacting proteins in random protein sets could be explained by low-abundant, tissue-specific and/or badly annotated proteins, we also determined the percentage of interacting proteins in four random sets of proteins that were extracted from the two large datasets of ubiquitinated proteins recently identified in peptide screens by Kim *et al.*[32] and Wagner *et al.*[33]. Because the enrichment step in both of these screens was performed at the peptide level – after a denaturing and digestion step – protein complexes were not isolated and all information about protein-protein associations was lost. For the random sets extracted from Kim *et al.*[32] and from Wagner *et al.*[33], the percentages of interacting proteins were on average 25% and 29%, respectively (Supplementary Figure 2). Although these percentages were higher than those found for the random sets collected from the Ensembl database, the percentages of interacting proteins for both datasets were similar and significantly lower than the 53% interacting proteins in the FK2-specific protein dataset ($p = 1.8 \times 10^{-12}$ for the Kim *et al.* dataset and 1.4×10^{-9} for the Wagner *et al.* dataset, Fisher's exact test). This clearly indicates that the optimized enrichment method described here indeed isolates endogenously ubiquitinated protein complexes.

DISCUSSION

We present here an immunoaffinity purification method for the proteomic analysis of endogenously ubiquitinated protein complexes. Proteins were successfully isolated using the FK2 antibody bound to protein G-beaded agarose, which recognizes mono-

fraction. IP, immunoprecipitated proteins. (**e**) Odyssey quantification of Figure 3a-d. Recovery efficiency was determined by normalization towards the total of ubiquitinated proteins as shown by the WCE. (**f**) Endogenously ubiquitinated protein complexes were isolated from HeLa WCE in two independent experiments. FK2 beads and control beads were washed 4x with either PBS or RIPA buffer before elution of bound proteins in 2x Laemmli buffer. The immunoblot was stained with FK2 and a polyclonal α-ubiquitin antibody. Total proteins levels were assessed with silver staining, WCE and NB were diluted 200x as compared to the IP fractions. M, molecular weight marker. WCE, whole-cell extract. NB, non-bound fraction. Wash, final wash fraction before protein elution. IP, immunoprecipitated proteins. (**g**) Odyssey quantification of Figure 3f. Recovery efficiency was determined by normalization to the total of ubiquitinated proteins as shown by the WCE.

a

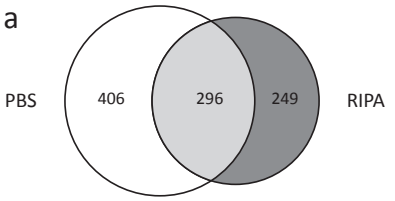

b

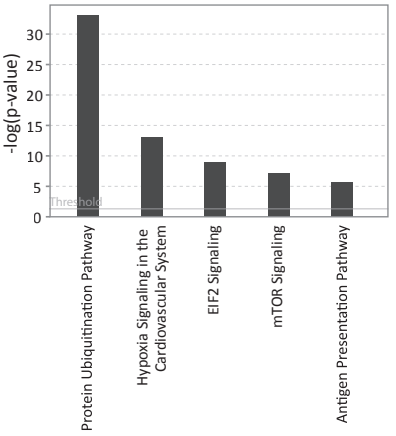

c

GO	Term	Fold Enrichment	Bonferroni
GO:0051443	positive regulation of ubiquitin-protein ligase activity	24.4	7.2E-30
GO:0051437	positive regulation of ubiquitin-protein ligase activity during mitotic cell cycle	24.3	1.2E-28
GO:0051444	negative regulation of ubiquitin-protein ligase activity	23.8	3.1E-27
GO:0051352	negative regulation of ligase activity	23.8	3.1E-27
GO:0031145	anaphase-promoting complex-dependent proteasomal ubiquitin-dependent protein catabolic process	23.6	4.8E-26
GO:0051436	negative regulation of ubiquitin-protein ligase activity during mitotic cell cycle	23.6	4.8E-26
GO:0051351	positive regulation of ligase activity	23.4	3.2E-29
GO:0051439	regulation of ubiquitin-protein ligase activity during mitotic cell cycle	23.2	5.1E-28
GO:0051438	regulation of ubiquitin-protein ligase activity	22.6	8.6E-30
GO:0051340	regulation of ligase activity	21.8	3.3E-29

d

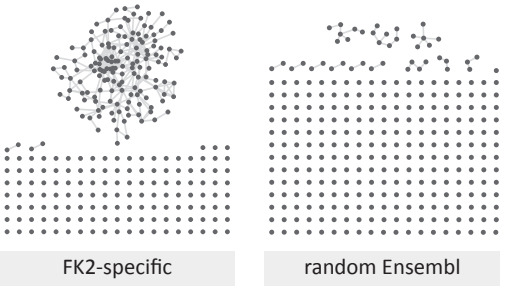

	Interacting
FK2-specific	53%
random Ensembl	15% ± 4%
random Kim, et al.	25% ± 5%
random Wagner, et al.	29% ± 4%

Figure 4: Mass spectrometric data analysis

(a) Venn diagram of the FK2-specific MS-identified proteins in two independently executed FK2 IPs. (b) Functional annotation of the FK2-specific proteins identified in both experiments into canonical pathways using IPA. The five most significant pathways are shown. The significance of the pathways was determined using Fisher's exact test (c) GO annotation enrichment analysis using DAVID. The 10 most enriched biological processes with $p < 0.005$ are shown. The p-values were corrected for multiple hypotheses testing using Bonferroni FDR. (d) Protein interaction networks were built using association data based on physical interactions, which were obtained through the GeneMANIA database and visualized using Cytoscape. Every dot represents a protein and connecting lines represent a physical interaction. Percentages of interacting proteins for the random protein sets are averages of n = 5. For the random protein set from the Ensembl database a representative protein interaction network is shown.

ubiquitinated and poly-ubiquitinated conjugates (Figure 1 and 3f). An optimal WCE/FK2 ratio was determined for the efficient isolation of ubiquitinated proteins and an IP incubation time of 4 h was shown to be sufficient for immunodepletion of ubiquitinated proteins from WCE of human cells (Figure 2a). A high degree of specific enrichment for ubiquitinated factors was achieved, as shown by the high recovery of ubiquitinated proteins (up to 86%, Figure 3g), while the total amount of proteins decreased strongly in the IP fraction (>200-fold, as assessed on a silver-stained gel in Figure 3f). Finally, the efficient elution of bound proteins with 2% SDS from the FK2 beads (Figure 2c) illustrates the compatibility of this method with large-scale proteomic assays.

The MS analysis of two small-scale FK2 IPs resulted in the identification of 296 FK2-specific proteins in both experiments (Figure 4a). The isolation of ubiquitinated proteins and ubiquitination-related proteins was confirmed by pathway analyses using IPA and GO-annotation enrichment (Figure 4b,c). Additionally, comparing the FK2-specific proteins with databases of ubiquitinated proteins in the literature indicated that a high percentage of proteins in the enriched fraction in our assay was indeed ubiquitinated (Supplementary Table 2b).

Further characterization of the FK2 IP, with immunoblot analysis using chain-linkage-specific antibodies and two different α-ubiquitin antibodies, suggested that there was no detectable bias for the FK2 antibody in binding specific types of ubiquitin chains or protein substrates under the conditions used (Figure 3a-d). This was further supported by MS analysis of FK2-enriched proteins, which identified six (out of seven possible) specific poly-ubiquitin chain-linkages. The fact that the K33 ubiquitin-modified peptide was not identified could be explained by the fact that it is the least abundant chain-linkage type in unperturbed cells[22] and that these experiments were performed on a small scale (IPs were performed on WCE from a single 9 cm dish).

The FK2 IP was performed under non-denaturing conditions, which allows the preservation of protein complexes. Most biological processes mainly rely on functional protein modules[36]; however, within complexes not all interactors are necessarily ubiquitin modified. Evaluation of protein-protein interactions within the FK2-specific protein group showed that a significantly higher percentage (53%) of the FK2-specific proteins are interacting among one another compared to proteins in random datasets from the Ensembl database (15%) or datasets of ubiquitinated-peptide IPs from Kim *et al.* (25%) and Wagner *et al.* (29%) (Figure 4d). This indicates that in our assay intact ubiquitinated protein complexes are indeed isolated. MS analysis identified 296 FK2-specific proteins in two FK2 IPs using PBS or RIPA buffer as the final wash buffer. Additionally, 655 proteins were found in only one of these IPs. Interestingly, 62% of the additional identified proteins were specific for the PBS-washed IP (Figure 4a and Supplementary Table 2a). Since PBS is a much milder buffer than RIPA buffer in terms of salt and detergent concentrations, our data suggest that changing the wash buffer stringency can result in a different amount of proteins isolated. It will be of interest to study whether changes in wash buffer stringency will result in the identification of additional ubiquitinated proteins or proteins that are transiently or weakly bound to ubiquitinated protein complexes.

We showed that the FK2 IP efficiently enriched for ubiquitinated proteins of different chain-linkages; however, we cannot be certain that all ubiquitinated factors were equally efficient isolated. For this reason we performed an isolation of endogenously ubiquitinated protein complexes using the UbiQapture-Q matrix under the same conditions as for the FK2 IP. MS analysis identified a total of 735 UbiQapture-Q-specific proteins (Supplementary Table 2a). From this set 351 overlapped with the FK2-specific proteins (Supplementary Figure 2b). This indicates that while these methods isolate identical proteins, a considerable amount of additional method-specific proteins was also isolated. This suggests that the FK2 isolation method can be combined with other isolation procedures for ubiquitinated proteins, to broaden the pool of proteins isolated and to overcome a putative bias in the isolation procedure.

A limitation of the FK2 isolation method presented here is that, apart from sites on ubiquitin itself, we identified only a few ubiquitination sites on substrate proteins (Supplementary Table 1). It is therefore not possible to differentiate with certainty between ubiquitinated and non-ubiquitinated proteins based on the results of the MS analysis alone. The low number of ubiquitination sites identified could be explained by the absence of an enrichment protocol for ubiquitinated peptides in our assay. The presence of ubiquitinated peptides is probably masked by large amounts of non-ubiquitinated peptides from the same protein and from non-ubiquitinated interactors of the ubiquitinated proteins. Enrichment strategies for the detection of ubiquitination sites are available and would be an ideal tool to complement the data generated with this FK2-enrichment strategy. The recently developed method for the immunoenrichment of ubiquitinated peptides using a diglycine-specific antibody[31-35] is highly efficient and could be implemented to discriminate between ubiquitinated proteins and interacting non-ubiquitinated proteins in our FK2 samples containing ubiquitinated protein complexes.

In conclusion, the use of the FK2 antibody for protein isolation enables the enrichment of endogenously ubiquitinated proteins. The advantage of this method is that possible negative side effects of introducing tagged ubiquitin into the cells – such as a biased incorporation into mono-ubiquitination or certain ubiquitin chains and/or interference with, e.g., the stability, activity, and localization of protein substrates – are therefore prevented. Additionally, the FK2 isolation method described here is broadly applicable as it can also be used to isolate proteins from tissues and cell types that are usually difficult to transfect.

In recent years, mass spectrometry has become the method of choice for studying the proteome and, more specifically, PTMs. It can be used not only to analyze proteins and protein complexes, but also to dissect biological pathways and identify proteins not previously known to be involved in specific processes. Moreover, various quantitative mass spectrometry strategies are available for detecting and quantifying the effects of a specific stimulus in a proteome-wide fashion[48]. Label-based quantification methods – such as stable isotope labelling by amino acids in cell culture (SILAC) and isobaric tags for relative and absolute quantitation (iTRAQ)[48] – are very suitable for comparing the abundance of proteins on a proteome-wide scale since they can provide a quantitative ratio for a large number of proteins. Combining the method we describe for the isolation

of endogenously ubiquitinated protein complexes using the FK2 IP with such quantitative proteomic techniques would therefore generate a powerful tool to study dynamic changes in the ubiquitinome following for example environmental stresses, drug treatment, knockdown of proteins, or when comparing two disease states.

Recently we showed a clear example of the successful application of this approach[49]. Combining the FK2 IP described here with SILAC-based proteomics identified several differentially ubiquitinated proteins in HeLa cells following UV-irradiation. The most prominent factors were DNA repair proteins that are involved in nucleotide excision repair (NER) and that are known to be ubiquitinated. Importantly, it also resulted in the identification of *UVSSA* (UV-stimulated scaffold protein A) as the causative gene for UV^{S}S (UV-sensitive syndrome), a previously unresolved NER deficiency disorder[49-51]. Follow-up experiments showed that the ubiquitination status of UVSSA remained unchanged after UV and that this protein was co-purified as part of a UV-induced ubiquitinated protein complex[49]. These data illustrate the value and advantage of our non-denaturing immunoaffinity purification method, which is capable of isolating both ubiquitinated proteins and their interacting proteins, for the proteomic analysis of endogenously ubiquitinated protein complexes.

ACKNOWLEDGEMENTS

We like to thank Genentech for providing the chain-linkage specific antibodies and we are grateful to K. Derks for his help in generating the random proteins lists. This work was funded by the Netherlands Genomics Initiative NPCII (to P.S.), 935.19.021 and 935.11.042 (to W.V., C.L. and J.A.M.), the Dutch Organization for Scientific Research ZonMW Veni Grant (917.96.120 to J.A.M.) and TOP grant (912.08.031 to W.V.), and the Association for International Cancer Research (10-594 to W.V.).

SUPPLEMENTARY MATERIAL

Supplementary data associated with this article can be found, in the online version, at http://dx.doi.org/10.1016/j.ab.2013.05.020.

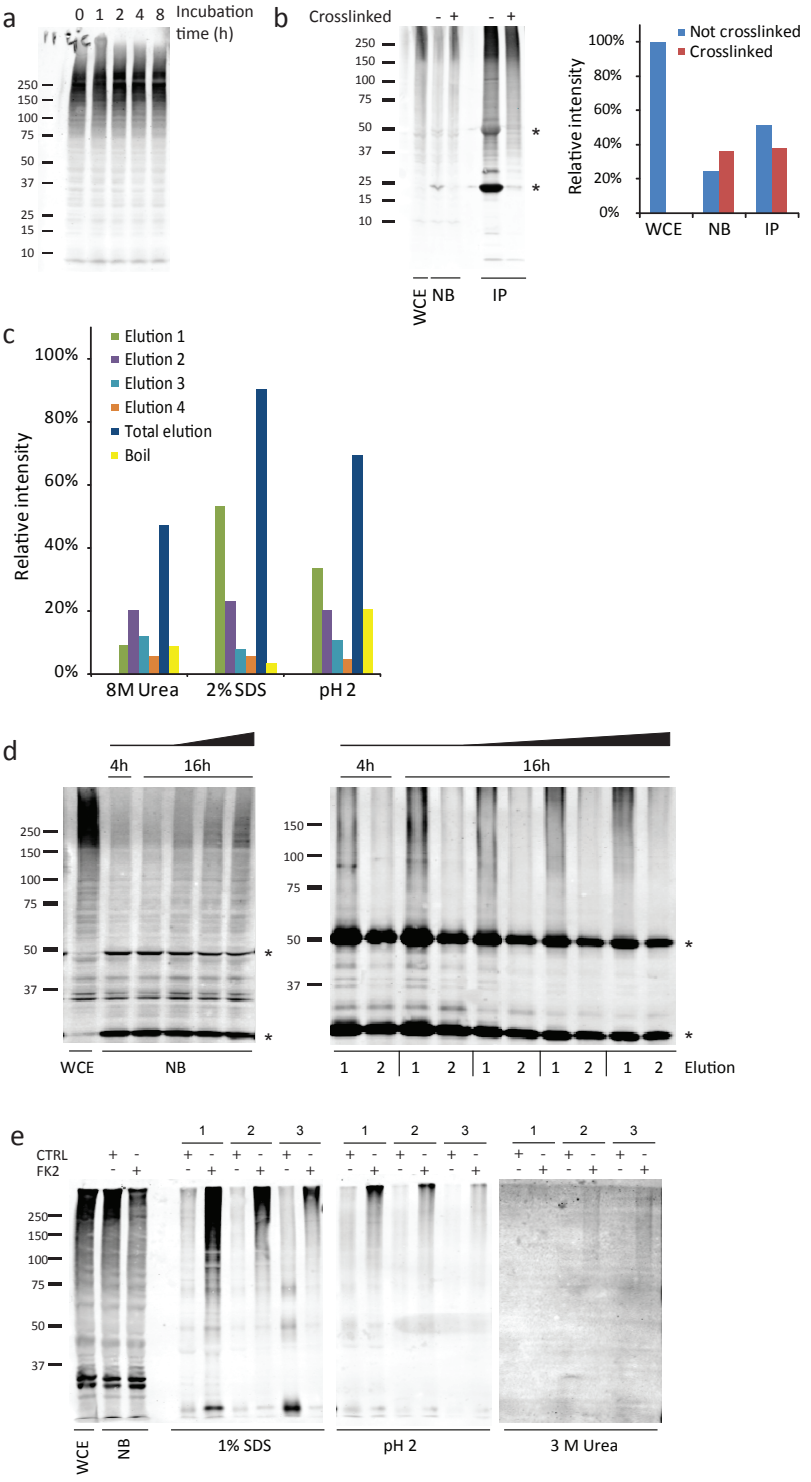
a
0 1 2 4 8 Incubation time (h)
250
150
100
75
50
37
25
15
10
b
Crosslinked
- + - +
250
150
100
75
50
37
25
15
10
*
*
WCE NB IP
Not crosslinked
Crosslinked
Relative intensity
100%
80%
60%
40%
20%
0%
WCE NB IP
c
Elution 1
Elution 2
Elution 3
Elution 4
Total elution
Boil
Relative intensity
100%
80%
60%
40%
20%
0%
8M Urea
2% SDS
pH 2
d
4h 16h
4h 16h
250
150
100
75
50
37
150
100
75
50
37
*
*
*
*
WCE NB
1 2 1 2 1 2 1 2 1 2 Elution
e
CTRL
FK2
1 2 3 1 2 3 1 2 3
250
150
100
75
50
37
WCE NB
1% SDS
pH 2
3 M Urea

Supplementary Figure 1: Optimization and elution of the FK2 IP
(a) HeLa WCE in RIPA buffer was incubated at 4°C for the indicated times. The immunoblot is stained with the FK2 antibody. A representative blot of this IP is shown (n=2) (b) Endogenously ubiquitinated protein complexes were isolated from HeLa WCE using either cross-linked or not cross-linked FK2 beads. Protein samples were loaded on SDS-PAGE gel in ratio, IP samples were loaded 3.6x the amount. The immunoblot is stained with the FK2 antibody. (c) Odyssey quantification of Figure 2c. Recovery efficiency was determined by normalization to the total of ubiquitinated proteins as shown by the WCE. (d) Endogenously ubiquitinated protein complexes were isolated using 40 µl FK2-beads (50% slurry) and incubated for 16 or 4 h with an increasing amount of XP2OS WCE (0.6 – 2.4 mg). Samples were loaded on SDS-PAGE gels. Immunoblots were stained with the FK2 antibody. The left immunoblot shows the WCE and NB fractions, the right immunoblot shows the eluted IP fractions. (e) FK2 beads and control beads were incubated for 16 h with HeLa WCE. Bound proteins were eluted from the beads in three consecutive steps with either 1% SDS, 0.1 M glycine pH 2 or 3 M Urea. Protein samples were loaded on an SDS-PAGE gel in ratio and stained on an immunoblot with a polyclonal α-ubiquitin antibody. WCE, whole-cell extract. NB, non-bound fraction. (*), heavy and light antibody chains.

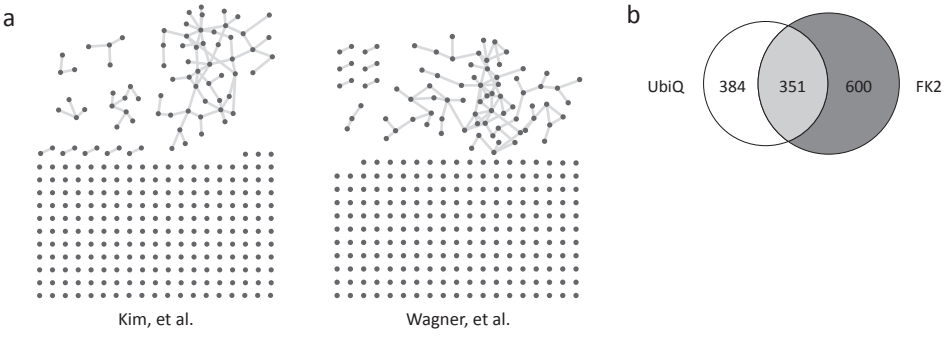

Supplementary Figure 2: Mass spectrometric data analysis
(a) Protein interaction networks were built using association data based on physical interactions, which were obtained through the GeneMANIA database and visualized using Cytoscape. A representative interaction network is shown for the random protein sets taken from the two large data sets of ubiquitinated proteins recently identified in peptide screens by Kim *et al.* and Wagner *et al.* Every dot represents a protein and connecting lines represent a physical interaction. (b) Venn diagram of the MS-identified specific proteins. UbiQapture-Q-specific proteins were compared with the FK2-specific proteins of the two FK2 IPs as shown in Figure 4a.

The supplementary tables 1-4 can be found at http://dx.doi.org/10.1016/j.ab.2013.05.020.

Supplementary Table 1: Identified GG-peptides
List of identified ubiquitination sites of substrate proteins. Ubiquitin-modified peptides on position K6, K11, K27, K29, K48 and K63 of ubiquitin, representing six of the seven possible chain-linkages of ubiquitin, were found.

Supplementary Table 2: MS-identified protein list
(a) List of FK2-specific proteins identified in two independently executed FK2 Ps with the label-free quantitation (LFQ) algorithm of the MaxQuant software. Identified proteins were considered true FK2 antibody interactors when either an LFQ intensity was listed in the FK2 IP and no signal was observed in the control IP, or when the ratio of the LFQ intensities for the FK2 IP versus control IP was >2. From the identified and validated 951 true interactors, 296 proteins were identified in both experiments. Additionally, the same criteria were applied to determine UbiQapture-Q-specific proteins and it is indicated if these proteins were identified in the FK2 IPs. (b) The GeneMANIA plugin in Cytoscape was used to build protein interaction networks. For each of the recognized 290 FK2-specific proteins found in both experiments it is indicated if the protein is not-interacting (NI) or interacting (complex). Additionally, it is indicated if the FK2-specific proteins were identified in two large data sets with ubiquitinated proteins of Kim *et al.* and Wagner *et al.*

Supplementary Table 3: Pathway analysis using IPA
Functional annotation of the 296 FK2-specific proteins into canonical pathways using IPA. The significance of the pathways was determined using Fisher's exact test.

Supplementary Table 4: GO annotation enrichment analysis
GO annotation enrichment analysis using DAVID. The p-values were corrected for multiple hypotheses testing using Bonferroni FDR. Enriched terms were required to have at least a two-fold enrichment and $p < 0.005$.

REFERENCES

1. Bergink, S. & Jentsch, S. Principles of ubiquitin and SUMO modifications in DNA repair. *Nature* **458**, 461-7 (2009).
2. Mocciaro, A. & Rape, M. Emerging regulatory mechanisms in ubiquitin-dependent cell cycle control. *J Cell Sci* **125**, 255-63 (2012).
3. Vucic, D., Dixit, V.M. & Wertz, I.E. Ubiquitylation in apoptosis: a post-translational modification at the edge of life and death. *Nat Rev Mol Cell Biol* **12**, 439-52 (2011).
4. Hershko, A. & Ciechanover, A. The ubiquitin system. *Annu Rev Biochem* **67**, 425-79 (1998).
5. Ciechanover, A. The ubiquitin-proteasome proteolytic pathway. *Cell* **79**, 13-21 (1994).
6. Kulathu, Y. & Komander, D. Atypical ubiquitylation - the unexplored world of polyubiquitin beyond Lys48 and Lys63 linkages. *Nat Rev Mol Cell Biol* **13**, 508-23 (2012).
7. Komander, D. & Rape, M. The ubiquitin code. *Annu Rev Biochem* **81**, 203-29 (2012).
8. Clague, M.J., Coulson, J.M. & Urbe, S. Cellular functions of the DUBs. *J Cell Sci* **125**, 277-86 (2012).
9. Nijman, S.M. *et al.* A genomic and functional inventory of deubiquitinating enzymes. *Cell* **123**, 773-86 (2005).
10. Komander, D., Clague, M.J. & Urbe, S. Breaking the chains: structure and function of the deubiquitinases. *Nat Rev Mol Cell Biol* **10**, 550-63 (2009).
11. Love, K.R., Catic, A., Schlieker, C. & Ploegh, H.L. Mechanisms, biology and inhibitors of deubiquitinating enzymes. *Nat Chem Biol* **3**, 697-705 (2007).
12. Low, T.Y., Magliozzi, R., Guardavaccaro, D. & Heck, A.J. Unraveling the ubiquitin-regulated signaling networks by mass spectrometry-based proteomics. *Proteomics* (2012).
13. Vertegaal, A.C. Uncovering ubiquitin and ubiquitin-like signaling networks. *Chem Rev* **111**, 7923-40 (2011).
14. Peng, J. *et al.* A proteomics approach to understanding protein ubiquitination. *Nat Biotechnol* **21**, 921-6 (2003).
15. Gururaja, T., Li, W., Noble, W.S., Payan, D.G. & Anderson, D.C. Multiple functional categories of proteins identified in an in vitro cellular ubiquitin affinity extract using shotgun peptide sequencing. *J Proteome Res* **2**, 394-404 (2003).
16. Hitchcock, A.L., Auld, K., Gygi, S.P. & Silver, P.A. A subset of membrane-associated proteins is ubiquitinated in response to mutations in the endoplasmic reticulum degradation machinery. *Proc Natl Acad Sci U S A* **100**, 12735-40 (2003).
17. Kirkpatrick, D.S., Weldon, S.F., Tsaprailis, G., Liebler, D.C. & Gandolfi, A.J. Proteomic identification of ubiquitinated proteins from human cells expressing His-tagged ubiquitin. *Proteomics* **5**, 2104-11 (2005).
18. Tagwerker, C. *et al.* A tandem affinity tag for two-step purification under fully denaturing conditions: application in ubiquitin profiling and protein complex identification combined with in vivocross-linking. *Mol Cell Proteomics* **5**, 737-48 (2006).
19. Jeon, H.B. *et al.* A proteomics approach to identify the ubiquitinated proteins in mouse heart. *Biochem Biophys Res Commun* **357**, 731-6 (2007).
20. Meierhofer, D., Wang, X., Huang, L. & Kaiser, P. Quantitative analysis of global ubiquitination in HeLa cells by mass spectrometry. *J Proteome Res* **7**, 4566-76 (2008).
21. Franco, M., Seyfried, N.T., Brand, A.H., Peng, J. & Mayor, U. A novel strategy to isolate ubiquitin conjugates reveals wide role for ubiquitination during neural development. *Mol Cell Proteomics* **10**, M110 002188 (2011).
22. Danielsen, J.M. *et al.* Mass spectrometric analysis of lysine ubiquitylation reveals promiscuity at site level. *Mol Cell Proteomics* **10**, M110 003590 (2011).
23. Shi, Y. *et al.* A data set of human endogenous protein ubiquitination sites. *Mol Cell Proteomics* **10**, M110 002089 (2011).
24. Lopitz-Otsoa, F. *et al.* Integrative analysis of the ubiquitin proteome isolated using Tandem Ubiquitin Binding Entities (TUBEs). *J Proteomics* **75**, 2998-3014 (2012).
25. Vasilescu, J., Smith, J.C., Ethier, M. & Figeys, D. Proteomic analysis of ubiquitinated proteins from human MCF-7 breast cancer cells by immunoaffinity purification and mass spectrometry. *J Proteome Res* **4**, 2192-200 (2005).
26. Matsumoto, M. *et al.* Large-scale analysis of the human ubiquitin-related proteome. *Proteomics* **5**, 4145-51 (2005).

27. Shimada, Y. *et al.* A protocol for immunoaffinity separation of the accumulated ubiquitin-protein conjugates solubilized with sodium dodecyl sulfate. *Anal Biochem* **377**, 77-82 (2008).
28. Igawa, T. *et al.* Isolation and identification of ubiquitin-related proteins from Arabidopsis seedlings. *J Exp Bot* **60**, 3067-73 (2009).
29. Argenzio, E. *et al.* Proteomic snapshot of the EGF-induced ubiquitin network. *Mol Syst Biol* **7**, 462 (2011).
30. Akimov, V., Rigbolt, K.T., Nielsen, M.M. & Blagoev, B. Characterization of ubiquitination dependent dynamics in growth factor receptor signaling by quantitative proteomics. *Mol Biosyst* **7**, 3223-33 (2011).
31. Povlsen, L.K. *et al.* Systems-wide analysis of ubiquitylation dynamics reveals a key role for PAF15 ubiquitylation in DNA-damage bypass. *Nat Cell Biol* **14**, 1089-98 (2012).
32. Kim, W. *et al.* Systematic and quantitative assessment of the ubiquitin-modified proteome. *Mol Cell* **44**, 325-40 (2011).
33. Wagner, S.A. *et al.* A proteome-wide, quantitative survey of in vivo ubiquitylation sites reveals widespread regulatory roles. *Mol Cell Proteomics* **10**, M111 013284 (2011).
34. Xu, G., Paige, J.S. & Jaffrey, S.R. Global analysis of lysine ubiquitination by ubiquitin remnant immunoaffinity profiling. *Nat Biotechnol* **28**, 868-73 (2010).
35. Udeshi, N.D. *et al.* Methods for quantification of in vivo changes in protein ubiquitination following proteasome and deubiquitinase inhibition. *Mol Cell Proteomics* **11**, 148-59 (2012).
36. Hartwell, L.H., Hopfield, J.J., Leibler, S. & Murray, A.W. From molecular to modular cell biology. *Nature* **402**, C47-52 (1999).
37. Nielsen, M.L. *et al.* Iodoacetamide-induced artifact mimics ubiquitination in mass spectrometry. *Nat Methods* **5**, 459-60 (2008).
38. Wilm, M. *et al.* Femtomole sequencing of proteins from polyacrylamide gels by nano-electrospray mass spectrometry. *Nature* **379**, 466-9 (1996).
39. Cox, J. *et al.* A practical guide to the MaxQuant computational platform for SILAC-based quantitative proteomics. *Nat Protoc* **4**, 698-705 (2009).
40. Cox, J. *et al.* Andromeda: a peptide search engine integrated into the MaxQuant environment. *J Proteome Res* **10**, 1794-805 (2011).
41. Warde-Farley, D. *et al.* The GeneMANIA prediction server: biological network integration for gene prioritization and predicting gene function. *Nucleic Acids Res* **38**, W214-20 (2010).
42. Cline, M.S. *et al.* Integration of biological networks and gene expression data using Cytoscape. *Nat Protoc* **2**, 2366-82 (2007).
43. Newton, K. *et al.* Ubiquitin chain editing revealed by polyubiquitin linkage-specific antibodies. *Cell* **134**, 668-78 (2008).
44. Hjerpe, R. *et al.* Efficient protection and isolation of ubiquitylated proteins using tandem ubiquitin-binding entities. *EMBO Rep* **10**, 1250-8 (2009).
45. Fujimuro, M., Sawada, H. & Yokosawa, H. Production and characterization of monoclonal antibodies specific to multi-ubiquitin chains of polyubiquitinated proteins. *FEBS Lett* **349**, 173-80 (1994).
46. Bebington, C., Bell, S.C., Doherty, F.J., Fazleabas, A.T. & Fleming, S.D. Localization of ubiquitin and ubiquitin cross-reactive protein in human and baboon endometrium and decidua during the menstrual cycle and early pregnancy. *Biol Reprod* **60**, 920-8 (1999).
47. Huang da, W., Sherman, B.T. & Lempicki, R.A. Systematic and integrative analysis of large gene lists using DAVID bioinformatics resources. *Nat Protoc* **4**, 44-57 (2009).
48. Nikolov, M., Schmidt, C. & Urlaub, H. Quantitative mass spectrometry-based proteomics: an overview. *Methods Mol Biol* **893**, 85-100 (2012).
49. Schwertman, P. *et al.* UV-sensitive syndrome protein UVSSA recruits USP7 to regulate transcription-coupled repair. *Nat Genet* **44**, 598-602 (2012).
50. Nakazawa, Y. *et al.* Mutations in UVSSA cause UV-sensitive syndrome and impair RNA polymerase IIo processing in transcription-coupled nucleotide-excision repair. *Nat Genet* **44**, 586-92 (2012).
51. Zhang, X. *et al.* Mutations in UVSSA cause UV-sensitive syndrome and destabilize ERCC6 in transcription-coupled DNA repair. *Nat Genet* **44**, 593-7 (2012).

3

QUANTITATIVE PROTEOMIC ANALYSIS REVEALS CHANGES IN UBIQUITINATED PROTEIN COMPLEXES WITHIN THE UV-INDUCED DDR

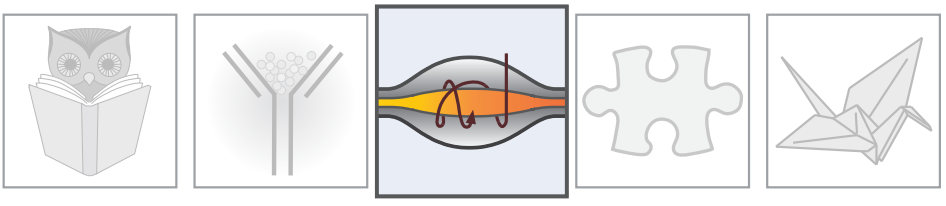

Petra Schwertman[1], Dick H W Dekkers[2], Jeroen A A Demmers[2], Wim Vermeulen[1] & Jurgen A Marteijn[1,]

[1]Department of Genetics and Netherlands Proteomics Centre, Centre for Biomedical Genetics, Erasmus University Medical Centre, 3015 GE Rotterdam, The Netherlands
[2]Proteomics Centre, Erasmus University Medical Centre, 3015 GE Rotterdam, The Netherlands

4

UV-SENSITIVE SYNDROME PROTEIN UVSSA RECRUITS USP7 TO REGULATE TRANSCRIPTION-COUPLED REPAIR

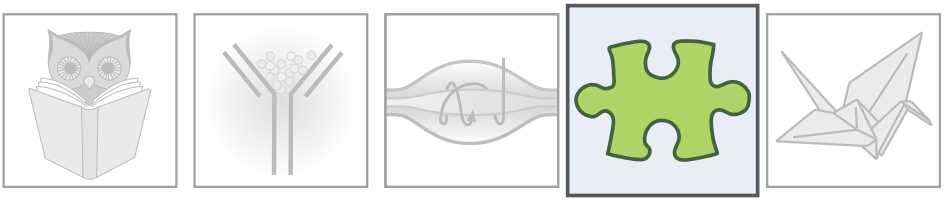

Petra Schwertman[1], Anna Lagarou[2], Dick H.W. Dekkers[3], Anja Raams[1], Adriana C. van der Hoek[1], Charlie Laffeber[1], Jan H.J. Hoeijmakers[1], Jeroen A.A. Demmers[3], Maria Fousteri[2], Wim Vermeulen[1,*] and Jurgen A. Marteijn[1,*]

[1]Department of Genetics and Netherlands Proteomics Centre, Centre for Biomedical Genetics, Erasmus University Medical Centre, 3015 GE Rotterdam, The Netherlands
[2]Institute of Molecular Biology and Genetics, Biomedical Sciences Research Centre Alexander Fleming, 16672 Vari, Athens, Greece
[3]Proteomics Centre, Erasmus University Medical Centre, 3015 GE Rotterdam, The Netherlands

* corresponding authors

Published in Nature Genetics 2012 May; 44(5):598-602

ABSTRACT

Transcription-coupled nucleotide-excision repair (TC-NER) is a subpathway of NER that efficiently removes the highly toxic RNA polymerase II blocking lesions in DNA. Defective TC-NER gives rise to the human disorders Cockayne syndrome and UV-sensitive syndrome ($UV^{S}S$)[1]. NER initiating factors are known to be regulated by ubiquitination[2]. Using a SILAC-based proteomic approach, we identified UVSSA (formerly known as KIAA1530) as part of a UV-induced ubiquitinated protein complex. Knockdown of *UVSSA* resulted in TC-NER deficiency. *UVSSA* was found to be the causative gene for $UV^{S}S$, an unresolved NER-deficiency disorder[3]. The UVSSA protein interacts with elongating RNA polymerase II, localizes specifically to UV-induced lesions, resides in chromatin-associated TC-NER complexes and is implicated in stabilizing the TC-NER master organizing protein ERCC6 (also known as CSB) by delivering the deubiquitinating enzyme USP7 to TC-NER complexes. Together these findings indicate that the UVSSA-USP7-mediated stabilization of ERCC6 represents a critical regulatory mechanism of TC-NER in restoring gene expression.

INTRODUCTION

Nucleotide-excision repair removes a wide range of DNA damage, including UV-induced lesions. Inherited NER defects lead to extreme cancer proneness (xeroderma pigmentosum) or dramatic premature aging (Cockayne syndrome), showing the clinical impact of NER[4]. NER is initiated by two damage recognition pathways: global genome NER (GG-NER) and transcription-coupled NER (TC-NER). DNA helix-distorting injuries located throughout the genome are repaired by GG-NER to avoid replication-induced mutations and resultant cancer. TC-NER targets transcription-blocking lesions to enable recovery of arrested transcription, thereby preventing damage-induced apoptosis and resultant aging. In addition, it was shown that TC-NER is also important in overcoming UV-induced transcription-associated mutations[5].

NER is regulated in response to UV irradiation by ubiquitination[2] of the process-initiating factors xeroderma pigmentosum group C (XPC)[6] and DNA damage-binding protein 2 (DDB2)[7] in GG-NER and Cockayne syndrome group B (CSB, also known as ERCC6) and the largest subunit of RNA polymerase II (RNA Pol II) in TC-NER[8-10]. However, how the entire pathway is controlled via ubiquitination remains enigmatic.

RESULTS AND DISCUSSION

To characterize the UV-induced ubiquitination network, we performed an unbiased proteomic analysis of differentially ubiquitinated protein complexes after UV irradiation. Using a ubiquitin-binding (FK2) resin and selecting for mono- and poly-ubiquitinated proteins[11], we achieved a strong and specific enrichment of endogenously ubiquitinated protein complexes (Supplementary Fig. 1a). With stable isotope labeling by amino acids in cell culture (SILAC)-based proteomics, we compared UV-treated and mock-treated cells and identified 50 upregulated and 13 downregulated proteins that were changed (by >1.5-fold) in response to UV (Fig. 1a). The prominent presence of four known ubiquitin-regulated NER factors, DDB2, XPC, RNA Pol II and ERCC6 (Fig. 1a)[6-9], at the very top of the list of enriched proteins shows the validity of our approach. The first unknown candidate was UVSSA (UV-stimulated scaffold protein A, encoded by a predicted gene *KIAA1530*[12]), which has been renamed, with support from the Human Gene Nomenclature Committee (HGNC) (Fig. 1a). UVSSA is a highly conserved 709 amino acid protein predicted to contain two conserved yet poorly characterized domains (Supplementary Fig. 1b,c): an N-terminal Vps27/Hrs/STAM (VHS) domain[13] and a C-terminal DUF2043 domain[14]. To verify UVSSA ubiquitination, we coexpressed HA-tagged ubiquitin (HA-Ub) and Flag-tagged UVSSA (UVSSA-Flag) in U2OS cells and identified mono-ubiquitinated UVSSA after both HA-Ub or Flag-UVSSA immunoprecipitation (Supplementary Fig. 1d,e). Unexpectedly, UVSSA ubiquitination did not increase in response to UV. As this screen was performed under non-denaturing conditions, it is possible that UVSSA was isolated as part of a UV-induced ubiquitinated protein complex and that it is implicated in the UV DNA damage response (DDR) independent of its own ubiquitination status. To test this possibility, we employed RNA interference to deplete *UVSSA* in NER-proficient U2OS cells (Supplementary Fig. 2a)

and observed clear UV hypersensitivity, similar to that achieved with knockdown of known NER factors (Fig. 1b). In addition, *UVSSA* knockdown resulted in IlludinS hypersensitivity (Fig. 1c), indicative of a role of UVSSA in TC-NER but not in GG-NER, as this drug specifically

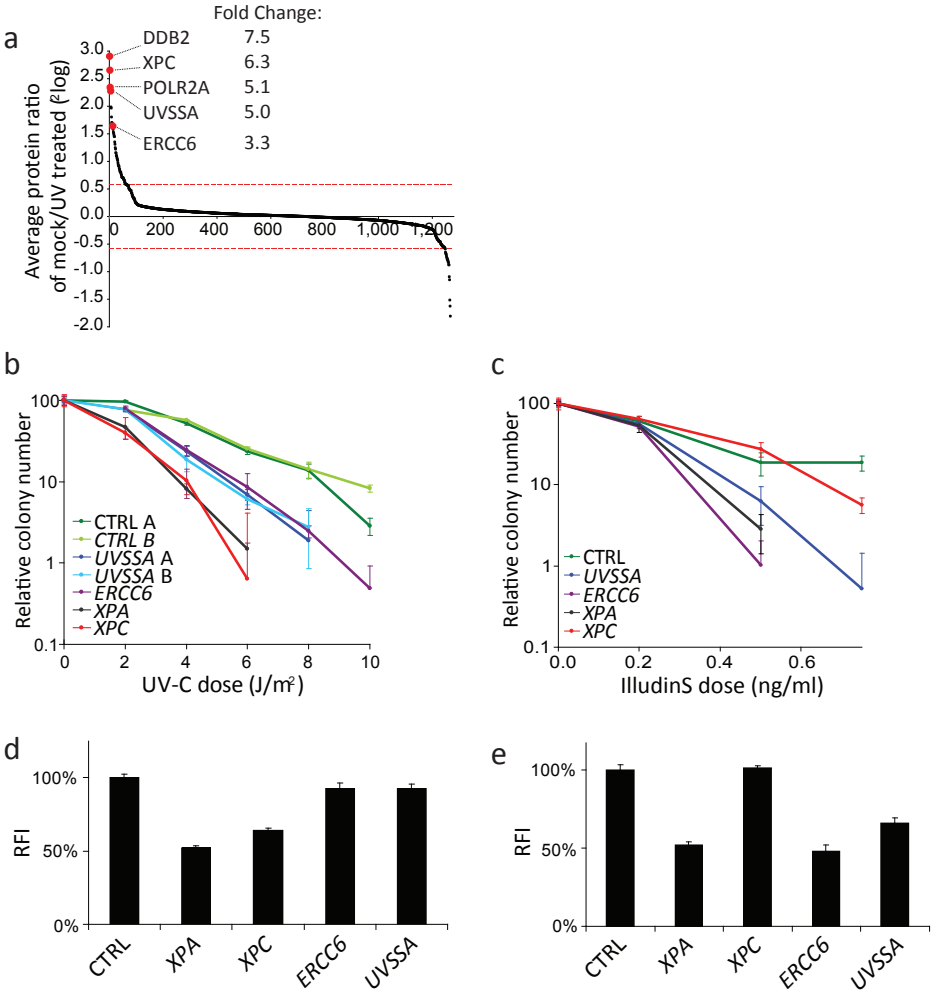

Figure 1: *UVSSA* knockdown results in reduced TC-NER activity.
(**a**) S-curve of the average $\log_2$ SILAC ratio of the forward and reverse experiment of ubiquitin (FK2 antibody) binding proteins 1 h after UV-C exposure (16 J/m²). The fold change of the SILAC ratio of NER proteins known to be ubiquitinated upon UV exposure and of UVSSA are indicated. (**b**,**c**) Sensitivity of U2OS cells with small hairpin RNA (shRNA)- or siRNA-mediated knockdown of the indicated factors to UV-C irradiation (**b**) and IlludinS (**c**), as determined by colony-forming ability (mean ± s.d.). (**d**) UDS determined by 5-ethynyl-2'-deoxyuridine (EdU) incorporation for 3 h after UV-C exposure (16 J/m²) in primary VH10 cells after siRNA-mediated knockdown of the indicated factors. (**e**) RRS after UV-induced inhibition, with 2 h of pulse labeling with 5-ethynyl uridine (EU), 16 h after UV-C exposure (12 J/m²) in U2OS cells with siRNA-mediated knockdown of the indicated factors. In **d** and **e**, n>200 cells per sample. RFI, relative fluorescence intensity (mean ± s.e.m).

sensitizes TC-NER-deficient cells[15]. The specific role of UVSSA in TC-NER was further shown, as knockdown resulted in a clear reduction of recovery of RNA synthesis (RRS) after UV irradiation, a measure that is specific for TC-NER[16], whereas no effect was found on UV-induced DNA repair synthesis (UDS), which is mainly a measure for GG-NER efficiency[16] (Fig. 1d,e and Supplementary Fig. 2b). Together, these data show that UVSSA is specifically implicated in TC-NERThe specific TC-NER deficiency after *UVSSA* knockdown strongly parallels the cellular TC-NER defect of individuals with UV-sensitive syndrome (UV^{S}S)[3,17]. UV^{S}S is a rare autosomal recessive disorder characterized by photosensitivity and mild freckling but, in contrast to Cockayne syndrome, occurs without neurological abnormalities. UV^{S}S is genetically heterogeneous, which is caused by mutations in either *ERCC6*, *ERCC8* (*CSA*) or the previously unknown UV^{S}SA causal gene[3,17-19]. To test whether UVSSA was the causative gene of UV^{S}S, we expressed differently tagged UVSSA proteins (Supplementary Fig. 2c) in the UV^{S}S group A (UV^{S}S-A) cell line TA-24[17]. UVSSA expression restored UV and IlludinS sensitivity (Fig. 2a,b) and RRS deficiency (Fig. 2c,d) to wild-type levels. In addition, immunoblot analysis showed that the UVSSA protein was absent in UV^{S}S-A cells relative to GG-NER-deficient (XP-C) or TC-NER-deficient (CS-B) cells (Fig. 2e). Together with mutational analysis of *UVSSA* in accompanying papers by Zhang *et al.*[20] and Nakazawa *et al.*[21], our data show that *UVSSA* is the causative gene in UV-sensitive syndrome and also establish that the encoded protein is a new TC-NER factor.

To investigate the *in vivo* role of UVSSA, we measured the dynamic association of UVSSA with NER in living cells. Green fluorescent protein (GFP)-tagged UVSSA, which was shown to be biologically active (Fig. 2a-d), accumulated at local UV-C DNA damage (LUD). LUD was either induced by a 266 nm UV-C laser[22] (Fig. 3a,b) or by irradiation with a 254 nm UV-C lamp through a microporous filter[23] (Supplementary Fig. 3a,b). Recruitment kinetics of GFP-UVSSA to LUD were strikingly similar to those of the TC-NER factor ERCC6 but were markedly different from the assembly rate of the GG-NER factors DDB2 and XPC (Fig. 3a,b). Inhibition of transcription by α-amanitin substantially attenuated the association of GFP-UVSSA with LUD (Fig. 3a,b), consistent with a role of UVSSA in TC-NER. UVSSA still accumulated at LUD in XP-C, XP-A, CS-A and CS-B cells (Fig. 3c), indicating that UVSSA accumulates early in the TC-NER process. Our ubiquitinome analysis, performed under non-denaturing conditions, showed that UVSSA was enriched to the same extent as RNA Pol II (fivefold; Fig. 1a), which is known to be poly-ubiquitinated in response to UV[8,10]. This might suggest that UVSSA is copurified as part of an RNA Pol II-containing protein complex, such as lesion-stalled elongating RNA Pol II. To test this possibility, we compared the mobility of GFP-UVSSA by measuring fluorescence recovery after photobleaching (FRAP) in the presence of different transcription inhibitors. The DNA-intercalating drug actinomycin D, which strongly immobilizes GFP-RNA Pol II as a result of stalling at intercalating molecules[24], also resulted in immobilization of GFP-UVSSA (Fig. 3d), as was the case with GFP-ERCC6[25]. In contrast, a-amanitin released RNA Pol II from DNA, which also resulted in increased mobility of UVSSA. The opposing effects by these transcription inhibitors on GFP-UVSSA mobility in living cells cannot be caused by an indirect UVSSA interaction with RNA Pol II via ERCC6[25], as similar effects were found in CS-B cells (Supplementary Fig. 3c).

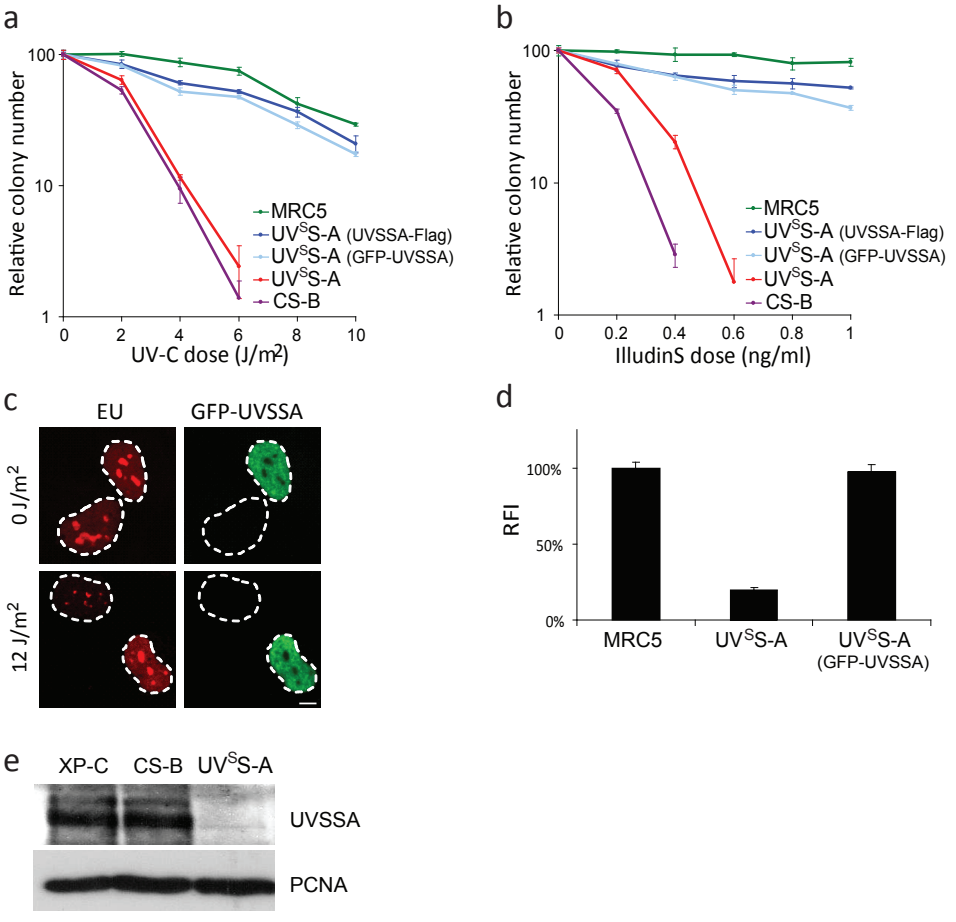

Figure 2. UVSSA expression rescues TC-NER deficiency in UV^{S}S-A (TA-24) cells.
(a, b) Colony survival of NER-proficient MRC5 cells, TC-NER-deficient CS-B (CS1AN) cells and the cell lines from subjects with UV^{S}S-A (TA-24) after UV-C irradiation (a) and IlludinS treatment (b). Expression of Flag- or GFP-tagged UVSSA rescues the UV-sensitive phenotype of UV^{S}S-A cells (mean ± s.d.). (c) *In situ* transcription in UV^{S}S-A cells with and without expression of GFP-UVSSA, before and 16 h after UV-C exposure (12 J/m^2), as measured by EU pulse labeling. Scale bar, 7 μm. (d) RRS activity of MRC5, UV^{S}S-A and GFP-UVSSA-expressing UV^{S}S-A cells using 2 h of pulse labeling with EU, 16 h after UV-C exposure (12 J/m^2) (n>200 cells, mean ± s.e.m.). RFI, relative fluorescence intensity. (e) Immunoblot analysis of UVSSA in chromatin fractions of XP-C (XP4PA), CS-B (CS1AN) and UV^{S}S-A (TA-24) cells. PCNA staining was used as loading control.

Because these findings argue for an interaction of UVSSA with the protein complex containing the elongating form of RNA Pol II (RNA Pol IIo), we performed coimmunoprecipitation experiments. Indeed, UVSSA-Flag coprecipitated with GFP-RNA Pol II in U2OS cells in equal amounts before or after UV damage (Fig. 3e). In addition, using a specialized chromatin immunoprecipitation (ChIP) procedure aimed at revealing endogenous TC-NER interacting proteins[26], we found that also chromatin-bound RNA Pol IIo

also interacts with UVSSA in a UV-independent manner (Supplementary Fig. 3d) in UVSSA-expressing UV^{S}S-A and CS-B cells. This UV-independent UVSSA-RNA Pol II interaction explains the enrichment of UVSSA in our ubiquitin screen after UV irradiation (Fig. 1a), as this protein will be copurified by virtue of the enhanced ubiquitination of RNA Pol IIo in response to UV[8], thereby explaining the similar SILAC ratio for both proteins. Together these data suggest that UVSSA dynamically interacts with active transcription complexes.

To examine whether UVSSA is also present in active, chromatin-bound TC-NER complexes via its interaction with RNA Pol IIo we performed ChIP experiments with antibodies against HGMN1, a chromatin remodeler that is enriched in lesion-stalled TC-NER complexes[26]. This analysis revealed a clear UV-dependent interaction of endogenous UVSSA with active chromatin-bound TC-NER complexes in TC-NER-proficient cells (Fig. 3f). The UVSSA-HMGN1 interaction was absent in CS-B cells, consistent with the notion that HMGN1 is not recruited to TC-NER complexes in the absence of ERCC6[26], showing that UVSSA only resides in HMGN1 complexes that are active in TC-NER. Using antibodies to ERCC6 for ChIP, we confirmed the UV-induced enrichment of UVSSA in active TC-NER complexes upon UV damage (Fig. 3g). Because UVSSA is targeted to active TC-NER complexes and is essential for efficient transcription restart after UV-damage[17], we tested whether UVSSA is involved in the recruitment of the TC-NER master organizer ERCC6 to sites of UV damage. Knockdown of *UVSSA* attenuated the assembly of GFP-ERCC6 on LUD (Fig. 4a), whereas it did not affect XPC (GG-NER) accumulation (Supplementary Fig. 4a). In addition, we noted that with *UVSSA* depletion in cells stably expressing GFP-ERCC6[25], the total level of GFP-ERCC6 fluorescence was decreased (Supplementary Fig. 4b). ERCC6 protein levels are controlled by the ubiquitin-proteasome system after UV damage[9]. To test whether UVSSA has an effect on ERCC6 stability, we quantified endogenous ERCC6 levels in UV^{S}S-A and GFP-UVSSA-complemented UV^{S}S-A cells at different time points after UV irradiation (Fig. 4b and Supplementary Fig. 4c). In UV^{S}S-A cells, we observed a clear proteasome- and UV-dependent decrease in ERCC6 levels compared to UVSSA-complemented UV^{S}S-A cells. The levels of RNA Pol II were equally reduced in both cell lines[8]; however, RNA Pol II reappeared 8 h after UV damage only in the complemented UV^{S}S-A cells. Whether this RNA Pol II recovery is a direct effect of UVSSA or an indirect consequence of rescued TC-NER remains to be determined.

In order to examine how UVSSA influences ERCC6 protein stability, we immunoprecipitated GFP-UVSSA and analyzed UVSSA-interacting proteins by mass spectrometry. Of note, we identified the deubiquitinating enzyme ubiquitin carboxyl-terminal hydrolase 7 (USP7, also called HAUSP) that is known to have various functions in DDR[27-30], as one of the most prominent interacting partners of UVSSA (Supplementary Fig. 4d). This interaction was confirmed by coimmunoprecipitation of UVSSA-Flag with Myc-USP7 (Fig. 4c). Moreover, we showed that endogenous USP7 resides in chromatin immunoprecipitated TC-NER complexes in a UV- and UVSSA-dependent manner (Fig. 4d and Supplementary Fig. 5a,b). Like the UVSSA-RNA Pol II interaction, the UVSSA-mediated USP7-RNA Pol II interaction is not increased after UV damage (Supplementary Fig. 5c). This suggests that USP7 is recruited to TC-NER complexes via its interaction with UVSSA. As UVSSA is missing in UV^{S}S-A cells, decreased ERCC6 stability after UV could be explained by the absence of USP7 deubiquitinating activity in the TC-NER

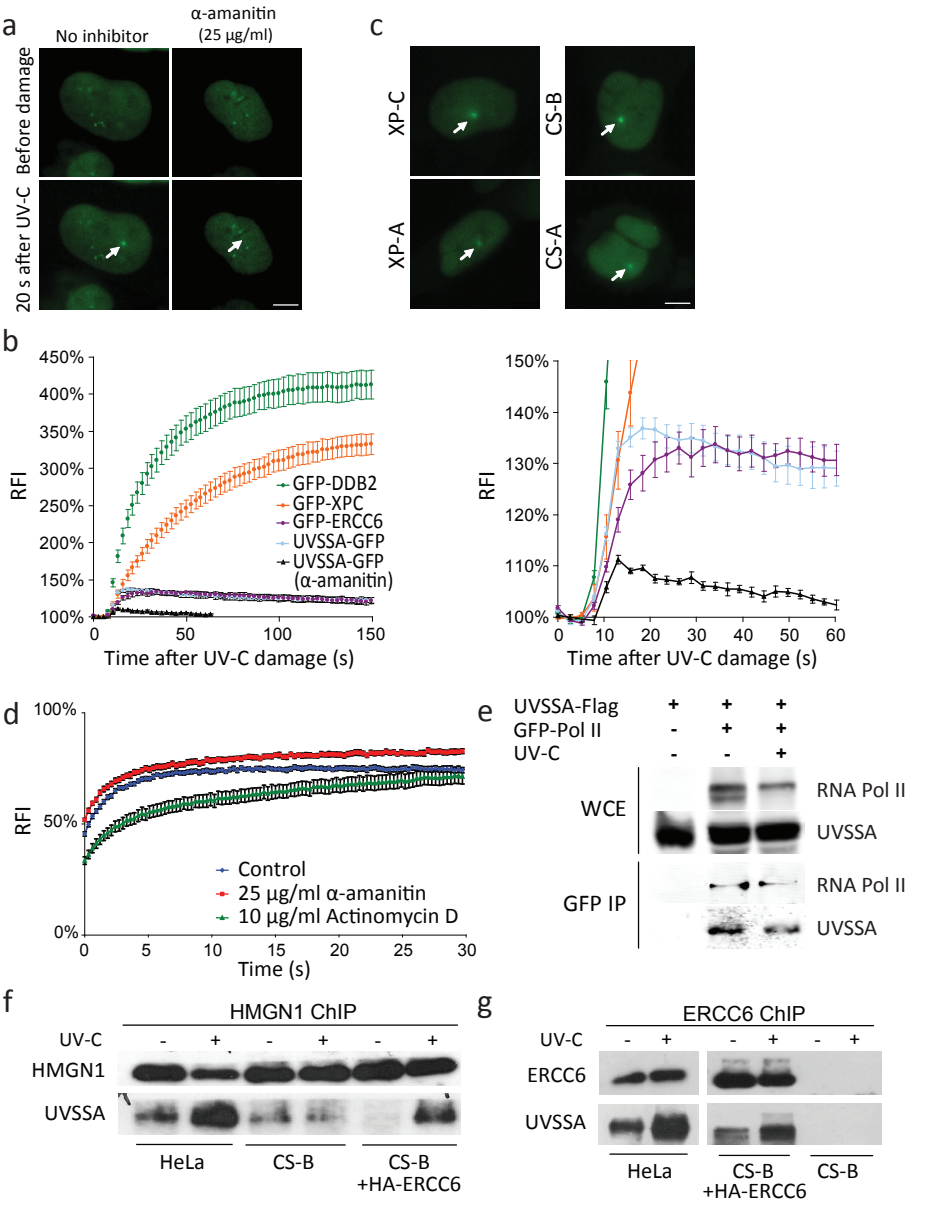

Figure 3. UVSSA is recruited to active TC-NER sites in a UV-damage- and transcription-dependent manner.

(a) LUD infliction (arrow) in MRC5 cells stably expressing UVSSA-GFP. Right, cells were pretreated with 25 μg/ml α-amanitin for 16 h. Scale bar, 7 μm. (b) GFP fluorescence intensities of the indicated proteins at LUD relative to pre-damage intensity were recorded over time using live-cell confocal imaging (n>10 cells, mean ± s.e.m.). Right, magnification of the early time points. (c) XP-C (XP4PA), XP-A (XP2OS), CS-B (CS1AN) and CS-A (CS3BE) cells stably expressing GFP-tagged UVSSA were exposed to UV-C (266 nm) laser-induced damage (arrows). Scale bar, 7 μm. (d) Graph of FRAP results in which

complex. Indeed, depletion of *USP7* by RNA interference (Supplementary Fig. 6a) caused a similar defect in RRS (Fig. 4e) and in reduction of ERCC6 levels (Fig. 4f and Supplementary Fig. 6b-d) after UV irradiation as UVSSA deficiency. These data suggest that USP7, recruited by UVSSA, has an important role in TC-NER. Additionally, the absence of further sensitization to the RRS defect by combined interference with *UVSSA* and *USP7* expression (Fig. 4e) suggests that these genes are epistatic.

In summary, within our mass spectrometry analysis of the UV-induced ubiquitinome, we identified an uncharacterized protein (UVSSA), which was highly enriched upon UV irradiation in immunopurified ubiquitinated protein complexes. Functional analysis indicated that UVSSA is a new factor implicated in TC-NER and, of note, is the causative gene in the unresolved UV^{S}S-A NER disorder. Two accompanying studies aimed at finding the genetic defect in UV^{S}S-A also identified *UVSSA* as the gene mutated in individuals with UV^{S}S-A[20,21]. Their further functional analysis is consistent with our observation that UVSSA has an important role in TC-NER and is part of the protein complex containing the elongating form of RNA Pol II. Our data argue for a UV-independent UVSSA-RNA Pol IIo interaction. In contrast to GFP-UVSSA, we were not able to observe RNA Pol IIo accumulation at LUD with current technology. The transient or low-affinity interaction between UVSSA and RNA Pol IIo might be stabilized upon UV irradiation, explaining the UV dependency observed in native immunoprecipitations[20] and the UV independence of the fixed interactions by cross-linking in ChIP shown here.

We propose a model (Supplementary Fig. 6f) in which one of the key functions of UVSSA in TC-NER is to protect ERCC6 against UV-induced degradation, by targeting the deubiquitinating enzyme USP7 to lesion-stalled RNA Pol II complexes. Of note, overexpression of ERCC6 in UV^{S}S-A cells did not correct the TC-NER defect (Supplementary Fig. 6e), suggesting that the reduced levels of ERCC6 observed in UV^{S}S-A cells is not sufficient to explain the UV^{S}S phenotype. This suggests that the deubiquitination of ERCC6 by UVSSA is an essential step for proper TC-NER, either to provide an increased time frame for this key assembly factor to orchestrate TC-NER complex formation or to inhibit a ubiquitin-mediated functional change in ERCC6. In cells with *UVSSA* knockdown, reduced interaction was observed between RNA Pol IIo and ERCC6 (Fig. 4d). Whether this reduced interaction is a direct consequence or is independent of the ERCC6 ubiquitination remains to be elucidated. Either way, our data show the importance of the delicate ERCC6 ubiquitination equilibrium during TC-NER by counteracting TC-NER-specific E3 ligases[9,31]. USP7 has multiple roles in

▶ the relative fluorescence recovery after bleaching is plotted against the time after UVSSA-expressing MRC5 cells were untreated or treated with 25 μg/ml α-amanitin (16 h) or 10 μg/ml actinomycin D (1 h). RFI, relative fluorescence intensity. (**e**) U2OS cells cotransfected with GFP-RNA Pol II and UVSSA-Flag were subjected to GFP immunoprecipitation. Cells were UV-C irradiated (60 J/m^2) 1 h before cell lysis. WCE, whole-cell extract; IP, immunoprecipitate. (**f**,**g**) ChIP analysis of *in vivo* cross-linked HeLa, CS-B (CS1AN) or HA-ERCC6-complemented CS-B cells, which were subjected to HMGN1 (**f**) or ERCC6 (**g**) ChIP 1 h after mock or UV-C treatment (20 J/m^2). Immunoblot analysis of the coimmunoprecipitated proteins was performed with the indicated antibodies.

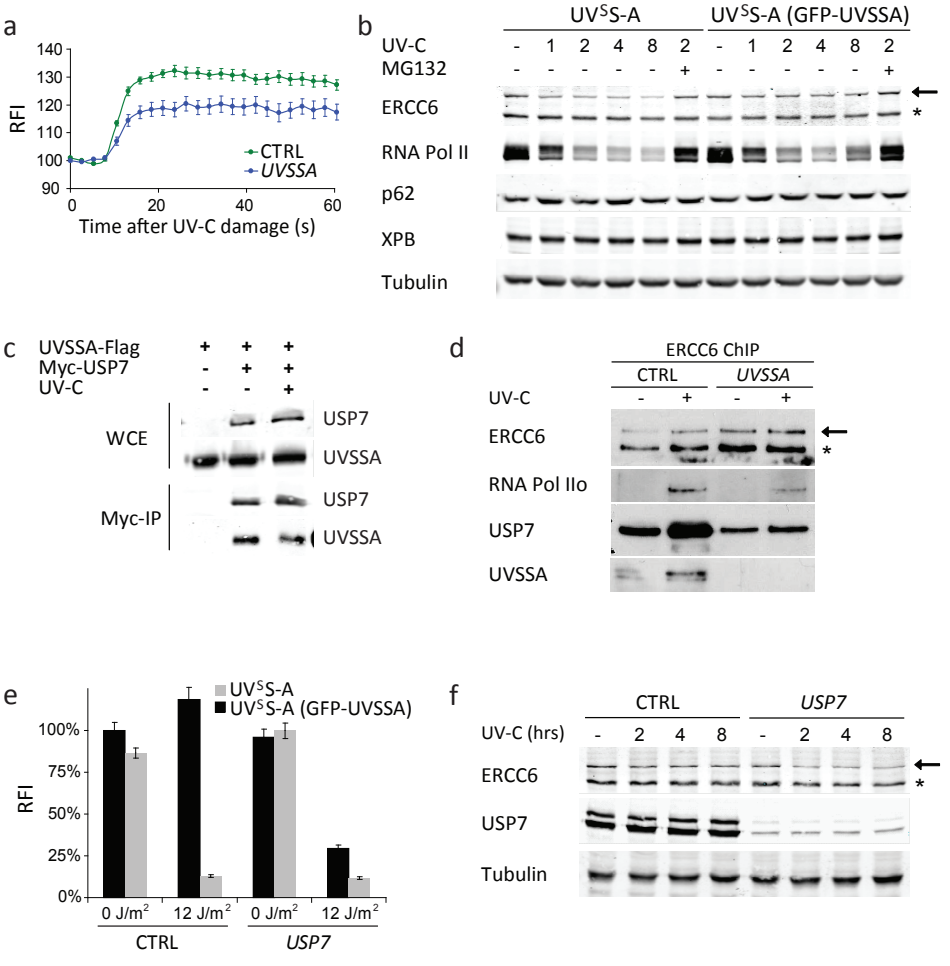

Figure 4. UVSSA-dependent recruitment of USP7 to active TC-NER complexes stabilizes ERCC6 and restores UV-inhibited RNA synthesis.

(**a**) GFP-ERCC6-complemented CS-B (CS1AN) cells transfected with the indicated siRNA were locally exposed to UV-C laser-induced damage. Relative fluorescence was followed in time at LUD (n>15 cells, mean ± s.e.m.). RFI, relative fluorescence intensity. (**b**) Immunoblot analysis of SDS lysates of TA-24 (UV^{S}S-A) and GFP-UVSSA-complemented TA-24 cells were analyzed with the indicated antibodies. Cells were recovered at the indicated times after UV-C (12 J/m^2) exposure. MG132 (50 μM) was added at the time of UV-C exposure. ERCC6 levels (arrow) were quantified relative to the ERCC6-PiggyBac Fusion protein[36] (asterisk) (Supplementary Fig. 4c). (**c**) U2OS cells cotransfected with Myc-USP7 and UVSSA-Flag were subjected to Myc immunoprecipitation. Cells were UV-C irradiated (20 J/m^2) 1 h before cell lysis. WCE, whole-cell extract, IP, immunoprecipitate. (**d**) U2OS cells stably expressing the indicated shRNA were subjected to ERCC6-specific ChIP followed by immunoblotting for the indicated proteins. (**e**) RRS activity of TA-24 (UV^{S}S-A) and GFP-UVSSA-complemented TA-24 cells transfected with the indicated siRNA before and 16 h after UV-C irradiation (12 J/m^2) (n>200 cells, mean ± s.e.m.). RFI, relative fluorescence intensity. (**f**) U2OS cells were transfected with control or *USP7* siRNA, harvested at the indicated time points after UV-C exposure (12 J/m^2) and stained for ERCC6, USP7 and Tubulin. ERCC6 levels (arrow) are quantified relative to those of the ERCC6-PiggyBac Fusion protein[36] (asterisk) (Supplementary Fig. 6b).

the DNA damage response[27-30], and its pleiotropic activity is even broader, targeting tumor suppressors, immune responders, viral proteins and epigenetic modulators[32]. An important role for UVSSA might be to deliver the deubiquitinating USP7 enzyme to TC-NER, thereby providing substrate specificity to this pleiotropic deubiquitinase. The implication of UVSSA in ubiquitination of the elongating form of RNA Pol II after UV-damage[21] seems to imply that UVSSA has functions in TC-NER beyond being a specific shuttle protein for USP7.

The causative genes for the two TC-NER defective disorders Cockayne syndrome and UV^{S}S (ERCC6, ERCC8 and UVSSA) are all cofactors of lesion-stalled RNA Pol II. However, the phenotypes of these two TC-NER deficiencies are strikingly different; Cockayne syndrome is characterized by severe neurological and developmental abnormalities in conjunction with UV sensitivity, whereas individuals with UV^{S}S mainly exhibit sun sensitivity, without any clear additional complications[1]. It has been proposed that this phenotypic difference is caused by the distinct abilities of affected individuals to process certain oxidative lesions: Cockayne syndrome cells are sensitive for oxidative base damage, whereas UV^{S}S cells are not[1,19,33-35]. This suggests that UVSSA and the subsequent deubiquitination of ERCC6 by USP7 are crucial for the execution of the complete NER process, but these seem to not be essential in processing oxidative damage in transcribed strands. Of course, the possibility is not excluded that additional functions of the Cockayne syndrome proteins also contribute to the severe Cockayne syndrome phenotype. The discovery of two new TC-NER factors, UVSSA and USP7, which are both implicated in regulating TC-NER activity, represents an important advance toward further elucidation of the transcription-coupled repair process.

METHODS

Cell lines and culture

For SILAC labeling, HeLa cells were cultured for 2 weeks in DMEM without lysine, arginine or leucine (AthenaES) supplemented with antibiotics, 10% dialyzed FCS (Invitrogen) and 105 µg/ml leucine (Sigma) and either 73 µg/ml light [$^{12}C_6$]-lysine and 42 µg/ml [$^{12}C_6$, $^{14}N_4$]-arginine (Sigma) or with heavy [$^{13}C_6$] lysine and [$^{13}C_6$, $^{15}N_4$]-arginine (Cambridge Isotope Laboratories) at 37°C and 5% CO_2.

U2OS, VH10 and the SV40-immortalized MRC5, TA-24 (UVSS-A), XP2OS (XP-A), XP4PA (XP-C), XP4PA (expressing GFP-XPC), CS3BE (CS-A), CS1AN (CS-B) and CS1AN (expressing GFP-ERCC6) cells were cultured in a 1:1 ratio of DMEM and Ham's F10 (Invitrogen) containing 10% FCS and antibiotics at 37°C and 5% CO_2. Medium was supplemented with hygromycin (25 µg/ml) for MRC5 (expressing UVSSA-GFP), TA-24 (expressing GFP-UVSSA) and TA-24 (expressing UVSSA-Flag) cells.

Cells were treated with 25 µg/ml α-amanitin (16 h), 10 µg/ml actinomycin D (1 h), or 50 µM MG132 (as indicated). DNA damage was inflicted by 24 h exposure to IlludinS[15] or by UV-C irradiation (254 nm; TUV Lamp, Phillips).

Plasmid constructs

The *UVSSA* cDNA was PCR amplified from a cDNA clone (BC110331) using the primers listed in Supplementary Table 1. The PCR product was cloned into pCR-Blunt-II-TOPO (Invitrogen)

and transferred into pENTR1A-GFP-N2 (Addgene, plasmid 19364) and pENTR1A-GFP-C1 (Addgene, plasmid 17396) using EcoRI-SacII sites or into pENTR4 (Addgene, plasmid 17424) using EcoRI-NotI sites[37]. Recombination into the pLenti CMV Hygro destination vector (Addgene, plasmid 17454)[37] was performed with the Gateway LR Clonase II Enzyme Mix (Invitrogen).

The GFP-RNA Pol II and Myc-USP7 constructs have been previously described[38,39]. DNA transfections were performed using Lipofectamine 2000 (Invitrogen) according to the manufacturer's instructions. Third-generation lentiviruses were made in HEK293T cells.

RNA interference

Sequences for siRNA oligonucleotides (Thermo Fisher Scientific) are shown in Supplementary Table 2. siRNA transfections were performed using RNAiMax (Invitrogen) or Hiperfect (Qiagen), according to the manufacturer's instructions. shRNAs from the MISSION shRNA library (Sigma) were used to make third-generation lentiviruses. Target sequences are provided in Supplementary Table 2.

Quantitative RT-PCR

Total RNA was isolated from siRNA-transfected or shRNA-transduced U2OS cells using the RNeasy mini kit (Qiagen). cDNA was synthesized using random hexamer primers and SuperScript II Reverse Transcriptase (Invitrogen).

UVSSA and *GAPDH* expression levels were analyzed using qRT-PCR with the TaqMan Gene Expression Assay using a Bio-Rad CFX96 device. *UVSSA* expression levels were normalized to *GAPDH* expression.

Antibodies

For immunoprecipitations, we used mouse monoclonal antibodies to mono-ubiquitinated and poly-ubiquitinated conjugates (FK2, BML-PW8810, Biomol) and Myc (9E10, sc-40, Santa Cruz Biotechnology) and Flag-M2 antibody conjugated to agarose beads (Sigma), HA-antibody conjugated to agarose beads (Sigma) and GFP antibody conjugated to agarose beads (ChromoTek). For ChIP, we used mouse monoclonal antibody to RNA Pol II (H5, Babco) and rabbit polyclonal antibodies to HMGN1 (Ab5212, Abcam) and ERCC6 (H-300, sc-25370, Santa Cruz Biotechnology).

For protein blots, we used monoclonal antibodies to GFP (Roche and Santa Cruz Biotechnology), CPD (TDM-2, MBL International), HA (3F10, Roche), RNA Pol II (8wG16, Ab5095, Abcam), XPA (Abcam) and P62 (3C9, kindly provided by J.M. Egly (Institut de Génétique et de Biologie Moléculaire et Cellulaire)). The polyclonal antibodies used were to Flag (F7425, Sigma), ubiquitin (Z0458, Dako), RNA Pol II (Ab5095, Abcam), Myc (9E10, sc-40, Santa Cruz Biotechnology), USP7 (A300-033A, Bethyl), ERCC6 (E-18, sc-10459, Santa Cruz Biotechnology), p89/XPB (S-19, sc-293, Santa Cruz Biotechnology), HMGN1 (Ab5212, Abcam), KIAA1530 (UVSSA) (NBP1-32598, Novus, and P-12, sc-138374, Santa Cruz Biotechnology) and XPC. Odyssey-compatible secondary antibodies were from Li-Cor, and horseradish peroxidase (HRP)-conjugated secondary antibodies were from Dako (to mouse and goat), Southern Biotech (to rabbit) and Sigma (to IgM).

Isolation of ubiquitinated protein complexes

SILAC-labeled HeLa cells were UV irradiated (16 J/m^2) or mock treated. Label swapping was performed to validate the biological findings, aid contaminant removal and exclude possible SILAC-derived differences. One hour after UV cells were washed twice in ice-cold PBS and harvested by scraping in RIPA buffer (PBS containing 1% NP-40, 0.5% sodium deoxycholate and 0.1% SDS) supplemented with 15 μM MG132 (Biomol), 10 mM N-Ethylmaleimide (Sigma), 20 μM PR-619 (LifeSensors) and Complete protease inhibitor cocktail (Roche). Lysates were centrifuged at 16,000*g* at 4°C for 15 min. Cleared UV treated and mock treated lysates were combined in a 1:1 ratio based on protein concentrations and added to the anti-ubiquitin resin (100 μl slurry per 5.3 mg of lysate) for 4 h at 4°C. The anti-ubiquitin resin was prepared by incubating 100 μl of 50% ProtG slurry (Pierce) with 87.5 μg of FK2 antibody (Biomol) for 40 min at room temperature, and four washes were performed with RIPA buffer. Protein complexes were eluted (after four washes with RIPA of lysate-bound resin) in two bead volumes of 4% SDS by shaking for 10 min at 1,000 rpm in an Eppendorf Thermomixer. The eluted sample was concentrated over 30-kDa spin columns (Millipore), supplemented with 2x Laemmli buffer and loaded onto 4-15% SDS-PAGE gradient gels (Jule).

Mass spectrometry

SDS-PAGE gel lanes were cut into 2-mm slices and subjected to in-gel reduction with dithiothreitol, alkylation with iodoacetamide (98%; D4, Cambridge Isotope Laboratories) and digested with trypsin (sequencing grade; Promega), as described previously[40]. Nanoflow liquid chromatography tandem mass spectrometry (LC-MS/MS) was performed on an 1100 series capillary liquid chromatography system (Agilent Technologies) coupled to an LTQ-Orbitrap XL mass spectrometer (Thermo Scientific) operating in positive mode. Peptide mixtures were trapped on a ReproSil C18 reversed phase column (Dr Maisch; 1.5 cm × 100 μm) at a rate of 8 μl/min. Peptides were separated on a ReproSil-C18 reversed-phase column (Dr Maisch; 15 cm × 50 μm) using a linear gradient of 0-80% acetonitrile (in 0.1% formic acid) during 170 min at a rate of 200 nl/min using a splitter. The elution was directly sprayed into the electrospray ionization (ESI) source of the mass spectrometer. Spectra were acquired in continuum mode; fragmentation of the peptides was performed in data-dependent mode.

Raw mass spectrometry data were analyzed with MaxQuant software (version 1.1.1.25)[41]. A false discovery rate of 0.01 for proteins and peptides and a minimum peptide length of 6 amino acids were set. The Andromeda search engine[42] was used to search the tandem mass spectrometry (MS/MS) spectra against the International Protein Index (IPI) human database (release 3.68). A maximum of two missed cleavages and mass tolerance of 0.6 Da was allowed. Further modifications were cysteine carbamidomethylation-2D (fixed), protein methionine oxidation and lysine ubiquitination (variable). MaxQuant automatically quantified SILAC peptides and proteins. From the 2,586 identified proteins in the forward and reverse experiments, we removed 116 known contaminants and reverse hits, 411 proteins that had less than 2 quantitation events, 441 proteins that were only found in the forward or reverse experiment, 71 hits with opposite ratios (>1.25-fold) in the label-swap experiment and

311 proteins with background levels (<1.25-fold) in one of the label-swap experiments. The remaining 1,236 proteins were plotted on the S-curve (Fig. 1a).

For the identification of UVSSA interactors, the software package Scaffold (version 3_00_03, Proteome Software Inc.) was used to validate MS/MS based peptide and protein identifications. Peptide identifications were accepted at >95.0% probability with the Peptide Prophet algorithm[43]. Protein identifications assigned by the Protein Prophet algorithm[38,44] were accepted at >95.0% probability.

Clonogenic survival assay

Cells from indicated cell lines were seeded in triplicate in 6-well plates (400 cells/well) and treated with UV-C or IlludinS[15] (24 h exposure) 1 d after seeding. After 1 week, colonies were fixed and stained in 50% methanol, 7% acetic acid and 0.1% Coomassie blue.

Recovery of RNA synthesis and unscheduled DNA synthesis after UV irradiation

Fluorescence-based RRS and UDS were performed as described[16]. In short, for RRS, the cell lines were UV irradiated with 12 J/m^2 of UV-C. Transcription levels were determined 16 h after UV irradiation by 2 h of incubation with 5-ethynyl uridine (EU) incorporation. For UDS, VH10 cells were UV irradiated with 16 J/m^2 of UV-C 48 h after siRNA transfection. UDS was determined by 3 h of incubation with 5-ethynyl-2'-deoxyuridine (EdU) incorporation. RRS and UDS were quantified by determining fluorescent intensities of >200 cells with ImageJ software of images obtained with a Zeiss LSM700. The cells displayed in Figure 2c were stained with antibody to GFP (Abcam) after the RRS procedure to visualize GFP signal.

Coimmunoprecipitation

Cells expressing Flag-, Myc-, HA- and/or GFP-tagged proteins were treated 24 h after transfection with the indicated UV-C doses and/or with 50 μM MG132 and lysed in RIPA buffer supplemented with Complete protease inhibitor cocktail (Roche) after 1 h recovery. Lysates were incubated on ice for 10 min and were centrifuged at 16,000*g* for 15 min at 4°C. The supernatant was incubated for 4 h at 4°C with antibody-conjugated agarose beads. Beads were washed four times with RIPA buffer and eluted with one bead volume of 2x Laemmli SDS sample buffer at 95°C.

In vivo cross-linking and ChIP

The procedure for ChIP has been described previously[26]. Briefly, cells were mock treated or exposed to UV-C light (20 J/m^2) and left to recover for 1 h at 37°C and then cross-linked *in vivo* by 1% formaldehyde at 4°C. Cross-linked cells were lysed, and purified chromatin was sheared with the Bioruptor Sonicator (Diagenode) using cycles of 30 s on, 60 s off. ChIP was performed on chromatin fragments of 200-600 bp. Reversal of the cross-linking and elution of the precipitated proteins was performed by extended boiling in Laemmli SDS sample buffer, and eluted proteins were analyzed by protein blotting[26].

Live-cell confocal laser-scanning microscopy and immunofluorescence

Confocal laser-scanning microscopy images were obtained with a Leica SP5 confocal microscope using a 100x quartz objective. Kinetic studies of GFP-tagged UVSSA, ERCC6,

DDB2 and XPC accumulation were performed using UV-C (266 nm) laser irradiation, as described previously[22]. FRAP experiments were performed as described previously[45]. All FRAP data (average of >15 cells) were normalized to the average fluorescence before bleaching after removal of the background signal.

Immunofluorescence experiments were executed as described[46], with or without pre-extraction by a 20 s treatment with 0.5% Triton X-100 before fixation. GFP-tagged proteins were visualized by staining with an antibody to GFP.

ACKNOWLEDGMENTS

We thank R. Bernards and M. Epping for Myc-tagged USP7 expression construct, P. Verrijzer and A. Reddy for shUSP7 expressing lentivirus. We thank H. Slor for the TA-24sv40 cell line and N.G.J. Jaspers and H. Lans for discussions and critical reading of the manuscript. This work was funded by the Netherlands Genomics Initiative, NPCII (P.S.), 935.19.021 and 935.11.042 (W.V., C.L. and J.A.M.), Dutch Organization for Scientific Research ZonMW Veni Grant 917.96.120 (J.A.M.) and TOP grant 912.08.031 (W.V.), the Association for International Cancer Research 10-594 (W.V.), Cancer Genomics Centre and ERC (advanced research grant, J.H.J.H.).

AUTHOR CONTRIBUTIONS

D.H.W.D. and J.D. performed the mass spectrometry analyses, A.R. performed UDS and RRS experiments, A.C.H. performed IP experiments, C.L. provided technical assistance, M.F. designed and together with A.L. performed ChIP experiments. J.H.J.H. provided support, advice and helped writing the article. P.S. and J.A.M. performed experiments and generated reagents. W.V. and J.A.M. designed the study and supervised the project. W.V., J.A.M. and P.S. wrote the article. All authors discussed the results and commented on the manuscript.

SUPPLEMENTARY MATERIAL

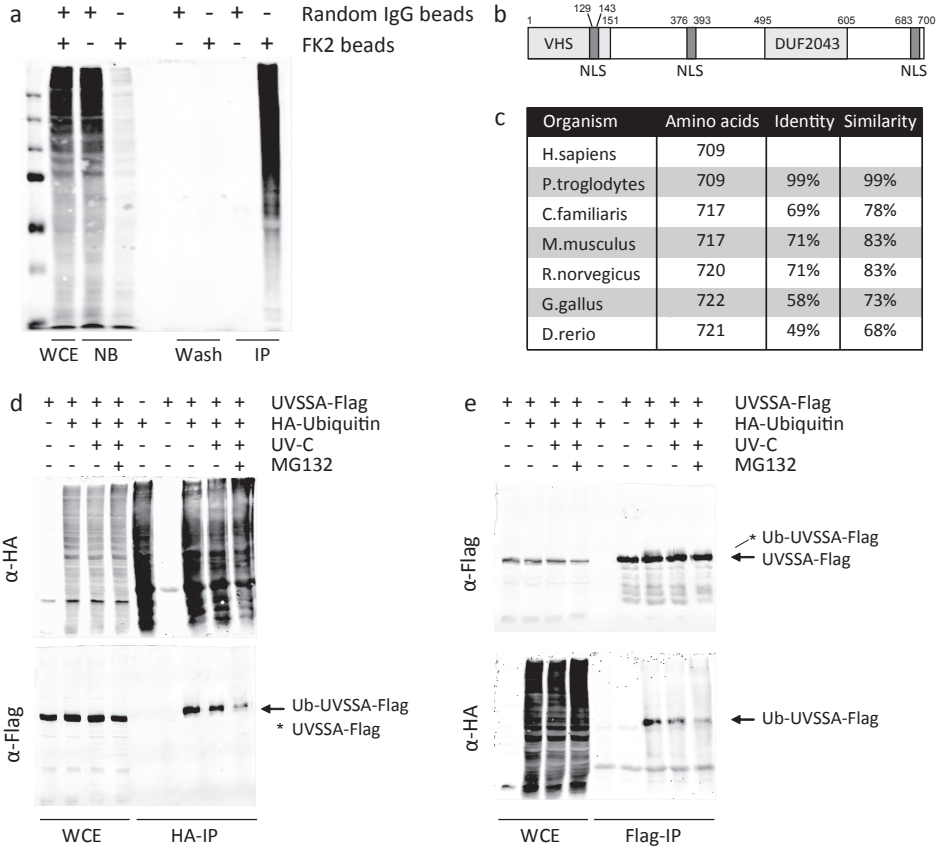

Organism	Amino acids	Identity	Similarity
H.sapiens	709		
P.troglodytes	709	99%	99%
C.familiaris	717	69%	78%
M.musculus	717	71%	83%
R.norvegicus	720	71%	83%
G.gallus	722	58%	73%
D.rerio	721	49%	68%

Supplementary Figure 1: UVSSA characteristics and ubiquitination.
(**a**) HeLa cell lysate was immunopurified by either random IgG, or FK2 loaded ProtG beads. WCE, whole-cell extract, NB, non-bound fraction, Wash, sample taken from last wash fraction, IP, immunoprecipitate. Samples are loaded in equal amounts compared to the WCE, IP sample is loaded twice the amount. The immunoblot is stained with a polyclonal antibody to ubiquitin (DAKO) and shows a high and specific enrichment of ubiquitinated proteins. (**b**) Putative protein domains of the human UVSSA protein, VHS- (predicted by Phyre2), NLS- (predicted by Prosite) and DUF2043-domains (predicted by PFAM) are indicated. (**c**) Homology of UVSSA protein between different species. (**d**,**e**) U2OS cells were transfected as indicated with HA-ubiquitin and UVSSA-Flag. 36 h after transfection cells were lysed and subjected to HA-IP (**d**) and Flag-IP (**e**). Cells were UV-C irradiated (20 J/m^2) 1 h before cell lysis, MG132 (50 μM) was added 1 h before UV-C exposure. Samples were analyzed on immunoblot using antibodies to Flag or HA. (arrow) indicates mono-ubiquitinated form of UVSSA, (asterisk) indicates unmodified form of UVSSA. WCE, whole-cell extract, IP, immunoprecipitate.

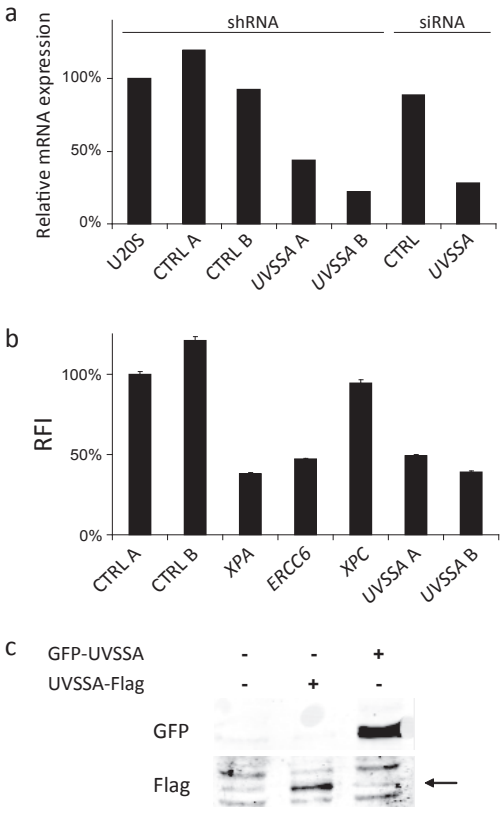

Supplementary Figure 2: UVSSA siRNA and expression controls.
(**a**) RNA was isolated from U20S cells stably expressing shRNA, or from U20S cells 48 h after siRNA transfection. UVSSA mRNA levels were analyzed using pre-designed TaqMan Assays and plotted as relative expression compared to untreated U2OS cells. (**b**) RRS after UV-induced inhibition, with 2 h of pulse labeling with 5-ethynyl uridine (EU), 16 h after UV-C exposure (12 J/m^2) in U2OS cells stably expressing shRNA targeting the indicated proteins (n > 150 cells, mean ± s.e.m.). (**c**) Expression of GFP-UVSSA and UVSSA-Flag in TA-24 (UV^{S}S-A) cells.

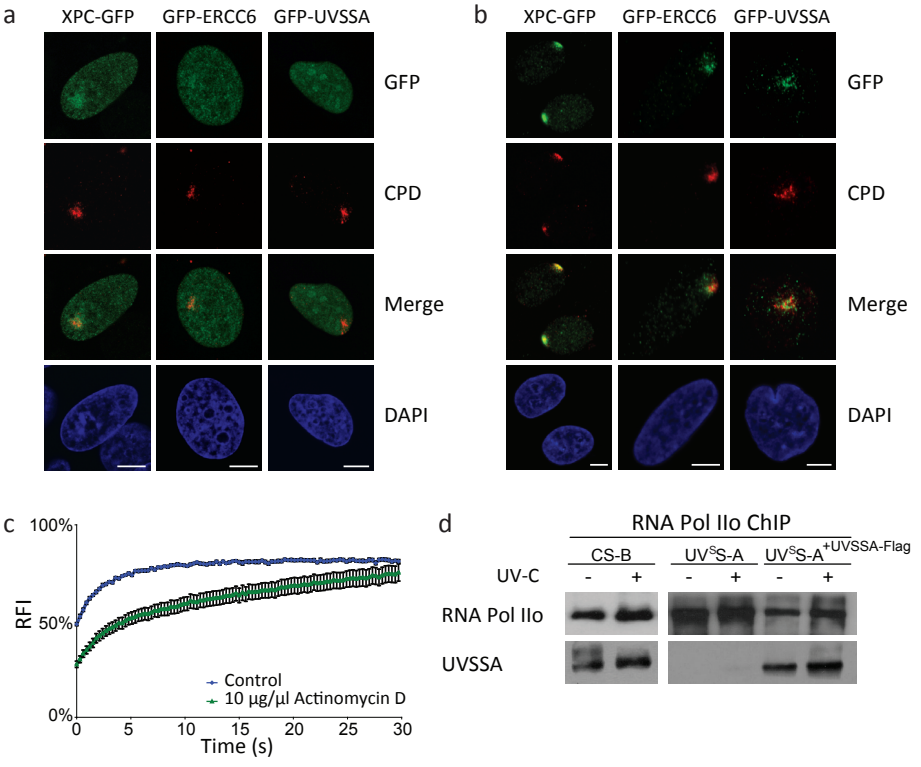

Supplementary Figure 3: UVSSA accumulation, kinetics and interaction with RNA Pol IIo.
(**a**,**b**) XPC-GFP-expressing XP-C (XP4PA) cells, GFP-ERCC6-expressing CS-B (CS1AN) cells and GFP-UVSSA-expressing UV^{S}S-A (TA-24) cells were locally UV irradiated with 60 J/m^2 (**a**) or 100 J/m^2 (**b**) UV-C. The local UV-irradiated area was visualized using CPD counterstaining. While XPC accumulates at LUD, no accumulation was visible for ERCC6 and UVSSA (**a**). However after pre-extraction (**b**) for 20 seconds with 0.5% Triton X-100 both GFP-ERCC6 and GFP-UVSSA accumulate at LUD. Scale bar, 7 µm. (**c**) FRAP graph in which the relative fluorescence recovery after bleaching is plotted against time of UVSSA-expressing CS-B (CS1AN) cells, untreated or treated with 10 µg/ml actinomycin D (1 h). RFI, relative fluorescence intensity. (**d**) ChIP analysis of CS-B (CS1AN), UV^{S}S-A (TA-24) and UVSSA-Flag-expressing UV^{S}S-A cells 1 h after UV-C treatment (20 J/m^2) or untreated were subjected to a RNA Pol IIo specific ChIP procedure and immunostained with an antibody to UVSSA.

a

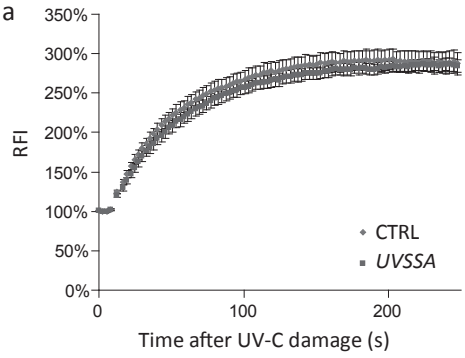

b

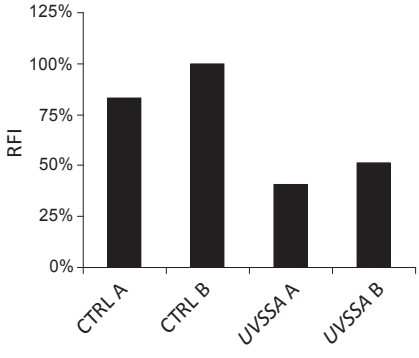

c

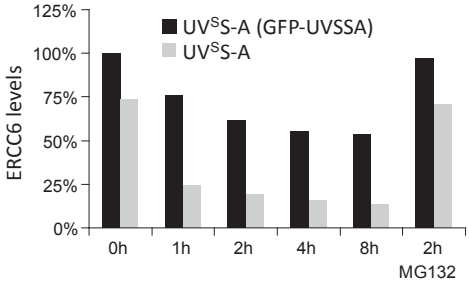

d

#	Identified Proteins	Accession Number	Unweighted Spectrum Count Values	
1	UVSSA	gi|7959327	22.08	624.76
2	GFP	gi|14595132	22.08	318.22
3	Heat shock cognate 71 kDa protein isoform 1	gi|5729877	45.17	89.53
4	Heat shock 70 kDa protein 1A/1B	gi|167466173	35.13	67.15
5	Polyubiquitin	gi|2627129	19.07	79.8
6	Histone H4	gi|32097	13.05	37.95
7	Desmoplakin I	gi|1147813	34.13	71.04
8	78 kDa glucose -regulated protein precursor	gi|16507237	17.06	24.33
9	Histone H2A type 1-D	gi|10800130	12.05	26.28
10	Ubiquitin carboxyl-terminal hydrolase 7	gi|150378533	0	23.36
			Background	GFP-UVSSA

Supplementary Figure 4: Effects of UVSSA on ERCC6 accumulation and protein levels and identified UVSSA-interactors.

(**a**) XPC-GFP-expressing XP-C (XP4PA) cells transfected with the indicated siRNA were locally exposed to UV-C (266 nm) laser-induced damage. Relative fluorescence was followed in time at the site of local damage (n>15 cells, mean ± s.e.m.). RFI, relative fluorescence intensity. (**b**) Relative fluorescence of GFP-ERCC6-expressing CS-B (CS1AN) cells transfected with the indicated siRNA were analyzed by FACS 48 h after transfection. (**c**) Immunoblot analysis quantification of ERCC6 levels of Fig. 4b using Odyssey software. Cells were recovered for the indicated times after UV-C (12 J/m^2) exposure. MG132 (50 μM) was added 30 min before UV-C exposure. ERCC6 levels are quantified relative to the ERCC6-PiggyBac Fusion protein[36]. (**d**) Table showing mass spectrometry analysis of a GFP-UVSSA pulldown experiment in MRC5 cells, sorted by highest Unweighted Spectrum Count after Scaffold analysis of proteins with a differential score compared to the negative control.

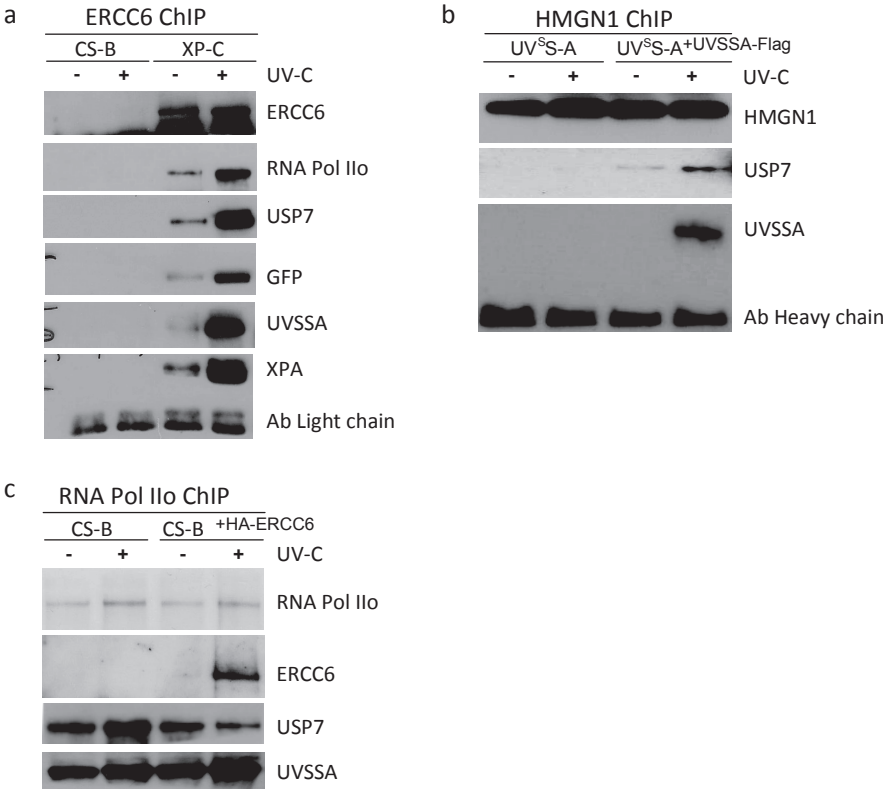

Supplementary Figure 5: ChIP experiments.
(a) Immunoblot analysis with the indicated antibodies of an ERCC6 ChIP procedure in XP-C (XP4PA) and CS-B (CS1AN) cells stably expressing GFP-UVSSA. Cells were UV-C irradiated (20 J/m^2) 1 h before fixing. (b) Immunoblot analysis with the indicated antibodies of a HMGN1 ChIP procedure in UV^{S}S-A (TA-24) and UVSSA-Flag-expressing UV^{S}S-A cells. Cells were UV-C irradiated (20 J/m^2) 1 h before fixing. (c) CS-B (CS1AN) and HA-ERCC6-expressing CS-B cells 1 h after UV-C treatment (20 J/m^2) or mock treated were subject to a RNA Pol IIo specific ChIP procedure and stained for ERCC6, UVSSA and USP7 on immunoblot.

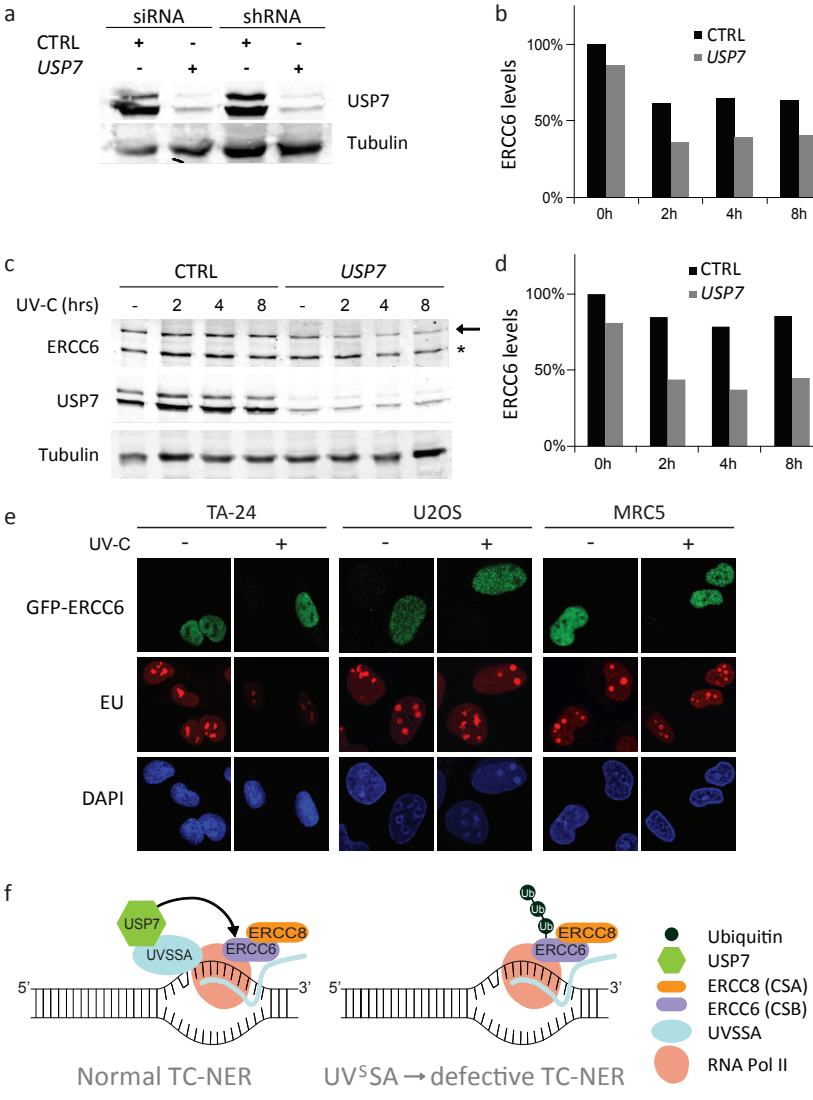

Supplementary Figure 6: Functional analysis and molecular model of TC-NER.
(**a**) Immunoblot of siRNA and shRNA knockdown of USP7 in U2OS cells 36 h after transfection. Tubulin staining was used as loading control. (**b**) Immunoblot analysis quantification of ERCC6 levels of Fig. 4f using Odyssey software. Cells were recovered for the indicated times after UV-C (12 J/m^2) exposure. ERCC6 levels are quantified relative to the ERCC6-PiggyBac Fusion protein[36]. (**c**) U2OS cells expressing Control or USP7 shRNA were harvested after the indicated time points after 12 J/m^2 UV-C and stained for ERCC6, USP7 and Tubulin. (**d**) Immunoblot analysis quantification of ERCC6 levels of Supplementary Fig. 6c using Odyssey software. ERCC6 levels are quantified relative to the ERCC6-PiggyBac Fusion protein[36]. (**e**) In situ transcription in UVSSA-deficient TA-24 (UV^{S}S-A) and NER-proficient MRC5 and U2OS cells with and without expression of GFP-ERCC6 before and 16 h after exposure with 12 J/m^2 UV-C for TA-24 and 6 J/m^2 UV-C for U20S and MRC5 cells, as measured by EU pulse labeling. Scale bar, 7 μm. (**f**) Model of UVSSA function in TC-NER. In normal cells ERCC6 is deubiquitinated by USP7, which is recruited by UVSSA. In UV^{S}S-A patient cells, mutated in UVSSA, USP7 is not targeted to the TC-NER complex resulting in increased ERCC6 ubiquitination and degradation.

Supplementary Table 1

	Site	Primer sequence
Forward	EcoRI	GAATTCTATGGATCAGAAACTTTCGAAG
Reverse GFP-UVSSA	SacII	CCGCGGTACTAGTTCAGTGCGTAGTTAAA
Reverse UVSSA-GFP	SacII	CCGCGGTAGTTCAGTGCGTAGTTAAACTG
Reverse UVSSA-FLAG	NotI	GCGGCCGCCTATTTGTCGTCATCGTCCTTG TAATCGTTCAGTGCGTAGTTAAACTGGTT

Supplementary Table 2

	Targeting gene	Targeting sequence
siRNA		
	XPA	5′-CUGAUGAUAAACACAAGCUUAUU-3′
	XPC	5′-CUGGAGUUUGAGACAUAUCUU-3′
	ERCC6 SMART pool	5′-GCAGUAACUUCUAAUCGAA-3′
		5′-GAAGCAAGGUUGUAAUAAA-3′
		5′-GCAUGUGUCUUACGAGAUA-3′
		5′-CAAACAGAGUUGUCAUCUA-3′
	UVSSA SMART pool	5′-GAUAAUCAGUUGACCAAAA-3′
		5′-GGCCAGGAGUUUAUAUGUA-3′
		5′-GCUCGUGGAUCCAGCGCUU-3′
		5′-GGUUCAGCACGGACGGAAU-3′
	USP7 SMART pool	5′-AAGCGUCCCUUUAGCAUUA-3′
		5′-GCAUAGUGAUAAACCUGUA-3′
		5′-UAAGGACCCUGCAAAUUAU-3′
		5′-GUAAAGAAGUAGACUAUCG-3′
	CTRL	siGENOME Non-targeting siRNA #5
shRNA		
	UVSSA (A)	5′-GCTTTGTCTATTACTGTGTTT-3′
	UVSSA (B)	5′-GCAGTAACCATGCTTTGTCTA-3′
	USP7	5′-CCAGCTAAGTATCAAAGGAAA-3′
		5′-CGTGGTGTCAAGGTGTACTAA-3′
	CTRL (A)	Empty Vector control (SHC001)
	CTRL (B)	Non-Target shRNA control (SHC002)

REFERENCES

1. Hanawalt, P.C. & Spivak, G. Transcription-coupled DNA repair: two decades of progress and surprises. *Nat Rev Mol Cell Biol* **9**, 958-70 (2008).
2. Bergink, S., Jaspers, N.G. & Vermeulen, W. Regulation of UV-induced DNA damage response by ubiquitylation. *DNA Repair (Amst)* **6**, 1231-42 (2007).
3. Itoh, T., Ono, T. & Yamaizumi, M. A new UV-sensitive syndrome not belonging to any complementation groups of xeroderma pigmentosum or Cockayne syndrome: siblings showing biochemical characteristics of Cockayne syndrome without typical clinical manifestations. *Mutat Res* **314**, 233-48 (1994).
4. Hoeijmakers, J.H. DNA damage, aging, and cancer. *N Engl J Med* **361**, 1475-85 (2009).
5. Hendriks, G. *et al.* Transcription-dependent cytosine deamination is a novel mechanism in ultraviolet light-induced mutagenesis. *Curr Biol* **20**, 170-5 (2010).
6. Sugasawa, K. *et al.* UV-induced ubiquitylation of XPC protein mediated by UV-DDB-ubiquitin ligase complex. *Cell* **121**, 387-400 (2005).
7. Rapic-Otrin, V., McLenigan, M.P., Bisi, D.C., Gonzalez, M. & Levine, A.S. Sequential binding of UV DNA damage binding factor and degradation of the p48 subunit as early events after UV irradiation. *Nucleic Acids Res* **30**, 2588-98 (2002).
8. Bregman, D.B. *et al.* UV-induced ubiquitination of RNA polymerase II: a novel modification deficient in Cockayne syndrome cells. *Proc Natl Acad Sci U S A* **93**, 11586-90 (1996).
9. Groisman, R. *et al.* CSA-dependent degradation of CSB by the ubiquitin-proteasome pathway establishes a link between complementation factors of the Cockayne syndrome. *Genes Dev* **20**, 1429-34 (2006).
10. Anindya, R., Aygun, O. & Svejstrup, J.Q. Damage-induced ubiquitylation of human RNA polymerase II by the ubiquitin ligase Nedd4, but not Cockayne syndrome proteins or BRCA1. *Mol Cell* **28**, 386-97 (2007).
11. Fujimuro, M., Sawada, H. & Yokosawa, H. Production and characterization of monoclonal antibodies specific to multi-ubiquitin chains of polyubiquitinated proteins. *FEBS Lett* **349**, 173-80 (1994).
12. Nagase, T., Kikuno, R., Ishikawa, K., Hirosawa, M. & Ohara, O. Prediction of the coding sequences of unidentified human genes. XVII. The complete sequences of 100 new cDNA clones from brain which code for large proteins in vitro. *DNA Res* **7**, 143-50 (2000).
13. Mizuno, E., Kawahata, K., Kato, M., Kitamura, N. & Komada, M. STAM proteins bind ubiquitinated proteins on the early endosome via the VHS domain and ubiquitin-interacting motif. *Mol Biol Cell* **14**, 3675-89 (2003).
14. Bateman, A., Coggill, P. & Finn, R.D. DUFs: families in search of function. *Acta Crystallogr Sect F Struct Biol Cryst Commun* **66**, 1148-52 (2010).
15. Jaspers, N.G. *et al.* Anti-tumour compounds illudin S and Irofulven induce DNA lesions ignored by global repair and exclusively processed by transcription- and replication-coupled repair pathways. *DNA Repair (Amst)* **1**, 1027-38 (2002).
16. Nakazawa, Y., Yamashita, S., Lehmann, A.R. & Ogi, T. A semi-automated non-radioactive system for measuring recovery of RNA synthesis and unscheduled DNA synthesis using ethynyluracil derivatives. *DNA Repair (Amst)* **9**, 506-16 (2010).
17. Spivak, G. UV-sensitive syndrome. *Mutat Res* **577**, 162-9 (2005).
18. Horibata, K. *et al.* Complete absence of Cockayne syndrome group B gene product gives rise to UV-sensitive syndrome but not Cockayne syndrome. *Proc Natl Acad Sci U S A* **101**, 15410-5 (2004).
19. Nardo, T. *et al.* A UV-sensitive syndrome patient with a specific CSA mutation reveals separable roles for CSA in response to UV and oxidative DNA damage. *Proc Natl Acad Sci U S A* **106**, 6209-14 (2009).
20. Zhang, X. *et al.* Mutations in UVSSA cause UV-sensitive syndrome and destabilize ERCC6 in transcription-coupled DNA repair. *Nat Genet* **44**, 593-7 (2012).
21. Nakazawa, Y. *et al.* Mutations in UVSSA cause UV-sensitive syndrome and impair RNA polymerase IIo processing in transcription-coupled nucleotide-excision repair. *Nat Genet* **44**, 586-92 (2012).
22. Dinant, C. *et al.* Activation of multiple DNA repair pathways by sub-nuclear damage

induction methods. *J Cell Sci* **120**, 2731-40 (2007).

23. Volker, M. *et al.* Sequential assembly of the nucleotide excision repair factors in vivo. *Mol Cell* **8**, 213-24 (2001).
24. Kimura, H., Sugaya, K. & Cook, P.R. The transcription cycle of RNA polymerase II in living cells. *J Cell Biol* **159**, 777-82 (2002).
25. van den Boom, V. *et al.* DNA damage stabilizes interaction of CSB with the transcription elongation machinery. *J Cell Biol* **166**, 27-36 (2004).
26. Fousteri, M., Vermeulen, W., van Zeeland, A.A. & Mullenders, L.H. Cockayne syndrome A and B proteins differentially regulate recruitment of chromatin remodeling and repair factors to stalled RNA polymerase II in vivo. *Mol Cell* **23**, 471-82 (2006).
27. Faustrup, H., Bekker-Jensen, S., Bartek, J., Lukas, J. & Mailand, N. USP7 counteracts SCFbetaTrCP- but not APCCdh1-mediated proteolysis of Claspin. *J Cell Biol* **184**, 13-9 (2009).
28. Khoronenkova, S.V., Dianova, II, Parsons, J.L. & Dianov, G.L. USP7/HAUSP stimulates repair of oxidative DNA lesions. *Nucleic Acids Res* **39**, 2604-9 (2011).
29. Li, M. *et al.* Deubiquitination of p53 by HAUSP is an important pathway for p53 stabilization. *Nature* **416**, 648-53 (2002).
30. Meulmeester, E. *et al.* Loss of HAUSP-mediated deubiquitination contributes to DNA damage-induced destabilization of Hdmx and Hdm2. *Mol Cell* **18**, 565-76 (2005).
31. Wei, L. *et al.* BRCA1 contributes to transcription-coupled repair of DNA damage through polyubiquitination and degradation of Cockayne syndrome B protein. *Cancer Sci* (2011).
32. Nicholson, B. & Suresh Kumar, K.G. The multifaceted roles of USP7: new therapeutic opportunities. *Cell Biochem Biophys* **60**, 61-8 (2011).
33. Spivak, G. & Hanawalt, P.C. Host cell reactivation of plasmids containing oxidative DNA lesions is defective in Cockayne syndrome but normal in UV-sensitive syndrome fibroblasts. *DNA Repair (Amst)* **5**, 13-22 (2006).
34. D'Errico, M. *et al.* The role of CSA in the response to oxidative DNA damage in human cells. *Oncogene* **26**, 4336-43 (2007).
35. Gorgels, T.G. *et al.* Retinal degeneration and ionizing radiation hypersensitivity in a mouse model for Cockayne syndrome. *Mol Cell Biol* **27**, 1433-41 (2007).
36. Newman, J.C., Bailey, A.D., Fan, H.Y., Pavelitz, T. & Weiner, A.M. An abundant evolutionarily conserved CSB-PiggyBac fusion protein expressed in Cockayne syndrome. *PLoS Genet* **4**, e1000031 (2008).
37. Campeau, E. *et al.* A versatile viral system for expression and depletion of proteins in mammalian cells. *PLoS One* **4**, e6529 (2009).
38. Epping, M.T. *et al.* TSPYL5 suppresses p53 levels and function by physical interaction with USP7. *Nat Cell Biol* **13**, 102-8 (2011).
39. Sugaya, K., Vigneron, M. & Cook, P.R. Mammalian cell lines expressing functional RNA polymerase II tagged with the green fluorescent protein. *J Cell Sci* **113 (Pt 15)**, 2679-83 (2000).
40. Wilm, M. *et al.* Femtomole sequencing of proteins from polyacrylamide gels by nano-electrospray mass spectrometry. *Nature* **379**, 466-9 (1996).
41. Cox, J. *et al.* A practical guide to the MaxQuant computational platform for SILAC-based quantitative proteomics. *Nat Protoc* **4**, 698-705 (2009).
42. Cox, J. *et al.* Andromeda: a peptide search engine integrated into the MaxQuant environment. *J Proteome Res* **10**, 1794-805 (2011).
43. Keller, A., Nesvizhskii, A.I., Kolker, E. & Aebersold, R. Empirical statistical model to estimate the accuracy of peptide identifications made by MS/MS and database search. *Anal Chem* **74**, 5383-92 (2002).
44. Nesvizhskii, A.I., Keller, A., Kolker, E. & Aebersold, R. A statistical model for identifying proteins by tandem mass spectrometry. *Anal Chem* **75**, 4646-58 (2003).
45. Houtsmuller, A.B. & Vermeulen, W. Macromolecular dynamics in living cell nuclei revealed by fluorescence redistribution after photobleaching. *Histochem Cell Biol* **115**, 13-21 (2001).
46. Marteijn, J.A. *et al.* Nucleotide excision repair-induced H2A ubiquitination is dependent on MDC1 and RNF8 and reveals a universal DNA damage response. *J Cell Biol* **186**, 835-47 (2009).

5

UVSSA AND USP7, A NEW COUPLE IN TRANSCRIPTION-COUPLED DNA REPAIR

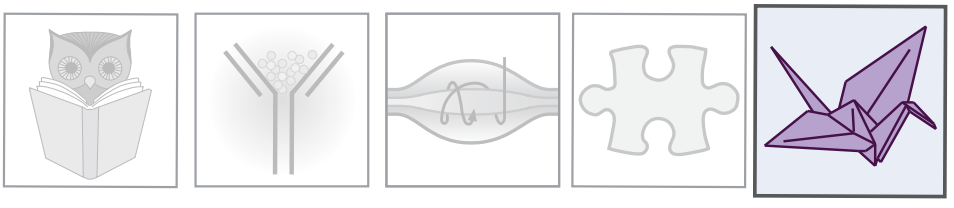

Petra Schwertman, Wim Vermeulen# and Jurgen A. Marteijn

Department of Genetics and Netherlands Proteomics Centre, Centre for Biomedical Genetics, Erasmus University Medical Centre, 3015 GE Rotterdam, The Netherlands
Corresponding author

Published in Chromosoma 2013 Aug; 122(4):275-84

ABSTRACT

Transcription-coupled nucleotide excision repair (TC-NER) specifically removes transcription-blocking lesions from our genome. Defects in this pathway are associated with two human disorders: Cockayne syndrome (CS) and UV-sensitive syndrome (UV^{S}S). Despite a similar cellular defect in the UV DNA damage response, patients with these syndromes exhibit strikingly distinct symptoms; CS patients display severe developmental, neurological, and premature aging features, whereas the phenotype of UV^{S}S patients is mostly restricted to UV hypersensitivity. The exact molecular mechanism behind these clinical differences is still unknown; however they might be explained by additional functions of CS proteins beyond TC-NER. A short overview of the current hypotheses addressing possible molecular mechanisms and the proteins involved are presented in this review. In addition we will focus on two new players involved in TC-NER which were recently identified: UV-stimulated scaffold protein A (UVSSA) and ubiquitin-specific protease 7 (USP7). *UVSSA* has been found to be the causative gene for UV^{S}S and together with USP7 is implicated in regulating TC-NER activity. We will discuss the function of UVSSA and USP7 and how the discovery of these proteins contributes to a better understanding of the molecular mechanisms underlying the clinical differences between UV^{S}S and the more severe CS.

INTRODUCTION

Alterations in the DNA structure that hinder the progression of RNA polymerases during transcription are highly toxic for the cell and if not properly resolved can lead to cellular apoptosis or senescence[1,2]. Helix-distorting lesions located in the transcribed strand of active genes initiate the transcription-coupled nucleotide excision repair (TC-NER) pathway to resolve the transcription-blocking DNA damage[3]. Lesion stalled elongating RNA polymerase II (RNA Pol II) triggers the recruitment of several TC-NER-specific factors to form a functional TC-NER complex, including the Cockayne syndrome A and B (CSA, CSB) proteins[4] (Figure 1a).

Cockayne syndrome versus UV-sensitive syndrome

In humans, defective TC-NER is associated with two autosomal recessive DNA repair-deficiency disorders: Cockayne syndrome (CS) and UV-sensitive syndrome (UV^{S}S)[5,6]. Although patient-derived cells are equally deficient in UV-induced TC-NER in vitro, the patients exhibit strikingly distinct clinical symptoms: CS individuals display severe developmental, neurological, and premature aging features, whereas UV^{S}S patients express much milder features, mostly restricted to UV hypersensitivity. CS is caused by mutations in two genes indispensable for TC-NER, *CSA* and *CSB*. UV^{S}S comprises three complementation groups, which are defined by specific mutations in *CSA*, *CSB,* and in the recently identified gene encoding for UV-stimulated scaffold protein A (*UVSSA)* (Table 1). Intriguingly, neither the site nor the nature of the mutations in CSA or CSB seems to correlate with the clinical differences observed among patients with CS and UV^{S}S[5,7]. Thus, an important question remains: how do molecular defects within the same TC-NER pathway and even different mutations within the same genes lead to such diverse pathologies?

Several models are proposed that try to explain the underlying molecular reason for the wide variety in TC-NER-deficient phenotype[8,9]. Most of these hypotheses are based on additional functions of the CS proteins outside of their role in TC-NER while assuming UVSSA is not implicated in these processes, hence explaining the milder phenotype in UV^{S}S[10] (Figure 2).

Table 1: Overview of UVSS mutations in CSA, CSB and UVSSA

Patient/Cell line	Gene affected	Mutation	References
KPS2	UVSSA	p.Lys123*	41, 42, 71, 72, 73
KPS3	UVSSA	p.Lys123*	41, 42, 71, 72, 73
UVS24TA	UVSSA	p.Ile31Phefs*9	41, 42, 74
XP24KO	UVSSA	p.Lys123*	41, 42, 75, 76
XP70TO	UVSSA	p.Cys32Arg	41, 75, 77
UVSS1VI	CSA	p.Trp361Cys	46
UVS1KO	CSB	p.Arg77*	38, 71, 72, 74, 78
CS3AM	CSB	p.Arg77*	37

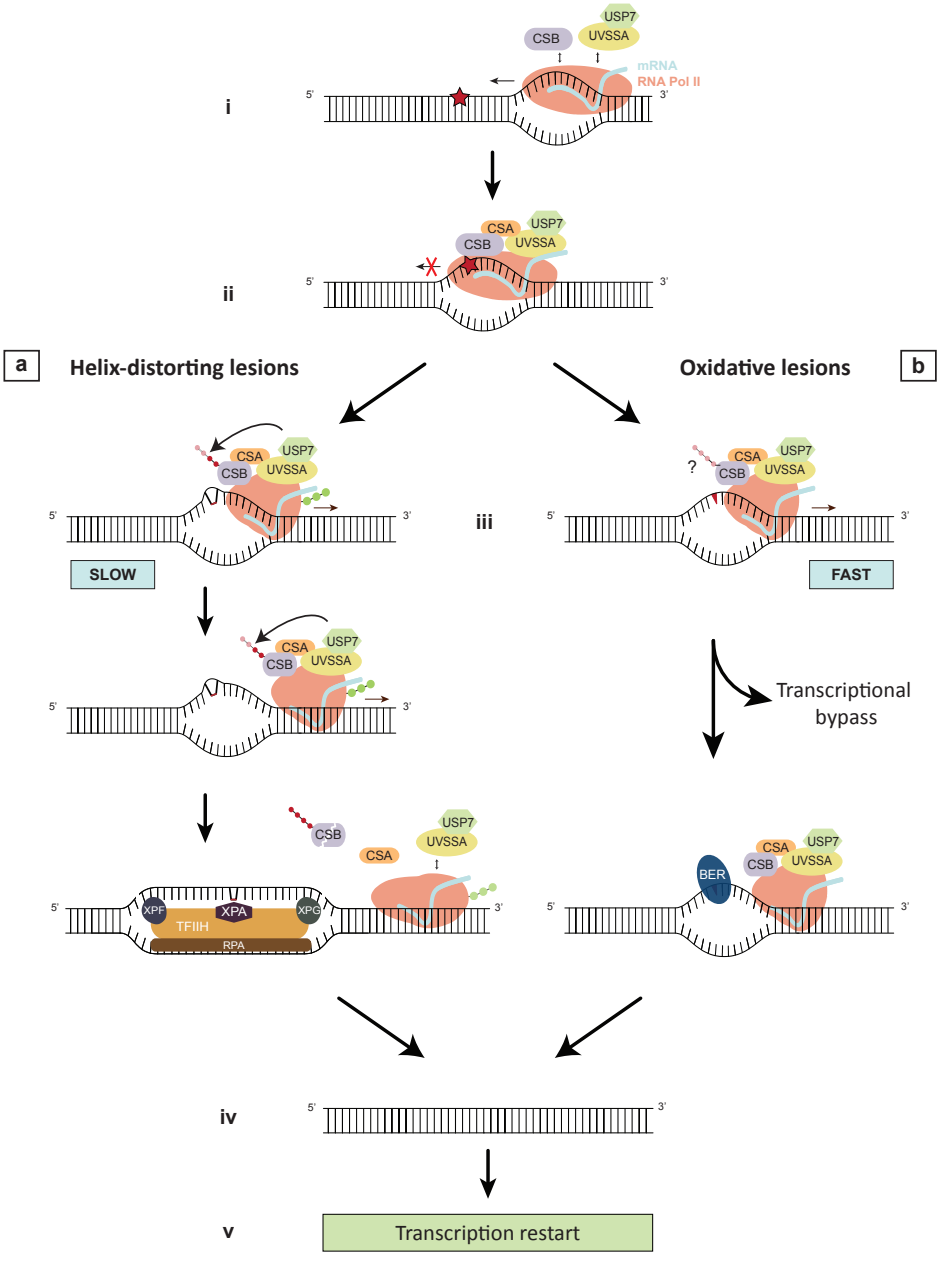

Figure 1: Model for resolving transcription-blocking lesions.
(i) During transcription UVSSA, USP7, and CSB interact transiently with elongating RNA Pol II. (ii) Upon encountering a lesion (indicated by star), stalled RNA Pol II stabilizes its binding with these proteins and triggers the recruitment of several other DNA repair factors, including CSA. Since RNA Pol II shields the DNA lesion in its active pocket, the stalled transcription complex must be remodeled to enable access of repair proteins to the lesion. In the case of helix-distorting lesions (iiia), TC-NER is initiated for which extensive modulation of stalled RNA Pol II is needed, causing a prolonged transcriptional arrest. During

One of these models, the transcription defect model, is mainly based on data obtained for the CSB protein. CSB is a member of the SNF2/SWI2 family of DNA-dependent ATPases[11] and is suggested to have chromatin remodeling abilities, possibly through recruitment of the p300 histone acetyltransferase[12-14]. CSB transiently interacts with elongating RNA Pol II and stimulates transcription[15-20]. This suggests that when CSB is absent or mutated, transcription would be affected even in the absence of DNA damage. There is a growing list of human diseases which are associated with defects in transcription, and many of these diseases are characterized by congenital defects[21], as also observed in CS patients. This suggests that the severe developmental and premature aging features of CS could partially be caused by a defect in transcription, while the sun sensitivity in these patients is most likely caused by the DNA repair deficiency of the TC-NER pathway.

Another hypothesis involves a role of the CS proteins in repairing endogenous DNA damage from reactive oxygen species (ROS), which is usually repaired by the base excision repair (BER) machinery[22]. Both human and mouse cell lines deficient in the CS proteins indeed display enhanced sensitivity to agents that produce oxidative DNA damage[23-28]. Furthermore, Menoni, *et al*.[29] recently showed recruitment of CSB to local oxidative DNA lesions in living cells without an accumulation of downstream NER factors, indicating the involvement of CSB in the response to oxidative DNA lesions independent of the downstream NER reaction. Importantly, CSB binding to oxidative damage was reduced upon transcription inhibition, which suggests a role of CSB in transcription-associated repair of oxidative lesions. In CS patients, the accumulation of unrepaired oxidative DNA damage and the subsequent prolonged transcription arrest at these lesions could result in apoptosis and consequentially tissue degeneration. Since active metabolism during development and a high level of oxidative metabolism in neural tissues may generate a considerable amount of oxidative damage, the consequences of the transcription arrest are mainly disclosed by developmental and neurological symptoms which are a hallmark of CS[30]. This model is further supported by transcriptomic analysis of CSB-deficient mice which revealed systematic suppression of growth and oxidative metabolism, an altered glycolysis and an upregulated anti-oxidant defense, collectively referred to as survival response[31].

this slow process, CSB assembles a functional TC-NER complex and assists in the remodeling of RNA Pol II. In response to DNA damage CSB is ubiquitinated and eventually degraded. In order to allow sufficient time for CSB to perform its function in TC-NER, its presence is protected by the concerted action of UVSSA and USP7 by counteracting the ubiquitination-dependent degradation. When the required remodeling of stalled RNA Pol II is completed, the TC-NER complex is destabilized and CSB is degraded by the proteasome. XPA, RPA, and the TFIIH complex are subsequently recruited. Following further helix unwinding and lesion verification, XPG and XPF are required for the double incision of the damaged DNA strand. The repair reaction is completed with DNA polymerase gap filling of the repair patch and sealing of the nicks. Oxidative lesions (**iiib**) have a minor effect on the DNA helix structure, which therefore requires relatively little remodeling of RNA Pol II for efficient repair. Consequently, RNA Pol II is only slowed down or transiently arrested in response to these lesions resulting in a faster response as compared to **iiia**. CSB remodeling helps to efficiently remove oxidative lesions likely via the BER pathway or to pass stalled complexes over the lesion (lesion bypass). However, due to the faster response, protection of CSB from ubiquitination-dependent degradation by UVSSA/USP7 is not necessary. After repair is completed (**iv**), transcription is resumed (**v**).

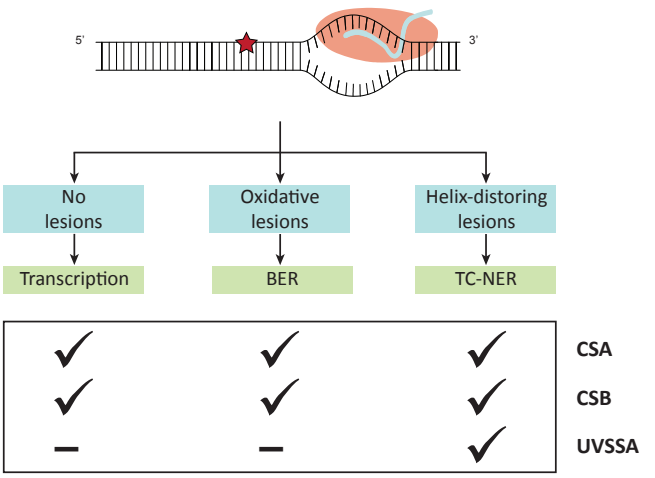

Figure 2: involvement of CSA, CSB and UVSSA in transcription, BER and TC-NER.
Involvement of CSA, CSB, and UVSSA in transcription, BER, and TC-NER. While the CS proteins have functions outside of TC-NER, a role for UVSSA in these other processes has presently not been shown.

Moreover, Pascucci, *et al.*[32] recently observed a disturbed redox balance in patient-derived CS cells. They showed increased intracellular ROS levels and oxidative DNA damage. In addition, alterations in cellular metabolism including the glycolysis pathway and oxidative metabolism were observed. Addition of antioxidants to the cells reduced ROS levels and at least partially reverted the alterations in cellular metabolism, suggesting that oxidative stress plays a causative role in CS pathology. Although there is compelling evidence supporting this hypothesis, no direct proof is currently present and it needs further exploration.

Within a third model, a role for the CS proteins in repair of oxidative DNA damage specifically in mitochondrial DNA (mtDNA) has been reported[33-35]. Mitochondria possess an independent repair machinery for oxidative lesions, which is thought to play a crucial role in protecting the integrity of mtDNA from the relatively high levels of ROS generated in this organelle. Certain clinical symptoms associated with mitochondrial dysfunction are also observed in CS patients, including the severe neurological and premature aging features[36]. This would suggest that the cause of these symptoms in CS results in part from the loss of mitochondrial function as a consequence of unrepaired oxidative mtDNA damage due to mutations in the CS proteins.

The abovementioned hypotheses to explain the severe phenotypical consequences of CS do not uphold, however, for the intriguing case of two unrelated patients with null mutations in CSB associated with mild UV^{S}S symptoms[37,38]. In contrast, two other patients with a deletion of the promoter sequence of CSB (resulting in no detectable CSB protein) have been found, which showed the most severe CS symptoms[39]. Thus, the absence of CSB alone cannot explain the striking variability in phenotype between CS and UV^{S}S. A factor possibly involved in this variability might be the expression of an evolutionary

conserved CSB-PGBD3 fusion protein, containing exons 1-5 of CSB joined in frame with the PiggyBac transposase. Reports have indicated that this fusion protein might play a role in the CS phenotype[40].

The UVSSA factor

Recently, three laboratories identified *UVSSA* (encoding UV-stimulated scaffold protein A) as the causative gene for the UV^{S}S-A complementation group. Microcell-mediated chromosome transfer[41], whole-exome sequencing[42] and quantitative proteomics[43] were used to identify *KIAA1530* as a new TC-NER factor, which was subsequently renamed *UVSSA*. Sequencing of this gene in five UV^{S}S-A patient cell lines revealed three different inactivating mutations in the *UVSSA* gene (Table 1).

Within UVSSA two conserved, though poorly characterized domains are identified with homology to the Vps27-Hrs-STAM (VHS) domain and the DUF2043 domain. UV^{S}S-A cells expressing UVSSA mutants without either of these domains fail to complement UV^{S}S-A deficiency[42], indicating that both domains are important for TC-NER activity. The UVSSA protein was shown to interact with the TC-NER factors RNA Pol II, CSA, CSB, and TFIIH[41-43]. A specialized chromatin immunoprecipitation (ChIP) procedure showed that UVSSA resides in active, chromatin-bound TC-NER complexes upon UV damage. Furthermore, GFP-tagged UVSSA accumulated at local UV damage in living cells with similar recruitment kinetics as the TC-NER factor CSB[43]. Together these results showed that UVSSA is a novel TC-NER factor.

UVSSA recruitment

There are two, though not mutual exclusive, models explaining how UVSSA is recruited to UV lesions: (1.) as an RNA Pol II interaction partner[43] and (2.) as a CSA interaction partner[41,44].

We observed a UV-independent interaction between RNA Pol II and UVSSA in ChIP experiments[43]. This interaction was also observed in CSB-deficient patient cells, indicative of a CSB-independent binding of UVSSA to TC-NER complexes. In line with this, a CSA- and CSB-independent accumulation of GFP-UVSSA was observed at sites of local UV damage using live cell imaging. In contrast, Zhang, *et al*.[41] observed UV dependency for the UVSSA-RNA Pol II interaction and showed a CSA-dependent interaction with UVSSA in the chromatin fraction using non-cross-linking IPs; the latter was also observed by Fei and Chen[44]. An explanation for this apparent discrepancy in UVSSA recruitment could be that the CS proteins may be required for stable integration into a functional TC-NER complex rather than for the recruitment of UVSSA. Transient or low-affinity interactions could appear CSA/CSB independent if interactions are fixed by cross-linking as in ChIP experiments[43] and CSA/CSB dependent as observed in non-cross-linking IPs[41,44].

The observed CSA-dependent stable association of UVSSA into TC-NER complexes provides the basis for a possible molecular explanation of the UV^{S}S/CS phenotypic difference. The CSA protein is a subunit of an E3 ubiquitin ligase complex[45] that is recruited to the site of damage by CSB[4]. Although essential for TC-NER, the precise role of CSA remains largely unknown. Nardo, *et al*.[46] described a patient with a specific missense *CSA* mutation, which causes the mild UV sensitive phenotype in the absence of the severe premature aging features common in CS. Cells of this UV^{S}S patient were hypersensitive to UV light,

but not to oxidative damaging agents. This finding thus implies a separable role for CSA in response to UV and oxidative DNA damage. Interestingly, Fei and Chen[44] showed that this same CSA mutant disrupts the interaction of CSA with UVSSA. This might suggest that an impaired interaction of UVSSA with mutated CSA at sites of DNA damage results in UV^{S}S in this patient, while an unaffected role of CSA in other processes – such as in oxidative DNA damage repair – prevents the additional CS symptoms.

UVSSA function: a role in CSB stability

In addition to its interaction with CSA and RNA Pol II, UVSSA forms a UV-independent protein complex with the deubiquitinating enzyme (DUB) ubiquitin-specific protease 7 (USP7). USP7 (also known as HAUSP) has multiple roles in the DNA damage response, as illustrated by the wide variety of substrates including Mdm2, p53, claspin, Chfr, and histone H2B[47-51]. Additionally, its diverse activity also includes targeting tumor suppressors, immune responders, viral proteins, and epigenetic modulators[52]. Through its interaction with UVSSA, USP7 is recruited to active TC-NER complexes upon UV damage[43]. Depletion of USP7 leads to a similar TC-NER deficiency as seen with UVSSA depletion, such as a decrease in UV survival and RNA synthesis recovery after UV[41,43]. From previous studies it is known that CSB is ubiquitinated and degraded by the proteasome in response to UV[53,54]. In the absence of either UVSSA or USP7 the degradation of CSB by the 26S proteasome is faster upon UV damage. It is therefore suggested that UVSSA stabilizes CSB after UV by targeting the pleiotropic DUB USP7 to TC-NER complexes, which subsequently removes UV-induced ubiquitin-chains. The purpose of this could be to provide an increased time frame for CSB to orchestrate TC-NER complex formation or to efficiently complete repair before CSB is degraded.

The stabilizing function of UVSSA/USP7 on CSB might be restricted to UV-induced TC-NER, since the reduced CSB levels in UV^{S}S-A cells do not result in developmental and neurological symptoms in UV^{S}S patients. Interestingly, overexpression of CSB in UV^{S}S-A cells did not correct the TC-NER defect[43]. This implies that the reduced level of CSB in UV^{S}S-A cells alone is not sufficient to explain the UV^{S}S phenotype. Therefore the ubiquitination state of CSB itself might have an additional function for proper TC-NER, for example to mediate a ubiquitin-mediated functional change in CSB, or UVSSA/USP7 might have additional substrates that can cause the UV^{S}S phenotype.

UVSSA function: a role in the processing of stalled RNA Pol II

Several transcription-associated factors recognize the C-terminal domain (CTD) of RNA Pol II by means of a conserved CTD-interacting domain (CID). The CID fold closely resembles that of VHS domains[55,56], suggesting that the observed interaction between UVSSA and RNA Pol II is mediated via the VHS domain of UVSSA. This interaction might be important for an additional function of UVSSA, as Nakazawa, *et al.*[42] showed that UVSSA is needed for processing stalled RNA Pol II at sites of UV damage. During TC-NER, elongating RNA Pol II can be recycled for a new round of transcription by means of dephosphorylating the elongating form of RNA Pol II into the hypophosphorylated initiating form[57]. Without the UVSSA protein this dephosphorylation step is substantially inhibited[42], as previously found in CS patient cells[57], leading to impaired resumption of transcription initiation.

Next to its possible involvement in RNA Pol II binding, the VHS domain has also been implicated in ubiquitin binding[58], raising the possibility that UVSSA binds ubiquitinated TC-NER proteins. Upon UV irradiation RNA Pol II is ubiquitinated and under specific conditions degraded[59-61]. Nakazawa, *et al.*[42] identified a UVSSA-dependent ubiquitination of RNA Pol II, which however is not subject to proteasomal degradation. Interestingly, this new ubiquitinated form of stalled elongating RNA Pol II is UV-specific, as it was not observed for oxidative DNA damage induced by hydrogen peroxide. Interaction of UVSSA with ubiquitinated RNA Pol II was indeed observed by Nakazawa, *et al.*[42]. Additionally, we identified UVSSA in a stable isotope labeling with amino acids in cell culture (SILAC)-based proteomic screen for differentially ubiquitinated proteins following UV irradiation[43]. While the ubiquitination status of UVSSA was not changed after UV, a similar SILAC ratio for UVSSA and RNA Pol II was observed. This would suggest that UVSSA was co-purified by virtue of the enhanced ubiquitination of RNA Pol II in response to UV. However whether this interaction is ubiquitination dependent remains unclear.

The VHS domain of UVSSA is suggested to be also involved in the interaction between UVSSA and CSB, since a UV^{S}S-A patient missense mutation (Cys32Arg) within the VHS domain disrupts the interaction with CSB in response to UV. Interestingly, UV^{S}S-A cells expressing UVSSA with this mutation were able to restore CSB stability to wild-type levels upon UV, while RNA Pol II ubiquitination and dephosphorylation remained absent[42]. This might indicate that while the VHS domain of UVSSA is dispensable for CSB stabilization, it is important for RNA Pol II processing. Apparently, the action of UVSSA on both CSB and RNA Pol II contributes to the UV^{S}S phenotype. Although the precise involvement of UVSSA in processing these RNA Pol II modifications remains to be elucidated, it is hypothesized that the modifications themselves contribute to the coordination of the removal of stalled RNA Pol II and formation of the TC-NER complex, and the subsequent resumption of transcription.

New insights in transcription-coupled DNA repair from a UVSSA perspective

Mutations in *UVSSA* were recently identified to cause UV^{S}S, a previously unresolved TC-NER deficiency disorder with rather mild clinical manifestations as compared to CS. UVSSA and its interaction partner USP7 were identified as new factors involved in TC-NER repair efficiency and cell survival after UV damage. Additionally, UVSSA is also important for the fate and ubiquitination state of both RNA Pol II and CSB. The identification of these new transcription-coupled DNA repair factors presents us with the opportunity to gain more insight into the molecular mechanisms underlying the clinical differences between UV^{S}S and CS.

The transcription defect model discussed previously is based on a role for the CS proteins in transcription, while assuming UVSSA is not involved in this process. The UV-independent transient interaction between UVSSA and RNA Pol II may suggest a role for UVSSA in transcription. However, no other data are currently available to conclude whether UVSSA is as equally important as CSB for transcription on undamaged DNA. Therefore, further studies are needed to determine the possible involvement of UVSSA in transcription.

One of the models including UVSSA involves the aberrant processing of elongating RNA Pol II when stalled at a lesion (Figure 3). For efficient repair to take place, the RNA Pol II complex must be remodeled since it will likely shield the DNA lesion and consequently

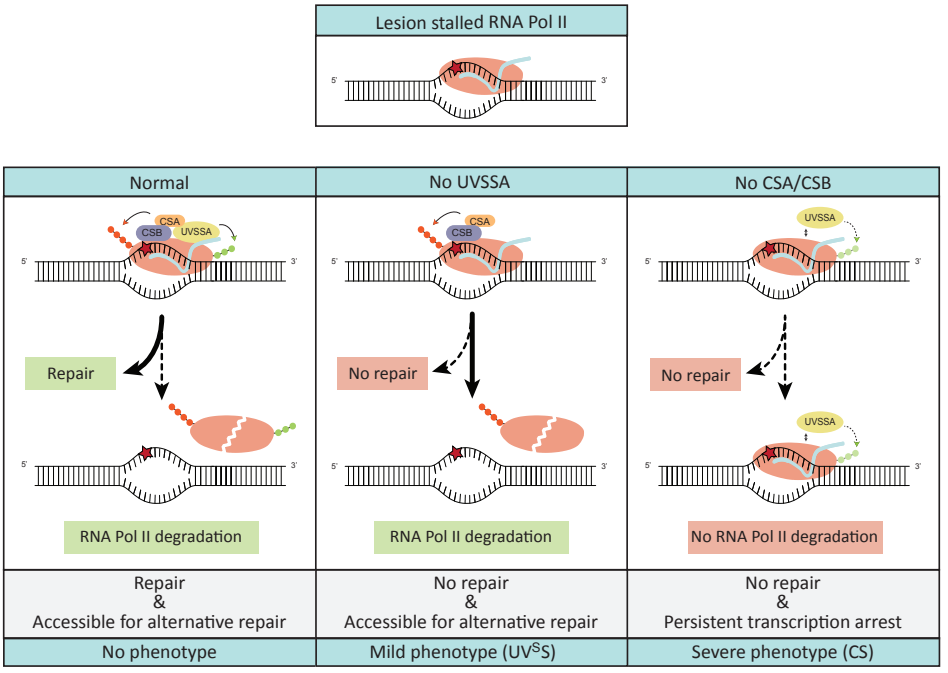

Figure 3: Differential aberrant processing of stalled elongating RNA Pol II is responsible for the differences in UV^{S}S/CS phenotype.
In wild-type cells, lesion stalled RNA Pol II initiates TC-NER to remove the transcription-blocking damage. In the infrequent cases that repair cannot take place, RNA Pol II is ubiquitinated and degraded by the proteasome to make the lesion accessible for alternative DNA repair. In UV^{S}S-A cells, TC-NER does not take place. Since the prolonged stalled RNA Pol II can still be ubiquitinated in a CSA/CSB dependent way, RNA Pol II is degraded and the lesion is made accessible to alternative DNA repair. In CS cells, TC-NER is blocked as well. In addition, the ubiquitination and degradation of RNA Pol II does not take place. The resultant persistent transcription arrest is more harmful for the cell, since it leads to apoptosis or senescence and might contribute to the more severe phenotype in CS patients.

prevent accessibility of repair proteins[62-66]. Additionally, when a lesion cannot be repaired or bypassed, stalled RNA Pol II is thought to be ubiquitinated and degraded in order to prevent persistent transcriptional arrest[66]. In the absence of UVSSA, stalled RNA Pol II can still be ubiquitinated in a CSA/CSB dependent way, which results in proteasomal degradation. In contrast, stalled RNA Pol II cannot be degraded by the proteasome in CS cells[3]. This would suggest that the lack of DNA repair combined with persistent arrest of RNA Pol II at DNA lesions in CS cells, which results in apoptosis or senescence, might be causative for the severe CS phenotype. In UV^{S}S-A cells prolonged arrest is prevented and the lesion is made accessible for alternative DNA repair by degradation of RNA Pol II, hence resulting in the milder UV^{S}S phenotype (Figure 3).

The CS proteins play important roles in both TC-NER and oxidative DNA damage repair, while the precise function of UVSSA in these processes remains unclear. The previously discussed oxidative damage model assumes that UVSSA does not play a role in oxidative

DNA damage repair[10], hence explaining the milder phenotype of UV^{S}S. We would like to postulate a model including UVSSA and its role in both repair pathways (Figure 1). We hypothesize that based on the nature of the DNA damage distinct modulations of lesion stalled RNA Pol II are required and that this involves a remodeling function of CSB. While oxidative lesions only slow down or transiently arrest RNA Pol II, more helix-distorting lesions (such as those induced by UV) would lead to a prolonged transcriptional arrest. In the case of transient transcription arrest, CSB remodeling assists in the efficient removal of a lesion or in bypassing the lesion[67-69]. In contrast, for a prolonged blocked transcription more time would be required for CSB to assemble a functional TC-NER complex and to assist in remodeling of the stalled RNA Pol II. The presence of CSB should, in the latter case, be protected by the concerted action of UVSSA/USP7 to allow sufficient time for CSB to perform its remodeling function. Whether the ubiquitination of CSB takes place at all after transient transcription arrest at oxidative DNA lesions, or if CSB is ubiquitinated but not degraded before the repair of these lesions is completed remains to be elucidated. In this proposed model, mutations in UVSSA would lead to dysfunctional TC-NER only, since the lack of CSB protection would not affect repair or restart of transcription blocked by oxidative lesions.

The discovery of UVSSA enables us to test the proposed models in greater detail and whether or not they are mutually exclusive. To further substantiate the hypothesis that the phenotypical difference between UV^{S}S and CS is derived from different sensitivities for endogenous levels of oxidative DNA damage, dedicated lesion-specific DNA repair assays are required[70]. Furthermore, dissecting the differences in molecular composition between repair complexes stalled at UV-induced lesions or oxidative lesions will help us to better understand the molecular mechanism of transcription-coupled repair for different types of DNA damage. Characterization of repair complexes present on the different lesions using immunoprecipitation (IP) combined with mass spectrometry (MS) would be a powerful tool to study this. Another interesting area for further investigation is the differential ubiquitination of several DNA repair factors, which is likely an important driver of protein hand over and passing of repair intermediates through successive steps during TC-NER. Especially the actual and/or precise involvement of USP7 in changing the ubiquitination state of CSB and RNA Pol II upon UV is of great interest, as is the establishment of identified or new E3 ubiquitin ligases responsible for the ubiquitin modifications. Finally, with the identification of UVSSA, a UV^{S}S-A mouse model can now be generated for a more extensive study of the UV^{S}S phenotype and molecular defect. Also an overall comparison of the UV^{S}S-A mouse with the already existing CS mouse models in an isogenic background will be a valuable source of information. Phenotypic consequences and possible differential responses to various genotoxic agents in the whole organism will contribute to our understanding of the clinical differences of CS versus UV^{S}S on a molecular level.

ACKNOWLEDGEMENTS

This work is funded by the Netherlands Genomics Initiative NPCII and the Dutch Organization for Scientific Research ZonMW: Horizon Zenith (935.11.042), Veni (917.96.120) and TOP grant (912.08.031 and 912.12.132).

REFERENCES

1. Ljungman, M. & Zhang, F. Blockage of RNA polymerase as a possible trigger for u.v. light-induced apoptosis. *Oncogene* **13**, 823-31 (1996).
2. Ljungman, M. & Lane, D.P. Transcription - guarding the genome by sensing DNA damage. *Nat Rev Cancer* **4**, 727-37 (2004).
3. Hanawalt, P.C. & Spivak, G. Transcription-coupled DNA repair: two decades of progress and surprises. *Nat Rev Mol Cell Biol* **9**, 958-70 (2008).
4. Fousteri, M., Vermeulen, W., van Zeeland, A.A. & Mullenders, L.H. Cockayne syndrome A and B proteins differentially regulate recruitment of chromatin remodeling and repair factors to stalled RNA polymerase II in vivo. *Mol Cell* **23**, 471-82 (2006).
5. Nance, M.A. & Berry, S.A. Cockayne syndrome: review of 140 cases. *Am J Med Genet* **42**, 68-84 (1992).
6. Spivak, G. UV-sensitive syndrome. *Mutat Res* **577**, 162-9 (2005).
7. Laugel, V. *et al.* Mutation update for the CSB/ERCC6 and CSA/ERCC8 genes involved in Cockayne syndrome. *Hum Mutat* **31**, 113-26 (2010).
8. Sarasin, A. UVSSA and USP7: new players regulating transcription-coupled nucleotide excision repair in human cells. *Genome Med* **4**, 44 (2012).
9. Cleaver, J.E. Photosensitivity syndrome brings to light a new transcription-coupled DNA repair cofactor. *Nat Genet* **44**, 477-8 (2012).
10. Spivak, G. & Hanawalt, P.C. Host cell reactivation of plasmids containing oxidative DNA lesions is defective in Cockayne syndrome but normal in UV-sensitive syndrome fibroblasts. *DNA Repair (Amst)* **5**, 13-22 (2006).
11. Troelstra, C. *et al.* Molecular cloning of the human DNA excision repair gene ERCC-6. *Mol Cell Biol* **10**, 5806-13 (1990).
12. Citterio, E. *et al.* ATP-dependent chromatin remodeling by the Cockayne syndrome B DNA repair-transcription-coupling factor. *Mol Cell Biol* **20**, 7643-53 (2000).
13. Newman, J.C., Bailey, A.D. & Weiner, A.M. Cockayne syndrome group B protein (CSB) plays a general role in chromatin maintenance and remodeling. *Proc Natl Acad Sci U S A* **103**, 9613-8 (2006).
14. Frontini, M. & Proietti-De-Santis, L. Cockayne syndrome B protein (CSB): linking p53, HIF-1 and p300 to robustness, lifespan, cancer and cell fate decisions. *Cell Cycle* **8**, 693-6 (2009).
15. Balajee, A.S., May, A., Dianov, G.L., Friedberg, E.C. & Bohr, V.A. Reduced RNA polymerase II transcription in intact and permeabilized Cockayne syndrome group B cells. *Proc Natl Acad Sci U S A* **94**, 4306-11 (1997).
16. Dianov, G.L., Houle, J.F., Iyer, N., Bohr, V.A. & Friedberg, E.C. Reduced RNA polymerase II transcription in extracts of cockayne syndrome and xeroderma pigmentosum/Cockayne syndrome cells. *Nucleic Acids Res* **25**, 3636-42 (1997).
17. Selby, C.P. & Sancar, A. Human transcription-repair coupling factor CSB/ERCC6 is a DNA-stimulated ATPase but is not a helicase and does not disrupt the ternary transcription complex of stalled RNA polymerase II. *J Biol Chem* **272**, 1885-90 (1997).
18. Tantin, D., Kansal, A. & Carey, M. Recruitment of the putative transcription-repair coupling factor CSB/ERCC6 to RNA polymerase II elongation complexes. *Mol Cell Biol* **17**, 6803-14 (1997).
19. van Gool, A.J. *et al.* The Cockayne syndrome B protein, involved in transcription-coupled DNA repair, resides in an RNA polymerase II-containing complex. *EMBO J* **16**, 5955-65 (1997).
20. van den Boom, V. *et al.* DNA damage stabilizes interaction of CSB with the transcription elongation machinery. *J Cell Biol* **166**, 27-36 (2004).
21. Villard, J. Transcription regulation and human diseases. *Swiss Med Wkly* **134**, 571-9 (2004).
22. Hegde, M.L., Hazra, T.K. & Mitra, S. Early steps in the DNA base excision/single-strand interruption repair pathway in mammalian cells. *Cell Res* **18**, 27-47 (2008).
23. Dianov, G., Bischoff, C., Sunesen, M. & Bohr, V.A. Repair of 8-oxoguanine in DNA is deficient in Cockayne syndrome group B cells. *Nucleic Acids Res* **27**, 1365-8 (1999).
24. Tuo, J., Jaruga, P., Rodriguez, H., Bohr, V.A. & Dizdaroglu, M. Primary fibroblasts of Cockayne syndrome patients are defective in cellular repair of 8-hydroxyguanine and 8-hydroxyadenine resulting from oxidative stress. *FASEB J* **17**, 668-74 (2003).

25. de Waard, H. *et al.* Different effects of CSA and CSB deficiency on sensitivity to oxidative DNA damage. *Mol Cell Biol* **24**, 7941-8 (2004).
26. Gorgels, T.G. *et al.* Retinal degeneration and ionizing radiation hypersensitivity in a mouse model for Cockayne syndrome. *Mol Cell Biol* **27**, 1433-41 (2007).
27. D'Errico, M. *et al.* The role of CSA in the response to oxidative DNA damage in human cells. *Oncogene* **26**, 4336-43 (2007).
28. Stevnsner, T., Muftuoglu, M., Aamann, M.D. & Bohr, V.A. The role of Cockayne Syndrome group B (CSB) protein in base excision repair and aging. *Mech Ageing Dev* **129**, 441-8 (2008).
29. Menoni, H., Hoeijmakers, J.H. & Vermeulen, W. Nucleotide excision repair-initiating proteins bind to oxidative DNA lesions in vivo. *J Cell Biol* **199**, 1037-46 (2012).
30. Hoeijmakers, J.H. Genome maintenance mechanisms are critical for preventing cancer as well as other aging-associated diseases. *Mech Ageing Dev* **128**, 460-2 (2007).
31. van der Pluijm, I. *et al.* Impaired genome maintenance suppresses the growth hormone--insulin-like growth factor 1 axis in mice with Cockayne syndrome. *PLoS Biol* **5**, e2 (2007).
32. Pascucci, B. *et al.* An altered redox balance mediates the hypersensitivity of Cockayne syndrome primary fibroblasts to oxidative stress. *Aging Cell* **11**, 520-9 (2012).
33. Osenbroch, P.O. *et al.* Accumulation of mitochondrial DNA damage and bioenergetic dysfunction in CSB defective cells. *FEBS J* **276**, 2811-21 (2009).
34. Kamenisch, Y. *et al.* Proteins of nucleotide and base excision repair pathways interact in mitochondria to protect from loss of subcutaneous fat, a hallmark of aging. *J Exp Med* **207**, 379-90 (2010).
35. Scheibye-Knudsen, M. *et al.* Cockayne syndrome group B protein prevents the accumulation of damaged mitochondria by promoting mitochondrial autophagy. *J Exp Med* **209**, 855-69 (2012).
36. Stevnsner, T. *et al.* Mitochondrial repair of 8-oxoguanine is deficient in Cockayne syndrome group B. *Oncogene* **21**, 8675-82 (2002).
37. Miyauchi-Hashimoto, H., Akaeda, T., Maihara, T., Ikenaga, M. & Horio, T. Cockayne syndrome without typical clinical manifestations including neurologic abnormalities. *J Am Acad Dermatol* **39**, 565-70 (1998).
38. Horibata, K. *et al.* Complete absence of Cockayne syndrome group B gene product gives rise to UV-sensitive syndrome but not Cockayne syndrome. *Proc Natl Acad Sci U S A* **101**, 15410-5 (2004).
39. Laugel, V. *et al.* Deletion of 5' sequences of the CSB gene provides insight into the pathophysiology of Cockayne syndrome. *Eur J Hum Genet* **16**, 320-7 (2008).
40. Bailey, A.D. *et al.* The conserved Cockayne syndrome B-piggyBac fusion protein (CSB-PGBD3) affects DNA repair and induces both interferon-like and innate antiviral responses in CSB-null cells. *DNA Repair (Amst)* **11**, 488-501 (2012).
41. Zhang, X. *et al.* Mutations in UVSSA cause UV-sensitive syndrome and destabilize ERCC6 in transcription-coupled DNA repair. *Nat Genet* **44**, 593-7 (2012).
42. Nakazawa, Y. *et al.* Mutations in UVSSA cause UV-sensitive syndrome and impair RNA polymerase IIo processing in transcription-coupled nucleotide-excision repair. *Nat Genet* **44**, 586-92 (2012).
43. Schwertman, P. *et al.* UV-sensitive syndrome protein UVSSA recruits USP7 to regulate transcription-coupled repair. *Nat Genet* **44**, 598-602 (2012).
44. Fei, J. & Chen, J. KIAA1530 protein is recruited by Cockayne syndrome complementation group protein A (CSA) to participate in transcription-coupled repair (TCR). *J Biol Chem* **287**, 35118-26 (2012).
45. Groisman, R. *et al.* The ubiquitin ligase activity in the DDB2 and CSA complexes is differentially regulated by the COP9 signalosome in response to DNA damage. *Cell* **113**, 357-67 (2003).
46. Nardo, T. *et al.* A UV-sensitive syndrome patient with a specific CSA mutation reveals separable roles for CSA in response to UV and oxidative DNA damage. *Proc Natl Acad Sci U S A* **106**, 6209-14 (2009).
47. Li, M. *et al.* Deubiquitination of p53 by HAUSP is an important pathway for p53 stabilization. *Nature* **416**, 648-53 (2002).
48. Meulmeester, E. *et al.* Loss of HAUSP-mediated deubiquitination contributes to DNA damage-induced destabilization of Hdmx and Hdm2. *Mol Cell* **18**, 565-76 (2005).

49. Faustrup, H., Bekker-Jensen, S., Bartek, J., Lukas, J. & Mailand, N. USP7 counteracts SCFbetaTrCP- but not APCCdh1-mediated proteolysis of Claspin. *J Cell Biol* **184**, 13-9 (2009).
50. Khoronenkova, S.V., Dianova, II, Parsons, J.L. & Dianov, G.L. USP7/HAUSP stimulates repair of oxidative DNA lesions. *Nucleic Acids Res* **39**, 2604-9 (2011).
51. Khoronenkova, S.V. *et al.* ATM-dependent downregulation of USP7/HAUSP by PPM1G activates p53 response to DNA damage. *Mol Cell* **45**, 801-13 (2012).
52. Nicholson, B. & Suresh Kumar, K.G. The multifaceted roles of USP7: new therapeutic opportunities. *Cell Biochem Biophys* **60**, 61-8 (2011).
53. Groisman, R. *et al.* CSA-dependent degradation of CSB by the ubiquitin-proteasome pathway establishes a link between complementation factors of the Cockayne syndrome. *Genes Dev* **20**, 1429-34 (2006).
54. Wei, L. *et al.* BRCA1 contributes to transcription-coupled repair of DNA damage through polyubiquitination and degradation of Cockayne syndrome B protein. *Cancer Sci* **102**, 1840-7 (2011).
55. Misra, S., Puertollano, R., Kato, Y., Bonifacino, J.S. & Hurley, J.H. Structural basis for acidic-cluster-dileucine sorting-signal recognition by VHS domains. *Nature* **415**, 933-7 (2002).
56. Meinhart, A. & Cramer, P. Recognition of RNA polymerase II carboxy-terminal domain by 3'-RNA-processing factors. *Nature* **430**, 223-6 (2004).
57. Rockx, D.A. *et al.* UV-induced inhibition of transcription involves repression of transcription initiation and phosphorylation of RNA polymerase II. *Proc Natl Acad Sci U S A* **97**, 10503-8 (2000).
58. Mizuno, E., Kawahata, K., Kato, M., Kitamura, N. & Komada, M. STAM proteins bind ubiquitinated proteins on the early endosome via the VHS domain and ubiquitin-interacting motif. *Mol Biol Cell* **14**, 3675-89 (2003).
59. Bregman, D.B. *et al.* UV-induced ubiquitination of RNA polymerase II: a novel modification deficient in Cockayne syndrome cells. *Proc Natl Acad Sci U S A* **93**, 11586-90 (1996).
60. Anindya, R., Aygun, O. & Svejstrup, J.Q. Damage-induced ubiquitylation of human RNA polymerase II by the ubiquitin ligase Nedd4, but not Cockayne syndrome proteins or BRCA1. *Mol Cell* **28**, 386-97 (2007).
61. Malik, S., Bagla, S., Chaurasia, P., Duan, Z. & Bhaumik, S.R. Elongating RNA polymerase II is disassembled through specific degradation of its largest but not other subunits in response to DNA damage in vivo. *J Biol Chem* **283**, 6897-905 (2008).
62. Donahue, B.A., Yin, S., Taylor, J.S., Reines, D. & Hanawalt, P.C. Transcript cleavage by RNA polymerase II arrested by a cyclobutane pyrimidine dimer in the DNA template. *Proc Natl Acad Sci U S A* **91**, 8502-6 (1994).
63. Tornaletti, S., Maeda, L.S., Lloyd, D.R., Reines, D. & Hanawalt, P.C. Effect of thymine glycol on transcription elongation by T7 RNA polymerase and mammalian RNA polymerase II. *J Biol Chem* **276**, 45367-71 (2001).
64. Brueckner, F., Hennecke, U., Carell, T. & Cramer, P. CPD damage recognition by transcribing RNA polymerase II. *Science* **315**, 859-62 (2007).
65. Fousteri, M. & Mullenders, L.H. Transcription-coupled nucleotide excision repair in mammalian cells: molecular mechanisms and biological effects. *Cell Res* **18**, 73-84 (2008).
66. Wilson, M.D., Harreman, M. & Svejstrup, J.Q. Ubiquitylation and degradation of elongating RNA polymerase II: The last resort. *Biochim Biophys Acta* **1829**, 151-7 (2013).
67. Doetsch, P.W. Translesion synthesis by RNA polymerases: occurrence and biological implications for transcriptional mutagenesis. *Mutat Res* **510**, 131-40 (2002).
68. Charlet-Berguerand, N. *et al.* RNA polymerase II bypass of oxidative DNA damage is regulated by transcription elongation factors. *EMBO J* **25**, 5481-91 (2006).
69. Damsma, G.E. & Cramer, P. Molecular basis of transcriptional mutagenesis at 8-oxoguanine. *J Biol Chem* **284**, 31658-63 (2009).
70. Spivak, G., Cox, R.A. & Hanawalt, P.C. New applications of the Comet assay: Comet-FISH and transcription-coupled DNA repair. *Mutat Res* **681**, 44-50 (2009).

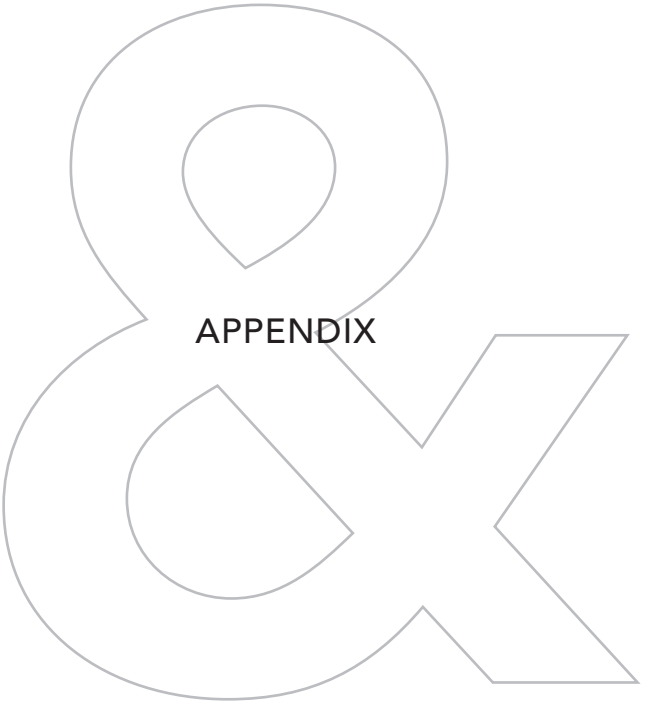

APPENDIX

SUMMARY

The integrity of our DNA is constantly threatened by genotoxic agents from both internal and external origin. DNA damage is a serious threat for cells as it disturbs replication and transcription. Persistent DNA damage can eventually lead to malignant transformation and accelerated aging. The DNA damage response (DDR), which consists of different dedicated DNA repair systems and signaling pathways, is evolved to overcome the severe consequences of DNA damage. One of these DNA processes is the versatile nucleotide excision repair (NER) mechanism, which removes a wide range of helix-distorting lesions including those induced by ultraviolet(UV)-light. NER is initiated by two damage recognition pathways: global genome NER (GG-NER) and transcription-coupled NER (TC-NER). While GG-NER can recognize and repair DNA damage located anywhere in the genome, TC-NER can only repair lesions in the transcribed strand of active genes. Together, over 30 different proteins are employed within NER to remove lesions from DNA. To ensure appropriate function and timing of these proteins at the right location, proper regulation of the NER pathway is crucial. This regulation relies for a big part on post-translational modification (PTM) of repair proteins themselves and of other proteins involved in the DDR pathway. This thesis focuses on protein modification by ubiquitin conjugation during the UV-induced DDR. Ubiquitination is known to control protein stability by targeting ubiquitinated proteins to the proteasome for degradation. Additionally, it was shown that modification of proteins with ubiquitin can also influence their activity, cellular localization and protein-protein interactions. In response to UV-irradiation several DDR proteins have been found to be ubiquitinated in order to orchestrate the complex UV-induced DDR. However, it is expected that more proteins involved within the UV-induced DDR are regulated by ubiquitination. To identify new ubiquitin modifications and proteins not previously known to be involved within the UV-DDR on a proteome-wide scale mass spectrometry (MS) was used. Since presumably not all proteins are ubiquitinated and as from those that are ubiquitinated only a small fraction is usually modified at a given time, methods to enrich for ubiquitinated proteins are necessary to study them by MS.

A general introduction to the DDR, ubiquitination and MS-based methods is provided in Chapter 1. In the following chapter, Chapter 2, an immunoaffinity purification method is described which we have developed to isolate endogenously ubiquitinated proteins, using the FK2 antibody that recognizes both mono-ubiquitinated and poly-ubiquitinated proteins. As this method is performed under non-denaturing conditions, it is especially suited for the proteomic analysis of ubiquitinated protein complexes.

Quantitative proteomic strategies – such as stable isotope labelling by amino acids in cell culture (SILAC)-based MS approaches – are designed to detect and quantify the effects of a specific stimulus on relative protein abundance in a proteome-wide fashion. In Chapter 3, SILAC-based MS was combined with the ubiquitinated protein isolation method described in Chapter 2, to identify UV-induced changes of ubiquitin modifications on proteins and protein complexes. Among the most enriched proteins in response to UV-induced DNA damage, NER factors known to be regulated by ubiquitin – including DDB2, XPC, CSB and POLR2A (the largest subunit of RNA Pol II) – were identified. This high enrichment of

established UV-induced ubiquitinated NER factors validates our approach for isolating UV-induced ubiquitinated proteins. In total we identified 65 up-regulated and 30 down-regulated proteins that were changed (>1.5 fold in two experiments) in response to UV, using a SILAC label-swap replication strategy. These UV-responsive proteins clustered into five major protein groups, representing biological processes that are in part expected to be affected in response to genotoxic stress, such as (1) NER, (2) chromatin remodelling and (3) transcription. In this analysis, NER is the most obviously expected biological pathway, as this is the sole mammalian repair process able to remove UV-induced DNA lesions and known to be controlled by ubiquitination. Also chromatin remodelling is commonly found associated to DDR and thought to aid loading of DNA repair and signalling factors. In addition, transcription is severely affected by UV-lesions, which triggers a dedicated repair pathway, transcription-coupled NER (TC-NER). Moreover, the largest subunit of RNA Pol II (POLR2A) was previously found to be poly-ubiquitinated in response to UV damage. The two other identified biological processes that appear to be regulated by ubiquitination in response to UV-light, (4) RNA splicing and (5) translation, were less expected and seem to represent novel branches of the DDR. Our results seem to indicate a global regulation of various interconnected biological processes by ubiquitination in order to ensure the right cellular response to UV-induced stress.

Chapter 4 describes the identification and molecular function of UV-stimulated scaffold protein A (UVSSA) and its interaction partner USP7 within TC-NER. The previously uncharacterized protein UVSSA was identified as one of the most enriched proteins in the MS screen described in Chapter 3, yet it was not found to be more ubiquitinated upon UV-damage. However, additional biochemical analysis demonstrated that UVSSA interacts with elongating RNA Pol II, localizes specifically to UV-induced lesions and resides in chromatin-associated TC-NER complexes. Therefore, we assume that this protein co-purified as part of the UV-induced ubiquitinated RNA Pol II protein complex, which explains its identification using our MS approach. Furthermore, we showed that UVSSA is implicated in stabilizing the TC-NER master organizing protein CSB by delivering the deubiquitinating enzyme USP7 to TC-NER complexes. Importantly, *UVSSA* turned out to be the causative gene for the UV-sensitive syndrome group A (UV^{S}S-A), a previously unresolved NER-deficiency disorder.

Chapter 5 discusses how the research on the role of UVSSA and USP7 in TC-NER contributes to a better understanding of the molecular mechanisms underlying the clinical differences between two human disorders associated with defective TC-NER: Cockayne syndrome (CS) and UV-sensitive syndrome (UV^{S}S). While CS patients display severe developmental, neurological, and premature aging features, the phenotype of UV^{S}S patients is mostly restricted to UV-hypersensitivity. The exact molecular mechanism behind these clinical differences is still unknown, however they might be explained by additional functions of the CS proteins beyond TC-NER. This chapter presents a short overview of the current hypotheses addressing possible molecular mechanisms and the proteins involved. In addition, the function of UVSSA and USP7 is discussed and how this knowledge can complement the existing models to explain the phenotypical difference between UV^{S}S and CS.

SAMENVATTING

Het menselijk lichaam is opgebouwd uit biljoenen cellen. Elke cel heeft zijn eigen kenmerken en werkt samen met de andere cellen in ons lichaam om het correct te laten functioneren. Zo bestaat ons lichaam uit verschillende typen cellen welke onderdeel uitmaken van grotere systemen, zoals weefsels en organen. De belangrijkste onderdelen in een cel zijn het DNA en de eiwitten. DNA is de blauwdruk van de cel, in het DNA staat alle informatie gecodeerd die nodig is voor het correct laten functioneren van cellen. DNA bestaat uit twee lange strengen nucleotiden die in de vorm van een dubbele helix met elkaar vervlochten zijn. Er zijn vier verschillende nucleotiden welke worden aangeduid met de letters A, C, G en T. De volgorde van deze letters vormt een codering; vergelijkbaar met hoe de letters in ons alfabet woorden en zinnen kunnen vormen. Deze genetische code kan vervolgens in onze cellen vertaald worden voor de productie van eiwitten. Dit gebeurd in twee stappen. Eerst wordt er een tijdelijke kopie van het stukje DNA gemaakt dat codeert voor een bepaald eiwit; dit proces noemen we transcriptie. Zo een kopie van een stukje DNA wordt boodschapper RNA genoemd (messenger RNA, mRNA). Het mRNA wordt vervolgens vertaald in een specifiek eiwit, waarbij elke drie letters samen coderen voor één bouwblok van een eiwit; dit proces noemen we translatie. Eiwitten zijn het gereedschap van de cel, hiermee wordt alles in de cel opgebouwd en aangestuurd.

Aangezien DNA de blauwdruk vormt voor de bouwstenen die essentieel zijn voor het correct functioneren van onze cellen is het bijzonder belangrijk dat er in de genetische code van het DNA geen fouten ontstaan. De integriteit van ons DNA wordt echter voortdurend bedreigd door genotoxische invloeden van buitenaf en ook door stoffen die door ons eigen lichaam worden gemaakt. Beschadigd DNA is gevaarlijk voor onze cellen, aangezien deze beschadigingen kunnen leiden tot een verstoring van de genetische code. Deze mutaties zouden uiteindelijk kunnen leiden tot het ontstaan van kanker. Onze cellen zijn echter uitgerust met een DNA-schade respons (DDR), welke bestaat uit een grote verscheidenheid aan specifieke DNA-herstelmechanismen en signaleringssystemen. Nucleotide excisie reparatie (NER) is een veelzijdig DNA-herstelmechanisme dat een breed scala aan helix-verstorende DNA-schade repareert, inclusief schade veroorzaakt door ultraviolette (UV) straling aanwezig in zonlicht. NER wordt geïnitieerd door twee verschillende schade-herkenningsmechanismen: globaal genoom NER (GG-NER) en transcriptie gekoppeld NER (TC-NER). GG-NER herkent en repareert DNA-schade overal in het genoom, terwijl TC-NER specifiek schade herkent in DNA wat actief getranscribeerd (gekopieerd) wordt. In totaal werken meer dan 30 eiwitten samen binnen NER om helix-verstorende schade in het DNA te verwijderen. Regulatie van het NER mechanisme is van essentieel belang om ervoor te zorgen dat de betrokken eiwitten hun functie uitvoeren op de juiste locatie en tijdstip. Deze regulatie wordt grotendeels bewerkstelligd door posttranslationele modificatie (PTM) (oftewel: een aanpassing maken aan een eiwit nadat het vertaald is van mRNA) van de reparatie eiwitten zelf of van andere eiwitten betrokken in de DDR. Dit proefschrift richt zich op de betrokkenheid van modificatie van eiwitten met ubiquitine tijdens de UV-geïnduceerde DDR. Ubiquitine is een klein eiwit dat covalent gebonden kan worden aan andere eiwitten. Het koppelen van een eiwit met ubiquitine wordt ubiquitinatie genoemd,

en kan invloed hebben op de activiteit, lokalisatie en stabiliteit van het gemodificeerde eiwit. Het is bekend van verschillende eiwitten dat deze worden geubiquitineerd als reactie op bestraling van cellen met UV licht en dat deze eiwitmodificaties functioneren om de complexe UV-geïnduceerde DDR in goede banen te leiden. Onze verwachting is echter dat naast deze bekende eiwitten, ook nog andere (onbekende) eiwitten gereguleerd worden door ubiquitinatie na UV-schade. Voor de identificatie van deze eiwitten is massaspectrometrie (MS) gebruikt. MS is een veel gebruikte techniek om eiwitten te kunnen identificeren. Hiervoor worden eiwitten in stukjes geknipt om vervolgens de massa van deze stukjes te meten. In **Hoofdstuk 1** worden de onderwerpen DNA-schade herstel, ubiquitinatie en MS-gebaseerde methoden geïntroduceerd.

Men neemt aan dat in een cel niet alle eiwitten geubiquitineerd worden en van de eiwitten die wel geubiquitineerd worden zal maar een kleine fractie gemodificeerd zijn op een bepaald tijdsstip. Er zijn dus, relatief gezien ten opzichte van alle andere eiwitten, maar weinig eiwitten die geubiquitineerd zijn. Om de kans te vergroten dat je deze eiwitten identificeert met behulp van MS is het dus erg nuttig om deze gemodificeerde eiwitten van tevoren te isoleren. In **Hoofdstuk 2** wordt een verrijkingsmethode besproken voor de isolatie van endogeen geubiquitineerde eiwitten. Deze methode is specifiek ontwikkeld voor de analyse van geubiquitineerde eiwitcomplexen met behulp van MS.

Kwantitatieve MS methoden – zoals op 'stable isotope labelling by amino acids in cell culture' (SILAC) gebaseerde MS – zijn ontworpen om de effecten van een specifieke stimulus op de relatieve hoeveelheid van eiwitten te detecteren en te kwantificeren in het gehele proteoom. In **Hoofdstuk 3** staat beschreven hoe op SILAC gebaseerde MS is gecombineerd met de verrijkingsmethode voor geubiquitineerde eiwitten beschreven in Hoofdstuk 2. Deze aanpak hebben wij gebruikt om UV-geïnduceerde veranderingen in geubiquitineerde eiwitcomplexen te identificeren. Bovenin de lijst van verrijkte eiwitten na behandeling met UV straling staan een aantal eiwitten waarvan al bekend is dat ze geubiquitineerd worden als reactie op UV-geïnduceerde DNA-schade: o.a. DDB2, XPC, RNA Pol II en CSB. De identificatie van deze eiwitten laat zien dat onze methode inderdaad goed gebruikt kan worden voor het isoleren van eiwitten met UV-geïnduceerde ubiquitine modificaties.

Na bestraling van cellen met UV licht hebben we in totaal 95 eiwitten geïdentificeerd waarvan de hoeveelheid eiwit minstens 1.5-voud meer of minder was geworden. Deze eiwitten konden gegroepeerd worden in vijf clusters en zo gekoppeld worden aan vijf biologische processen: (1) NER, (2) chromatine herstructurering, (3) transcriptie, (4) translatie en (5) RNA splicing. De identificatie van NER was het meest voor de hand liggende proces, aangezien dit het enige reparatie-mechanisme is in zoogdieren welke UV-geïnduceerde DNA schade kan verwijderen en waarvan bekend is dat het door middel van ubiquitinatie gereguleerd wordt. Ook chromatine herstructurering wordt vaak geassocieerd met de DDR, omdat dit proces de toegang tot beschadigd DNA kan vergemakkelijken voor DNA reparatie eiwitten en signaleringsfactoren. Daarnaast is bekend dat transcriptie ernstig belemmerd wordt door UV-schade, wat leidt tot de activering van TC-NER. De identificatie van de overige twee biologische processen, translatie en RNA splicing, was minder verwacht en zou nieuwe takken binnen de UV-DDR kunnen vertegenwoordigen. De gevonden resultaten

lijken te wijzen op een globale ubiquitine-gemedieerde regulatie van verschillende onderling verbonden biologische processen welke er voor moeten zorgen dat de cel de juiste acties onderneemt in reactie op UV-geïnduceerde stress.

Hoofdstuk 4 beschrijft de identificatie en moleculaire functie van 'UV-stimulated scaffold protein A' (UVSSA) en het interacterende eiwit USP7 in TC-NER. Het voorheen ongekarakteriseerde eiwit UVSSA is geïdentificeerd in de MS lijst van UV-geïnduceerde eiwitten gegenereerd in Hoofdstuk 3. Hoewel UVSSA is gevonden als één van de meest verrijkte eiwitten in deze lijst werd het eiwit zelf niet meer geubiquitineerd in reactie op UV straling. Verdere biochemische analyse heeft echter aangetoond dat UVSSA interactie aangaat met RNA Pol II, zich specifiek begeeft naar UV-geïnduceerde DNA-schade en zich bevindt in chromatine-gebonden TC-NER complexen. We nemen daarom aan dat UVSSA is geïsoleerd als onderdeel van het UV-geïnduceerde geubiquitineerd RNA Pol II complex. Verder laten we zien dat UVSSA betrokken is bij de stabilisatie van CSB door middel van het rekruteren van het de-ubiquitinerend enzym USP7 naar TC-NER complexen. Een belangrijke ontdekking was dat mutaties in het *UVSSA* gen verantwoordelijk zijn voor 'UV-gevoeligheids syndroom groep A' (UV^{S}S-A), een voorheen onopgeloste NER-deficiënte ziekte.

In **Hoofdstuk 5** wordt bediscussieerd hoe het onderzoek naar de rol van UVSSA en USP7 binnen TC-NER een bijdrage kan leveren aan een beter begrip van de mechanismen welke ten grondslag liggen aan de klinische verschillen tussen twee TC-NER-deficiënte ziekten: het Cockayne syndroom (CS) en het UV-gevoeligheids syndroom (UV^{S}S). Hoewel deze ziekten een moleculair defect hebben in hetzelfde proces (TC-NER), is het fenotype van deze patiënten zeer verschillend. Terwijl CS gekenmerkt wordt door ernstige groeiachterstand, neurologische problemen en een versnelde veroudering is het UV^{S}S fenotype voornamelijk beperkt tot UV-overgevoeligheid van de huid. Het precieze moleculaire mechanisme dat ten grondslag ligt aan deze klinische verschillen is nog steeds onbekend, echter de verschillen zouden verklaard kunnen worden door additionele functies van de CS eiwitten buiten TC-NER. Hoofdstuk 5 geeft een kort overzicht van de huidige hypotheses van mogelijke mechanismen en de bijbehorende betrokken eiwitten. Daarnaast wordt de functie van UVSSA en USP7 besproken en wordt bediscussieerd hoe deze kennis de bestaande moleculaire modellen, welke de fenotypische verschillen tussen UV^{S}S en CS proberen te verklaren, kan complementeren.

CURRICULUM VITAE

Name:	Pieterke Schwertman (Petra)
Date of birth:	5 September 1983
Nationality:	Dutch
E-mail:	p.schwertman@gmail.com

Education

2013-present	Postdoc, Ubiquitin signaling group, the Novo Nordisk Foundation Center for Protein Research, Copenhagen
2008-2013	PhD-student, department of Genetics, Erasmus MC, Rotterdam
2005-2008	MSc, Life Science & Technology, Leiden University/Technical University Delft, the Netherlands, specialization: Functional Genomics (Cum Laude)
2001-2005	BSc, Life Science & Technology, Leiden University/Technical University Delft, the Netherlands
1995-2001	Dollard College High School (Gymnasium), Winschoten, the Netherlands

PUBLICATIONS

Schwertman P, Bezstarosti K, Laffeber C, Vermeulen W, Demmers JAA, Marteijn JA. An immunoaffinity purification method for the proteomic analysis of ubiquitinated protein complexes. Anal Biochem. 2013 Sep 15;440(2):227-36.

Schwertman P, Vermeulen W, Marteijn JA. UVSSA and USP7, A new couple in Transcription-coupled DNA repair. Chromosoma. 2013 Aug;122(4):275-84

Schwertman P, Lagarou A, Dekkers DH, Raams A, van der Hoek AC, Laffeber C, Hoeijmakers JH, Demmers JA, Fousteri M, Vermeulen W, Marteijn JA. UV-sensitive syndrome protein UVSSA recruits USP7 to regulate transcription-coupled repair. Nat Genet. 2012 May;44(5):598-602

Marteijn JA, Bekker-Jensen S, Mailand N, Lans H, **Schwertman P**, Gourdin AM, Dantuma NP, Lukas J, Vermeulen W. Nucleotide excision repair-induced H2A ubiquitination is dependent on MDC1 and RNF8 and reveals a universal DNA damage response. J Cell Biol. 2009 Sep 21;186(6):835-47

Janssen GM, **Schwertman P**, Wanga TA, Tafrechi RS, van den Broek PJ, Raap AK. Transient and constitutive repression of cytoplasmic translation signaling in cells with mtDNA mutation. Cell Mol Life Sci. 2009 Feb;66(4):721-30

PHD PORTFOLIO

General courses

Veilig werken in laboratoria/ Safely working in the laboratory	2009
ML-1 (work permit for GMOs)	2008
ML-2 (work permit for Adenovirus and Lentivirus)	2010
Workshop: Photoshop and Illustrator CS4	2010
Workshop: Indesign CS5	2011
Biomedical English Writing and Communication	2011
EHBO/First aid	

Specific courses

Molecular and Cell Biology	2008
Genome Maintenance and Cancer	2008
Biomolecular MS course	2008
Confocal microscopy	2009
MaxQuant Summer school	2010

Conferences and seminars

Journal club	2009-2013
MGC DNA repair group meetings	2008-2013
NPC progress meetings	
Utrecht, the Netherlands, oral update presentations	2009-2012
The 18th MGC-Symposium	
Rotterdam, the Netherlands, attended	2008
CGC/CBG meeting "Molecular mechanisms and mouse models in cancer"	
Amsterdam, the Netherlands, attended	2008
NCMLS Symposium "New frontiers in ubiquitination"	
Nijmegen, the Netherlands, attended	2008
NWO-CW study groups protein research, nucleic acids, lipids & biomembranes	
Veldhoven, the Netherlands, poster presentation	2008
CGC Scientific Meeting	
Rotterdam, the Netherlands, attended	2009
3rd EU - IP DNA Repair Workshop for Young Scientists	
Taormina, Sicily, oral presentation	2009
PhD workshop	
Bruges, Belgium, attended	2009
The 19th MGC-Symposium	
Leiden, the Netherlands, attended	2009
NWO-CW study groups protein research, nucleic acids, lipids & biomembranes	
Veldhoven, the Netherlands, poster presentation	2009
PhD workshop	
Cologne, Germany, poster presentation	2010

8th Dutch Chromatin meeting
Leiden, the Netherlands, poster presentation 2010
EMBO Workshop 'Interface between the Ubiquitin family and the DNA damage response'
Rovinj, Croatia, poster presentation 2010
PhD workshop
Maastricht, the Netherlands, oral presentation 2011
The 21th MGC-Symposium
Leiden, the Netherlands, oral presentation 2011
9th Dutch Chromatin meeting
Groningen, the Netherlands, oral presentation 2011
Responses to DNA damage: from molecular mechanism to human disease
Egmond aan Zee, the Netherlands, poster presentation 2011
PhD workshop
Luxembourg, Luxembourg, oral presentation 2013

Students

Summer internship student 2009
Junior Science Program (2 high school students) 2009
HBO student (final thesis) 2010-2011
MSc student (literature study) 2013

Miscellaneous

Reisbeurs/travelling grant (Simonsfonds - EMBO workshop 2010)

DANKWOORD

Daar ligt het dan voor je. Mijn proefschrift. Het koste af en toe wat moeite, er was af en toe wat stress. Maar het is nu helemaal klaar en af. :) Ik ben erg blij mee en ben er onwijs trots op! Een proefschrift is echter geen solo project, het is een team effort. Ik wil dan ook graag iedereen ontzettend bedanken die een bijdrage heeft geleverd aan de totstandkoming van dit boekwerk; zowel wetenschappelijk als daarbuiten. Een aantal mensen wil ik dan nog in het bijzonder bedanken.

Jurgen! Ik heb ontzettend veel van je geleerd. De deur stond altijd voor me open, en je had altijd een oplossing en een antwoord. Daarnaast waren we prima compatible qua directheid en foute grappen; ik heb bijzonder vaak met/om je gelachen (die kano-outfit staat op mn netvliezen gebrand ^^). Samenwerken ging ook als een speer, met als hoogtepunt het KIAA verhaal natuurlijk. Al met al konden we het goed vinden en ben ik er trots op om jouw OIO te mogen zijn geweest.

Wim, bedankt dat ik in je groep mocht komen werken (boeiend transcriptie/translatie). Ik ben altijd met veel plezier naar het lab gekomen, mede ook dankzij de goede sfeer die er altijd hangt. Die gezelligheid was ook goed zichtbaar op de jaarlijkse labuitjes en de BBQs bij jou thuis (ook een dikke dank je wel voor Hanny!), die waren altijd leuk. Ook kon ik altijd bij je terecht voor wetenschappelijke feedback (hoewel je van sommige wellicht iets spijt hebt…droog, saai en kil enzo… ;)).

Jan, bedankt voor je inspirerende enthousiasme voor wetenschap. We hebben weinig met elkaar gesproken in mijn tijd als OIO, maar tijdens besprekingen wist je altijd resultaten in de juiste context te plaatsen en nuttige input te geven.

Leden van de leescommissie en overige commissieleden: bedankt voor het kritisch lezen van dit proefschrift.

Dit proefschrift bevat een flinke vleug massspec. En dat is mede mogelijk gemaakt door de massspec-mannen. Bedankt voor het runnen van al mijn samples en de nuttige input tijdens de data analyse en interpretatie van de resultaten.

Thank you Vermeulen lab, past and present! It was good to be part of the group and it has always been fun coming to the lab. Maikel, mijn eerste OIO-buddy! Bijna samen begonnen, veel samen geleerd. En later, als ouwe lullen, de 'jonkies' de stad in sleuren voor biertjes. Daarnaast was je mijn gids in R'dam en heb je me geïntroduceerd bij Het Apparaat. Supermove! Soon there were more however: Loes, Özge & Kasper. I will fondly remember our time together in the too small office and then in the somewhat bigger office, but also the fun we had on the workshops and conferences. :D Good luck with finishing your PhDs! Also a thank you for the newest batch of OIOs, the peaches: Imke, Franzi, Christina, Serena, Yasemin and Mariangela. We had a short overlap, but you made a lasting impression. Then

the 'old/more experienced' people, I learned so much from you and you made me laugh. Vooral Hannes, want jouw humor is stiekem best grappig. ;) Arjan, na die laatste paar maanden als roomy weet ik het zeker: veel herrie, maar eigenlijk een schatje. (En je kan niet zingen.) Nils, superhandig zo'n inside ITer.^^ En we moeten nog steeds eens vliegeren! Hervé, merci beaucoup, and thx for letting me teach you origami at the end. ;) Karen, Maria, Joris, Koos, Anja and Jan de Wit, thx for your scientific input and help along the way. Ook nog een dikke dank je wel voor Charlie! Je hebt me ontzettend goed geholpen in mijn begindagen. And finally all the students that came along! En dan in het bijzonder Rianne, voor al die prachtige IPs die je voor me gedaan hebt. :)

Also outside of the Vermeulen lab there are many people at the EMC that brightened my time as a PhD student. The people at the 'other' side and on the 6th floor, thank you for the scientific discussions and sharing cake & beers! The people outside of the EMC: especially all the attendees of the MGC PhD workshops; in addition to the science we had so much fun, and so many bad pictures. O:)

Verder werd experimenteren makkelijker gemaakt door de efficiënte infrastructuur: de dames van de keuken, de mannen van het computer-problemen-crisis-centrum, de schoonmakers, afdeling inkoop en de altijd behulpzame secretaresses!

Mange tak for my new colleagues at the CPR in Copenhagen. I had such a warm welcome and look forward to the time to come.

De Delftse delegatie! Ondertussen door het hele land verspreidt en daarbuiten: alle Kurkjes, SWAMPY (en aanhang) en Jasper voor de begindagen van mn PhD.

De Rotterdamse delegatie! Pleinbuurtjes, ik mis onze BBQs! Apparaten, ontzettend bedankt dat jullie me zo snel in jullie armen hebben gesloten. Jullie hebben me in no-time helemaal thuis laten voelen in Rotterdam: Bedankt! HEA's: ik kan nog steeds niet shoppen!!! o.O Maar ben wel erg goed geworden in breien, kletsen, sauna-en, sleep-overs, en cocktails drinken. Bedankt: Karin, Renée, Linda, Martine, Sabje, Astrid en Ines! Ik ben klaar voor Rome, wanneer gaan we?

Bert-Jaap. Ik ben zo blij dat je mijn paranimf wilde zijn! We zaten dan wel niet helemaal in hetzelfde lab, maar onze voorliefde voor eenzelfde soort geekyness is natuurlijk allesoverkomend-epic-awesome. ;) En, zoals verwacht, was je ontzettend capabel in het soepel laten verlopen van alles wat ik van je vroeg! Erg belangrijk voor een paranimf. Dank je wel voor al je hulp, zowel in je paranimf-functie als tijdens het gehele PhD traject. Ik verwacht nog steeds wel goeie boekentips van je trouwens, met de laatste twee series ben ik bij en ben ik alweer ontzettend ongeduldig aan het wachten.

Lieve Bert, lief broertje van me. Je grote zus gaat promoveren. Ik ben zo ontzettend trots dat jij op deze bijzondere dag naast me zal staan. Je bent er altijd voor mij als ik iets nodig heb. Niets is je te gek. Bedankt dat je zo'n fantastische broer bent!!

Lieve, lieve Thomas. Ik vind het nog steeds ongelofelijk, maar je bent mijn mirror. Onze to-do lijst puilt uit, we gaan ze allemaal doen en ik heb ontzettend zin in al onze toekomstige avonturen. En dank je wel dat je mijn stressballetje wilde zijn. :*

Pap, Mam en Opa&Oma, jullie hebben me altijd gestimuleerd om te studeren, te onderzoeken en te doen wat ik leuk vind. En ook al is het niet altijd even duidelijk wat ik nu allemaal voor moeilijke dingen doe, jullie hebben altijd naar me geluisterd (poging tot in ieder geval), me altijd gesteund en ik weet dat jullie ontzettend trots op mij zijn. Ik hou van jullie, dank jullie wel!!!